The Henryk Niewodniczański Institute of Nuclear Physics
Polish Academy of Sciences

Nanomechanics in skin cells' interactions

Barbara Orzechowska

Thesis submitted for the Degree of Doctor of Philosophy in Physics
Prepared under the supervision of
Prof. dr hab. Małgorzata Lekka (thesis supervisor)
Dr Joanna Zemła (auxiliary supervisor)

Kraków 2018

To my Mom.

Acknowledgements

Firstly, I would like to express my sincere gratitude to my advisor, the head of Department of Biophysical Microstructures Prof. dr hab. Małgorzata Lekka for the continuous support of my Ph.D study and related research, for her patience, motivation, and immense knowledge. Her guidance helped me in all the time of research and writing of this thesis. I could not have imagined having a better advisor and mentor for my Ph.D study.

I would also like to thank my co-supervisor, Dr Joanna Zemła, for her help, insightful comments and expertise that greatly assisted the research.

My deepest thanks to all my current and former colleagues from our research group (DBM, IFJ PAN) for the stimulating discussions, friendly and welcoming atmosphere, and for all the fun we have had in the last five years.

I would also like to thank to all my colleagues from the Department of Experimental Physics of Complex Systems (IFJ PAN) headed by Prof. dr hab. Wojciech Kwiatek.

I am also grateful to Mrs. Joanna Wiltowska-Zuber, Mrs. Joanna Pabijan and Mrs. Klaudia Suchy for their laboratory support.

To my friends for their love, patience and help. Especially, to my friend Kasia who supported me at all times, good and bad. I know I owe you. Thank you.

And, finally, to my family, my husband Dariusz and my beloved son Filip, who always believe in me, and give me wings in my moments of doubts. To my Dad who supported me not only with a good word but also helped to speed up the data analysis.

Abstract

Nowadays, a broad range of research methods is used to gather additional information about various kinds of diseases that appear in society. The main goal of researchers is to expand the possibilities of faster diagnosis and treatment of patients. In recent years, both physical and biophysical tests have become extremely important and they are one of the basic research and diagnostic tools. One of the methods extensively used in many research fields is Atomic Force Microscopy (AFM). This technique is currently used, among others, to study changes in mechanical properties of alive cells as they indicate alterations in various cellular functions. Nanomechanical properties seem to be a promising marker dependent on changes taking place in the cell structure resulting from pathological alterations.

The main objective of the presented thesis was to ascertain how mechanical properties of living cells change in the processes of wound healing and melanoma formation. For this purpose, an innovative approach of conducting cell cultures was elaborated basing on the mixing of two types of cells originating from skin. Co-cultures consisting of keratinocytes and fibroblasts were used to study the interactions occurring between these cells in the process of wound healing. Mixtures of melanoma cells either with fibroblasts or with keratinocytes allowed to study the mechanical response from mutually interacting cells involved in the melanoma progression.

Obtained results indicate that alterations in elastic properties of living cells accompany both wound healing and melanoma progression. Cells adapt their mechanical properties to the external environment, reduce or increase their stiffness in response to given conditions. Elasticity measurements revealed an increase in deformability of melanoma cells in the presence of fibroblasts. This enhance the ability of cancer cells to form metastases. Lack of changes in mechanical properties of melanoma cells in the presence of keratinocytes indicate high level of cellular adaptability to changing external conditions.

Streszczenie

W obecnych czasach stosuje się różnorodne metody badawcze do pozyskiwania nowych, dodatkowych informacji dotyczących różnego rodzaju schorzeń i chorób pojawiających się w społeczeństwie. Głównym celem badaczy jest poszerzenie możliwości szybszego diagnozowania i leczenia pacjentów. W ostatnich latach zarówno badania fizyczne jak i biofizyczne nabierają ogromnego znaczenia i stają się jednymi z podstawowych narzędzi badawczych i diagnostycznych. Jedną z metod wykorzystywanych do badań w wielu dziedzinach jest skaningowa mikroskopia sił atomowych (ang. *Atomic Force Microscopy*, AFM). Technika ta jest obecnie wykorzystywana między innymi do badań zmian własności mechanicznych żywych komórek, które wskazują na zmiany zachodzące w ich funkcjonowaniu. Właściwości nanomechaniczne komórek wydają się być również obiecującym markerem zależnym od zmian zachodzących w samej strukturze komórki, w efekcie zmian chorobowych.

Głównym celem niniejszej rozprawy było badanie zmian oraz roli własności mechanicznych żywych komórek, zachodzących w procesach gojenia ran i powstawaniu czerniaka. W tym celu użyto nowatorskiego podejścia prowadzenia hodowli komórkowych polegającego na wymieszaniu ze sobą dwóch rodzajów komórek pochodzących ze skóry ludzkiej. Mieszanina składająca się z keratynocytów i fibroblastów została wykorzystana do badania oddziaływań, które występują pomiędzy komórkami uczestniczącymi w procesie gojenia ran. Mieszaniny komórek czerniaka z fibroblastami lub keratynocytami pozwoliły zbadać odpowiedź mechaniczną pochodzącą z komórek, które w procesie powstawania czerniaka kontaktują się ze sobą i wzajemnie na siebie oddziaływają.

Uzyskane wyniki pokazały zmiany własności elastycznych żywych komórek występują w procesach gojenia ran oraz powstaniu czerniaka. Komórki dostosowują swoje własności mechaniczne do środowiska zewnętrznego zmniejszając bądź zwiększając nanomechniczną odpowiedź na określone warunki. Pomiary elastyczności pokazały wzrost deformowalności komórek czerniaka w obecności fibroblastów, związaną z większą zdolnością komórek do formowania przerzutów. Brak zmian elastyczności tych komórek o środowisku zawierającym keratynocyty wskazuje na wysoki stopień adaptacji komórek czerniaka do zmiennych warunków zewnętrznych.

Table of contents

List of abbreviations:

AFM – atomic force microscopy
BM – basal membrane
DERMAL – cells culture medium, Dermal Cell Basal Medium
ECM – extracellular matrix
EMEM – cell culture medium, Eagle's Minimum Essential Medium
FB, CCL-110 – normal fibroblasts cells derived from dermis layer of the skin
HGF – Hepatocyte Growth Factor
IL-1 – interleukin-1
IL-6 – interleukin-6
HaCaT – normal keratinocytes i.e. HaCaT cells derived from epidermis layer of the skin
KGF – keratinocyte growth factor
RPMI-1640 – cell culture medium developed at Roswell Park Memorial Institute in 1966 by Moore and his co-workers
TGF-β – Transforming Growth Factor β
WM35 – melanoma cells originating from primary melanoma site (skin) in a radial growth phase (RGP)

1. Introduction

The development of advanced spectroscopic techniques that allow to measure living cells in conditions close to natural ones at the cellular or even molecular levels opens the possibility to identify pathologically-related changes, also in the case of cancer. Such a precise recognition can potentially enable a faster diagnosis and disease treatment. Moreover, recent research evidence directly demonstrated that biochemical as well as molecular alterations define pathological state and bring the idea of mechanisms involved. It is also important to elaborate changes in biophysical properties of the studied cells, in parallel. This is particularly significant for cancer development as recent data have demonstrated the importance of mechanical forces in the formation of metastasis.[1,2] One of the techniques that enables to measure biomechanical properties of cells in conditions mimicking the natural ones is the atomic force microscopy (AFM). It is widely applied in the field of cancer research through delivering a well-accepted information that cancer cells are more deformable as compared to their normal, healthy counterparts.[3–5] However, so far, all measurements were carried out on single, isolated cells what questions the applicability of the technique in cancer recognition in tissue context. To overcome it, there is a need to study the deformability of cells being in contact with other cells. In the presented thesis, the cellular interaction between skin cells was quantified by means of AFM.

Wound healing is a process where the interaction between keratinocytes and fibroblasts proceeds through a double paracrine signaling pathway.[6,7] However, most of studies showing details of signaling pathway involvement were performed using immunostaining, immunodepletion.[8] Such experiments, frequwntly, neglect the role of direct physical interactions. In the presented studies, the main stress has been placed on alterations in cellular deformability of skin cells. By determining a deformability of single cells, any potential influence of paracrine signaling pathways can be obtained. In such a case, the direct cellular interaction is minimized. Studying cell clusters allows to get insight on the interactions of cells being in a direct contact. Here, paracrine signaling pathways is less pronounced. Dominant contribution in cell mechanical properties stem from physical contact between cells and is governed by cytoskeleton remodelling.[7] Healthy skin cells such as fibroblasts and keratinocytes affect the growth of melanoma cells. Some exemplary research has shown that at the early stage of melanoma progression, fibroblasts can inhibit growth of cancer cells whereas at more advanced tumour stages, especially, for metastasis, growth of melanoma cells can be stimulated.[9–11] Fibroblast-derived signals can allow cancer cells to escape from a local growth place both in the primary tumour site and at distant tissue sites. These results have been verified for a variety of experimental systems, particularly for that composed of human dermal fibroblasts and melanoma cells from distinct stages of cancer progression.[11] One of the molecules involved is an interleukin-6, which is a result of double paracrine signaling pathways occurring in keratinocyte-fibroblast interaction, in a similar manner to that observed in wound healing process.[10] So far, there is no knowledge how such signaling induced changes in deformability of melanoma cells, especially during early stages of melanoma progression, where interaction with normal skin cells has been reported, inhibit cancer development. Therefore, the main objective of the presented studies was to evaluate alterations in mechanical properties of melanoma cells derived from a radial growth phase in the interactions with two types of skin cells (both keratinocytes and fibroblasts). To

demonstrate that cells interact both indirectly through signaling molecules (secreted by other cells and attaching to receptors of target cells) and, also, directly by various types of cell-cell junctions, mechanical properties of single cells, cell clusters and border cells were investigated for cellular mixtures composed of a particular pair of cells either keratinocytes/WM35 melanoma cells or fibroblasts/WM35 melanoma cells.

The presented thesis is organized as follows. *Chapter 2* introduces the basic information about skin biology, structure and function. Brief descriptions of two processes involving a basal membrane interruption, namely, wound healing and melanoma progression, are presented, and followed by introducing the basic elements of cell structure and its relation to biomechanics. The end of *Chapter 2* presents the main objectives of the thesis. In *Chapter* 3, a characterization of the studied biological material is included. Three chosen cell lines (human skin fibroblasts, keratinocytes and melanoma cells from radial growth phase) are described together with their culture conditions. As growing cells in cellular mixtures is not an easy task, a part of preparatory studies were devoted to an optimization of culture conditions. Resulting modifications are described based on results obtained from cell viability (MTT) assay tests and elasticity measurements. After this chapter, a description of the technique, namely, AFM is presented. It is accompanied by short depictions of the viability assay and fluorescence microscope. A large part of *Chapter 4* is devoted to data analysis. As obtained results do not follow normal distributions several approaches to data analysis are presented. The comparison between them enabled me to identify mechanical fingerprints characteristic for each of skin cell types, namely, keratinocytes, fibroblasts and melanoma cells. In the approach, presented here, elasticity data were fitted with lognormal function describing non-symmetric histograms (normality tests were also applied to quantify the character of the distributions). Next two chapters (*Chapter 5 and Chapter 6*) present the gathered results. A comparison between various cell populations was performed basing on an expected modulus values determined from lognormal distribution accompanied by a standard error. Mood's median test was applied to estimate the statistical differences. The results included in *Chapter 5* show changes in mechanical properties of two cell types, i.e. keratinocytes and fibroblasts. These cells participate in keratinocyte-fibroblast interaction that occurs during wound healing. Their biomechanical properties were related to two ways of intercellular communication that are secretion of signaling molecules by other cells and direct connections between two adjacent cells. To resolve which way of cellular communications is dominating in mechanical response to surrounding environment, single cell, cell clusters and border cells were measured. Obtained distinct mechanical properties were found to be related to actin cytoskeleton organization. As melanoma is derived from single melanocytes surrounded by keratinocytes and during the invasion melanoma cells interact with fibroblasts, further studies focus on the interactions of melanoma cells (WM35 cells originating from the radial growth phase) either with keratinocytes or fibroblasts (*Chapter 6)*. The final chapter (*Conclusions*) summarizes the obtained results.

2. Skin biology – introduction

2.1. Skin structure and function

Skin is the largest human organ. It is composed of three main layers i.e. epidermis, dermis and hypodermis.[12] In healthy skin, epidermis and dermis are separated by basal membrane (BM, **Figure 1**) being a result of cooperative interactions between keratinocytes and fibroblasts producing extracellular matrix (ECM) proteins.[13,14]

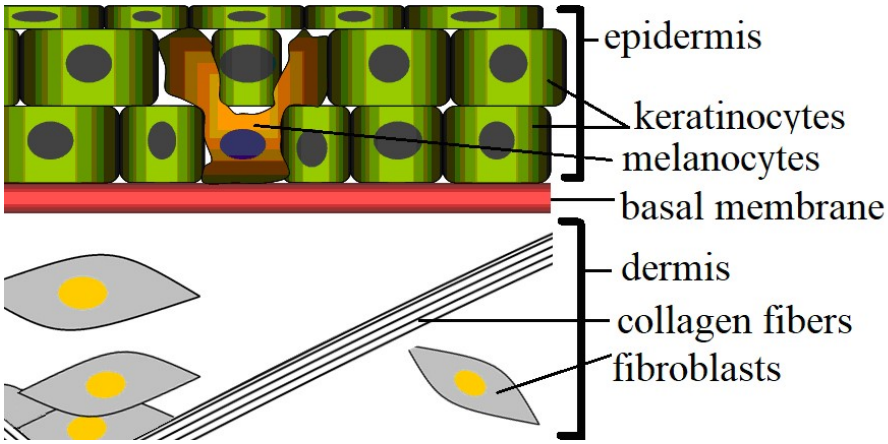

Figure 1. Schematic structure of human skin. Epidermis consists mainly of keratinocytes (green cells) with embedded melanocytes (orange cell). Fibroblasts (grey cells) are present in the dermis, in which collagen fibers are observed, too.

Keratinocytes in the epidermis layer of the skin are arranged into several layers. During keratinization*,[15,16], these cells move from regions close to the basal membrane to external layers of the skin. Here, keratinocytes lose cell nuclei and they form so-called *stratum corneum,* which protects the skin against a water loss mainly. Among deeper layers of epidermis, keratinocytes are mixed with melanocytes. Melanocytes are responsible for skin pigmentation since they have ability to produce and distribute melanin (a skin pigment).[17] Below the basal membrane, within the dermis layer, fibroblasts are present. These cells produce many factors and participate in the formation of collagen fibers and form the extracellular matrix filling the dermis.

* Keratinization (also called cornification) is the process of terminal differentiation of the epidermis. The keratinocytes move from the basal membrane, where they are in post germinative state, to finally differentiated, hardened cells. The outermost layer comprised of dead cells is called *stratum corneum*[7,8].

The main functions of the skin are:

- *protection* the body against the action of external factors of mechanical, chemical and biological origins,[18]
- *sensation* allowing to feel a heat, cold, pressure, touch, vibration or injury (pain). It is the consequence of skin interaction with the presence of several nerves that ended in the skin,[19]
- *temperature regulation* – in hot conditions, the sweat glands present in dermis layer of human skin help to regulate the temperature through a release of sweat from the body, which causes evaporative cooling; in cold conditions – the blood vessels placed under the skin shrink what leads to their isolation from the cold external environment. Simultaneously, arrector pili muscles attached to individual hair follicles start to act by trapping the air between the erected hairs what provides insulating layer trapping the heat release from the body,[20]
- *synthesis of vitamin D* – the 7-dehydrocholesterol which is present in a plasma membrane of epidermal keratinocytes and dermal fibroblasts is converted to previtamin D_3 under UVB exposure provided by the sunlight,[21]
- *excretion* – the waste product of body (water, ammonia, uric acid or urea) are released through the skin surface that is regulated by the composition and volume of sweat,[22]
- *immunological response* – Langerhans and epidermal dendritic cells present in the skin recognize and destroy of the microorganism pathogens.[23]

Disruption of basal membrane integrity frequently leads to some dysfunctions of the skin such as an increase of fragility, wounds, blister, congenital skin disorders or cancers (e.g. melanoma).[24–26]

2.2. Wound healing

One of the process leading to interruptions of basal membrane integrity is the formation of a wound. After an injury, fibroblasts migrate to the edges of a cutaneous region and start to produce growth factors that stimulate keratinocytes to proliferate through double paracrine signaling pathway. The keratinocytes differentiation influences fibroblasts activity, too.[6,27–29] Such cooperation indicates that the process of skin repair plays an important role in the healing of wounds of distinct origins.

The main role in the wound healing is to preserve both keratinocytes and fibroblasts, which interact with each other during the tissue repair. They affect each other through the secretion (i.e. production) of several factors such as keratinocyte growth factor (KGF), hepatocyte growth factor (HGF), transforming growth factor beta (TGF-β), interleukin-6 (IL-6) or interleukin-1 (IL-1) in a manner schematically shown in Figure 2.

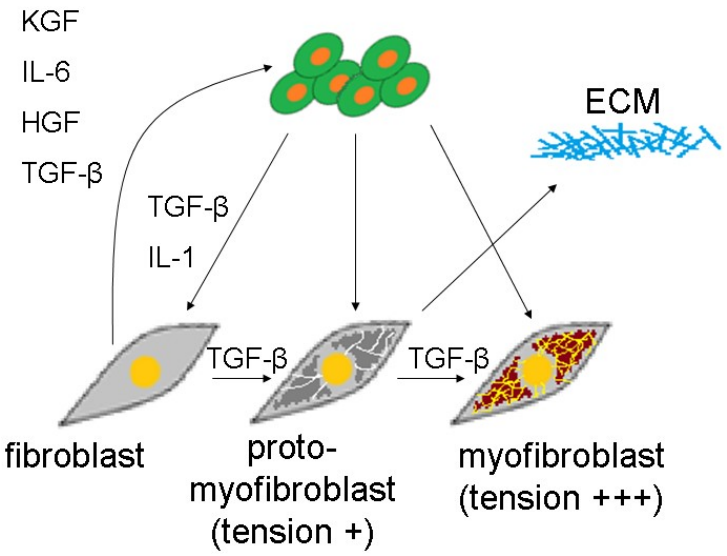

Figure 2. Scheme of skin cells interplay observed during wound healing (green cells denotes keratinocytes, grey cells – fibroblasts, ECM – extracellular matrix). Several types of signaling molecules are involved in the interactions between keratinocytes and fibroblasts. They are: transforming growth factor β (TGF-β), keratinocyte (KGF) and hepatocyte (HGF) growth factors, interleukins 6 (IL-6) and 1 (IL-1) (adapted from Werner et al., 2007]).[6]

Signaling molecules stimulate a proliferation of keratinocytes. At the same time keratinocytes influence fibroblasts *via* TGF-β and IL-1 and induce their transformation to proto-myofibroblasts and, finally, to myofibroblasts. Additionally, proto-myofibroblasts are stimulated by TGF-β to produce collagen I, collagen IV, collagen V, collagen VI, hyaluronan synthetase 2, syndecan 2, tenascin C and many other ECM components.[6]

Wound repair is a very complex process. It evolves over time, thus, several phases can be distinguished,[30] namely, *hemostasis*, *inflammation*, *proliferation* and *maturation*.[31]

Hemostasis occurs immediately after an injury. Within it, the blood starts clothing and many factors, necessary for injure closing, start to be produced. Clotting can be seen as preventing action against losing body fluids or electrolytes. The clot is composed of fibrin mesh and the platelets settle on them forming the skeleton for keratinocytes and fibroblasts migration to the injure.[32]

Inflammation is characterized by an increase of the body temperature, redness, or pain in the injury space. During this phase, the blood vessels dilate and white blood cells are released. The leukocytes clean the wound region by phagocytosis.[33]

Proliferation can be characterized by the presence of proliferating fibroblasts. They are moving into the wound region under the cytokines influence. These signaling molecules are also responsible for angiogenesis and epithelialization.[34,35] In this phase, keratinocytes and fibroblasts cooperate and act through double paracrine pathway.

Maturation occurs at the last phase of wound healing and is followed by the scar remodeling. The main task during maturation is a conversion of small, short collagen fibers to an organized, well-mannered network. It starts on 8th day after the injure and it can last through the years.[36]

2.3. Melanoma invasion

The other process leading to disruptions of basal membrane integrity is melanoma invasion. Melanoma is one of the most common cancers of the skin.[37] Several risk factors can be defined leading to the large incidence of the disease, e.g. a fair complexion, light eyes, red or blond hairs.[38–40]
Melanoma is derived from oncogenically altered melanocytes localized within the first layer of the skin, i.e. within epidermis (**Figure 3**).

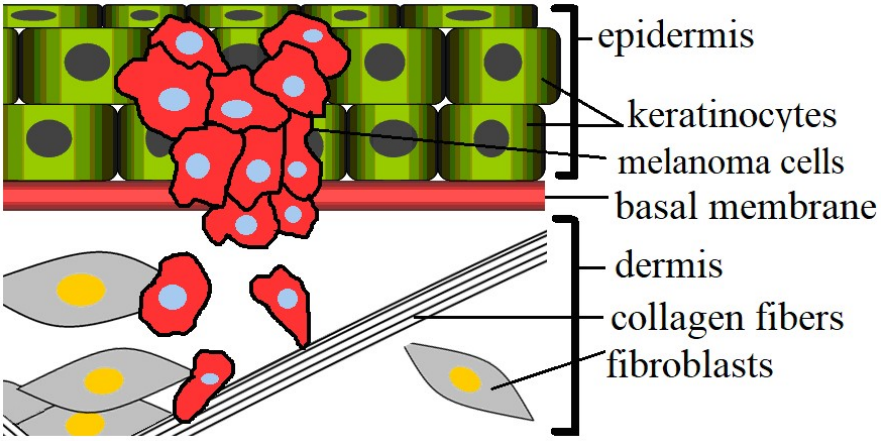

Figure 3. Spreading of melanoma cells into deeper parts of the skin (green cells – keratinocytes, grey cells – fibroblasts, red cells – melanoma).

The melanoma cells, present in epidermis, between keratinocytes, start to grow and to proliferate. When melanoma cells gain the migratory phenotype, cells start to disseminate. They break BM and invade to deeper parts of the skin. Thus, they move from epidermis to dermis and further on. As a consequence, several stages of melanoma progression can be defined (**Figure 4**).[41]

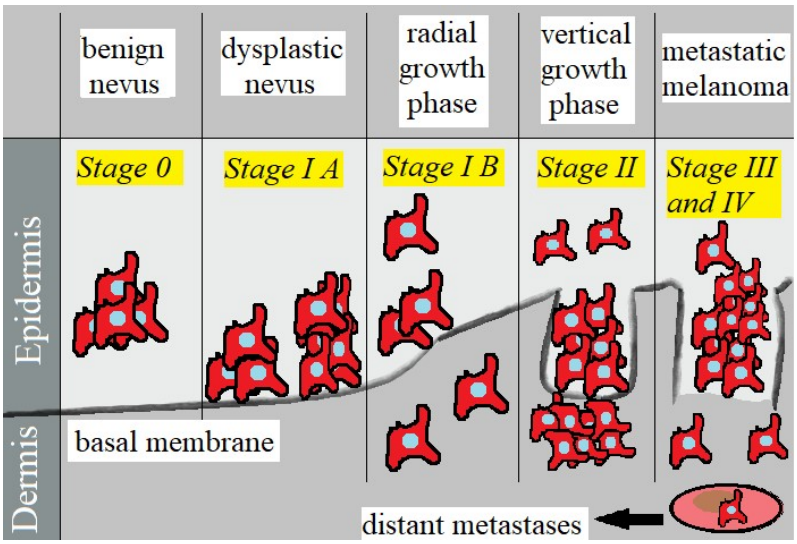

Figure 4. Stages of malignant melanoma progression (adapted from Arrangoiz et al., 2016]).[42]

In *Stage 0 (*called *benign nevus)* melanocytes are abnormal but still they are present only in the epidermis. Once cells gather migratory and invasive phenotypes, they invade to the surrounding normal tissue. *Stage IA (*called *dysplastic nevus)* characterizes a tumor, which is thinner than 1 mm without ulcer. *Stage IB (*called *radial growth phase)* represents tumor with thickness from 1 mm to 2 mm with or without ulcer. Up to these stages cells do not spread to deeper parts of the body. *Stage II (*called *vertical growth phase)* is characterized by melanoma thicker than 2 mm with or without ulceration[†]. Often, cells from this stage can form micrometastasis. *Stage III* represents metastatic melanoma. Cancer cells have capacity to spread to both the lymph nodes and vessels. Very small tumors (< 2 cm) can be found on or under the skin. During further melanoma progression, metastatic sites can be found in the other parts of the body e.g. in bones, liver, lung or brain (being a *Stage IV* of melanoma progression).[43]

2.4. Basics of cell structure and its relation to biomechanics

The use of physics methods to describe the living cells requires an introduction of some principles describing a cell structure.[44] A cell is a very complex system that is composed of various structurally and also mechanically distinct elements.[45] A cell can be briefly described as a nucleus surrounded by a cytoplasm. A barrier between cell's interior and exterior is a cell membrane, which consists of the lipid bilayer. Its function mainly lies in protection of the cell from many external (mechanical, chemical, biological) factors.[46] Cell membrane is a two-dimensional phospholipid structure which is permeable mainly for water and small non-polar molecules such as CO_2 or O_2.[47,48] There are various molecules like proteins or other lipids that are embedded in the cell membrane. They are able to create channels responsible for transport of nutritive, metabolites or ions.[49] A significant component of the cell membrane is cholesterol, which increases the stability of the membrane.[50,51] The cytoplasm of the cell is composed of both liquid and solid phases. Liquid phase contains mainly water molecules, ions, enzymes, etc. Solid phase encompasses various organelles such as mitochondria, endoplasmic reticula, and the cytoskeleton.[45] The latter one serves as a scaffold for cellular organelles, however, studies gathered till now, point out its regulating role by governing organelles' organization, and thus, determining behavior of the cells.[52–54]

A cytoskeleton is a main structure that is responsible for a cellular shape and mechanical resistance. It actively participates in bending, stretching or creeping of the cell what is its response to various internal or external stimuli and conditions. The cytoskeleton is composed of three main fibrous elements (**Figure 5**):

- intermediate filaments,
- microtubules, and
- actin filaments.

[†] The formation of a break on the skin or on the surface of an organ. An ulcer forms when the surface cells die and are cast off. Ulcers may be associated with cancer and other diseases.

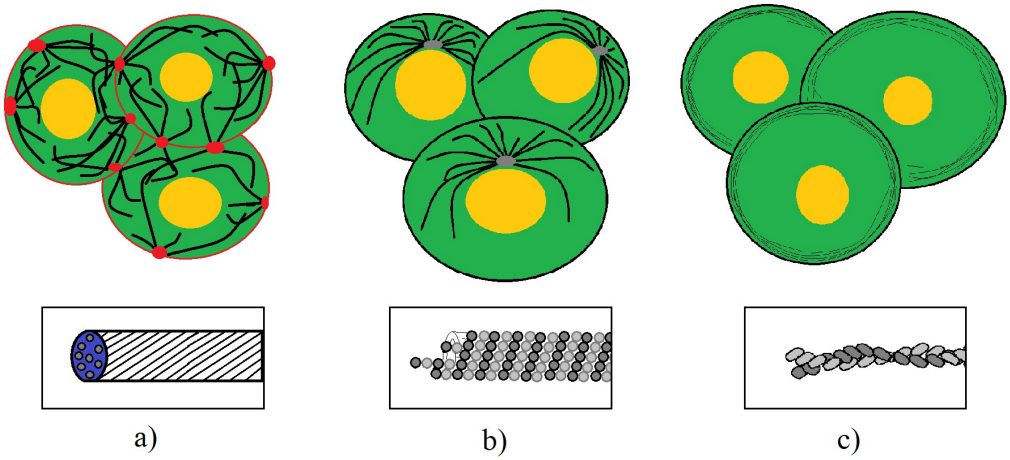

Figure 5. Localization of three main filamentous structures of cell cytoskeleton: a) intermediate filaments, b) microtubules, and c) actin fibers (adapted from [Alberts, 2009)].[45]

Intermediate filaments (IF) are the strongest and the most resistant filaments **(Figure 5a)**. Their structure is created by individual fibers of about 10 nm in diameter, which resembles a rope composed of many thin and long fibers, twisted around each other. Intermediate filaments are present in the cytoplasm of most animal cells. Usually, they form a network spanning over a whole cell body. They are densely packed around a cell nucleus. Such dense packing decreases for filaments located within a region of cell membrane. IF are also present in nuclear lamina which is attached to the cell nuclei and creates the reinforcement for them. The main role of intermediate filaments is to provide mechanical resistance towards tension or stretching. They help to distribute the forces over a cell body.[45]

Microtubules are long, empty inside and very dynamic tubes, which have a capacity to disassembly in one place and assembly in the other **(Figure 5b)**. They are built of two globular proteins: α-tubulin and β-tubulin and keep the cells' shape. In the typical animal's cell, microtubules grow out from centrosomes, which are placed near the nucleus. In the assembly process, they create the unidirectional trails, from the centrosomes toward the cell membrane, along which the organelles or other cell's elements can move.[45]

Actin filaments, the third type of cytoskeletal building element, are present in all eukaryotic cells. An individual filament is composed of α and β monomers of actin that are organized into a fibrous filament composed of polymerized actin (i.e. F-actin), twisted around filament main axis. A diameter of the single filament is around 7 nm. A bundle of actin fibers, called a stress fiber, is an assembly of individual actin filaments. There are two forms of their organization, they create either bundles (stress fibers) or nets composed of short, thin filaments **(Figure 5c)**. The latter one is localized just beneath the cell membrane while stress fibers can span over a whole cell body. It is widely accepted that actin filaments are responsible for mechanical properties of cells.

In the tissue, cells can adhere to each other. This is realized by specific types of molecules called cell-adhesion molecules (CAM). These molecules are often clustered into specialized junctions. Cells can also adhere indirectly through extracellular matrix proteins. Independently of the interaction type, such cellular connections would introduce additional

components in maintaining mechanical strength. Several types of cell-cell contacts (so called cell-cell junctions) can be distinguished:

- tight junctions whose function is to prevent the diffusion of various substances present in the extracellular space between cells,
- gap junctions that allow for the rapid diffusion of small molecules and ions through small channels,
- adherens junctions connecting membranes of the adjacent cell to another cell via bunches of actin fibers,
- desmosomes that are like contact points between cells linked with bunches of intermediate fibers,
- hemidesmosomes being junctions of epithelial cells with the basement membrane, anchoring cells to the underlying ECM.

All abovementioned types of junctions are critical for maintaining the integrity of the epithelium. Simultaneously, they transmit mechanical forces in both directions, i.e. inside and outside of the cells. Transferred force can significantly influence the global mechanical properties of the cell.[45]

2.5. Aim of the thesis

The main goals of the presented thesis were to elaborate how mechanical properties of skin cells change in response to the presence of neighboring cells, in phenomena leading to disruption of basal membrane integrity. Therefore, both wound healing and cancer (melanoma) cells' dissemination were studied for three chosen types of the skin cells (keratinocytes, fibroblasts, and melanoma cells from radial growth phase). The biochemical and biomolecular profile characteristics of these processes are relatively well-known. However, the knowledge how mechanics influences the process of cell migration or what is the effect of neighboring cells on deformability of single cells is still not well elaborated. Alterations in biomechanical properties of cellular mixtures have not been investigated much before, even though it is known that cells interact with each other. Moreover, majority of studies in cell mechanics realized by AFM have been carried out on single isolated cells, thus, changes in deformability resulting from the direct cellular interaction have not been quantified yet. Therefore, the main questions to be answered here were:

- how the mechanical properties of skin cells change in the studied specific processes, i.e. during wound healing and initial stages of cancer dissemination,
- how the mechanical properties of individual cells depend on the type of neighboring cells,
- in which pair of cells, the mechanical-based interaction is the strongest one.

To realize thesis objectives, the experiments were designed as follows. Studies were carried out for three types of skin cells, namely, fibroblasts, keratinocytes and melanoma cells. The interaction between fibroblasts and keratinocytes is a basic interaction in wound healing

process while melanoma cells during spreading to distant locations involve themselves in the interactions with both fibroblast and keratinocytes. Specific tasks of the studies were:

- to optimize the culture conditions for cells growth in cellular mixtures,
- to characterize mechanical properties of all studied cell types (single cells and clusters),
- to characterize mechanical properties of cellular mixtures (single cell and clusters).

Mechanical properties were investigated for cellular mixtures composed of two cell types **(Figure 6)**.

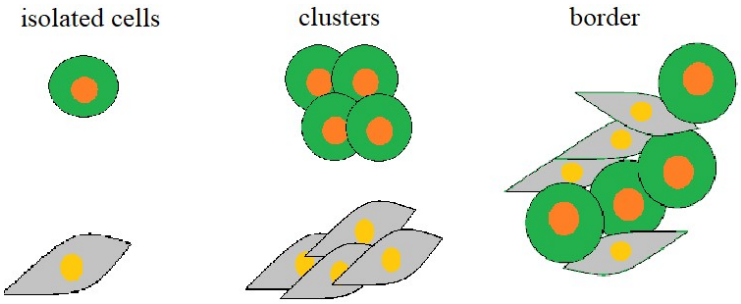

Figure 6. Graphical representation of AFM-based elasticity measurements for cellular mixtures.

Thus, for each particular pair of cells, measurements were carried out for each cell type separately (referred here as **single cells**), for each single cell type embedded within a cluster of 5-10 cells separately (referred here as **cell clusters**), and for cells being in the direct contact with each other (referred here as **border cells**). Measurements were conducted on individual cells and on single cells embedded within clusters of 5–10 cells as mechanical properties of single cells and cells in clusters are different.[55] Chosen cellular mixtures were fibroblasts/keratinocytes, fibroblasts/melanoma cells, and keratinocytes/melanoma cells.

3. Materials

3.1. Cell cultures

The cells lines, used in the experiments, were derived from human healthy skin (fibroblasts and keratinocytes) and from melanoma at the radial phase of the growth (RGP, radial growth phase). All chosen cells lines are commercially available and have been in use for many years at the Department of Biophysical Microstructures (NZ55) at the Institute of Nuclear Physics in Cracow (Poland). All cells were grown in an appropriate culture medium, in culture flasks (Saarstedt) at 37°C in 98% air/5% CO_2 atmosphere, in the CO_2 incubator (Nuaire). For AFM and fluorescent microscopies, cells were moved from the culture flasks onto circular coverslips (with a diameter of 2.5 cm).

3.1.1. Keratinocytes

Keratinocytes (HaCaT cells, a kind of gift of Dr Tomasz Kobiela, Warsaw University of Technology, Poland) are *in vitro* spontaneously transformed keratinocytes from histologically normal skin. They are derived from human epidermis. HaCaT cell line was cultured in Eagle's Minimum Essential Medium (EMEM, LGC Standards), supplemented with 10% heat-inactivated fetal bovine serum (FBS, Sigma-Aldrich), 1% HEPES (Sigma). Keratinocytes are round cells with the spherical nucleus located in the center of their body.

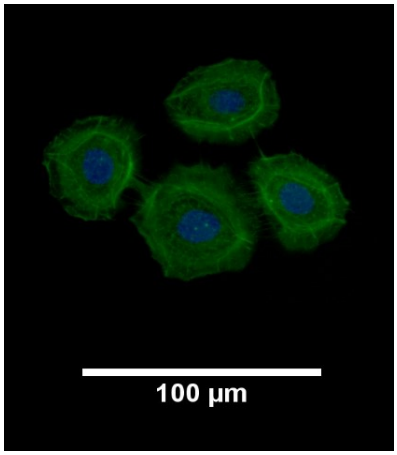

Figure 7. Fluorescent image of keratinocytes. Green denotes F-actin labeled with phalloidin–Alexa Fluor 488 dye, blue – cell nucleus stained with Hoechst.

The organization of actin filaments in keratinocytes is shown in **Figure 7**. They are located at a periphery of the cell's body, usually forming a ring-like structure around the cell nucleus. The main roles of keratinocytes are forming the protection barrier against many pathogens (fungi, bacteria, viruses), heat, UV radiation or water loose.[6] After the injury, keratinocytes are the first cells actively participating within initial stages of wound healing by introducing cytokines in the system.

3.1.2. Fibroblasts – human normal skin cells

Fibroblasts (FB, cell line CCL-110, ATCC, LGC Standards) are cells derived from human dermis. They are large, spindle-shape cells with clearly visible stress fibers composed of F-actin being a polymerized actin form. Stress fibers are usually spanning over a whole cell area (**Figure 8**). Similarly as keratinocytes, fibroblasts were cultured in Eagle's Minimum Essential Medium (EMEM, LGC Standards), supplemented with 10% heat-inactivated fetal bovine serum (FBS, Sigma-Aldrich), 1% HEPES (Sigma).

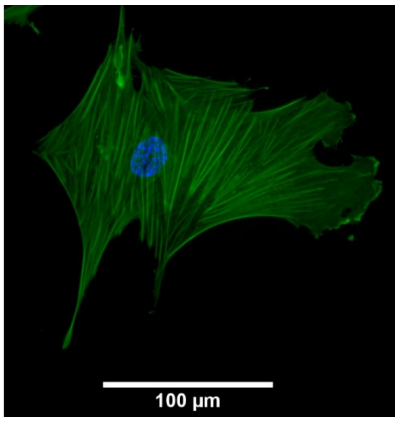

Figure 8. Fluorescent image of a fibroblast. F-actin (actin filaments) are labeled with phalloidin – Alexa Fluor 488 dye (green) while cell nucleus is stained with Hoechst (blue).

The main function of fibroblasts are the synthesis of collagens and other extracellular proteins leading to the formation of extracellular matrix and secretion of various cytokines or growth factors needed during wound healing process.[27,28,56] Fibroblasts play a significant role in epithelial-mesenchymal transition (EMT) stimulating epidermal proliferation and differentiation.[57] Furthermore, they endow the skin resistance against the mechanical stimulus and maintained its integrity.

3.1.3. Malignant melanoma cells (WM35)

Melanoma cells used in this research originating from WM35 cell line representing cells derived from the primary melanoma site of the patient's skin diagnosed with radial growth phase (RGP) melanoma[58]. At this stage of melanoma progression, cells start to move under the basal membrane but not forming metastasis structure. WM35 melanoma cells were cultured in RPMI-1640 (Sigma), supplemented with 10% heat-inactivated fetal bovine serum (FBS, Sigma-Aldrich), 1% HEPES (Sigma).

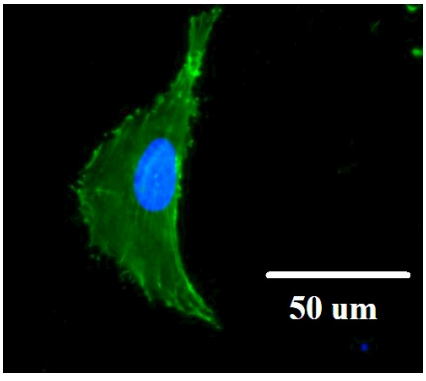

Figure 9. Fluorescent image of melanoma cells (WM35). Green – F-actin labeled with phalloidin – Alexa Fluor 488 dye, blue – cell nucleus stained with Hoechst.

WM35 melanoma cells (**Figure 9**) are characterized by a spindle-like shape with a large centralized cell nucleus. Actin filaments forming a cortex layer are visible, however, it is poorly developed.

3.2. Optimization of culture conditions for cellular mixtures.

In standard conditions, provided by ATCC, cell culturing is carried out at given conditions, in particular, in a culture medium specific for a given cell line. The culture media, advised by ATCC, for:

- CCL-110 fibroblasts is Eagle's Minimum Essential Medium (EMEM),
- HaCaT cells is Eagle's Minimum Essential Medium (EMEM),
- WM35 melanoma cells is RPMI 1640 developed at Roswell Park Memorial Institute in 1966 by Moore and his co-workers.[59]

Culture media differs in their composition (see **Annex 1**). To maintain the co-cultures composed of cells requiring two different media, an optimization of culture conditions is required. Here, the optimization of growth conditions started from cultures of each cell line separately in three types of culture media, referred here as *DERMAL*, *EMEM*, and *RPMI 1640.* The culture medium that resembles a rich environment of the skin is *DERMAL*, while EMEM is the common widely applied medium for culturing of various cells, including fibroblasts. In the presented studies, due to culture media cost and high sensitivity of fibroblasts to altered environment, culture conditions were optimized towards the use of EMEM as a culture medium to grow all predicted combinations of cellular mixtures. In the first step of the optimization, viability of cells in given culture conditions was verified using MTT assay applied towards the determination of a doubling time (details are presented in the section ***Methods***). A comparison of doubling time obtained for all studied combinations is presented in **Figure 10**.

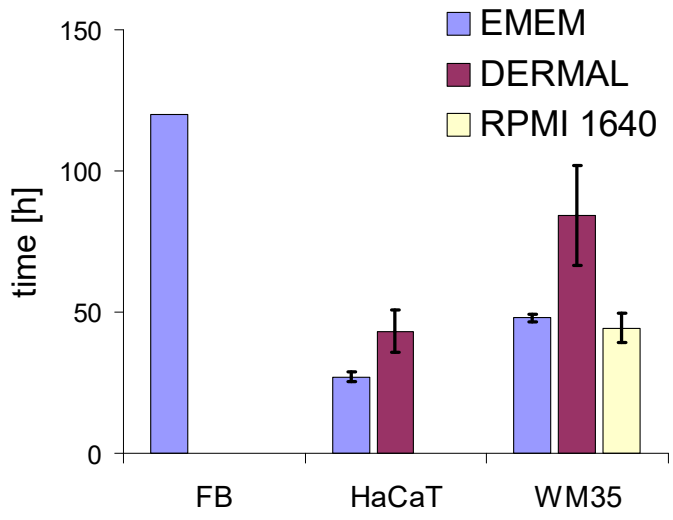

Figure 10. Doubling time calculated basing on results of MTT assay performed for keratinocytes cultured in EMEM and DERMAL, and melanoma cells cultured in EMEM, DERMAL and RPMI 1640. Doubling time for fibroblasts was set to 120 h[7].

Results from MTT show that all studied cell lines can be cultured in chosen culture media. However, their growth rate is related to the composition of medium. Lower doubling time denotes faster cell proliferation. Thus, the MTT results show that the best culture conditions for HaCaT and WM35 melanoma cells were provided by *EMEM*. The determined doubling time was 35.3 ± 2.3 h and 53.3 ± 5.5 h, respectively. Rich *DERMAL* medium in both cases increased the rate of cell division to 43.2 ± 7.4 h and 84.3 ± 17.6 h for HaCaT and WM35 melanoma cells, correspondingly. The other parameter that should be taken into account is elasticity of cells. It is known that culture medium composition influences mechanical properties of cells[60]. Thus, elasticity of cells cultured in *DERMAL*, *EMEM* and *RPMI 1640* was determined for single cells and cells in clusters according to methodology presented in the ***section 2.5***.

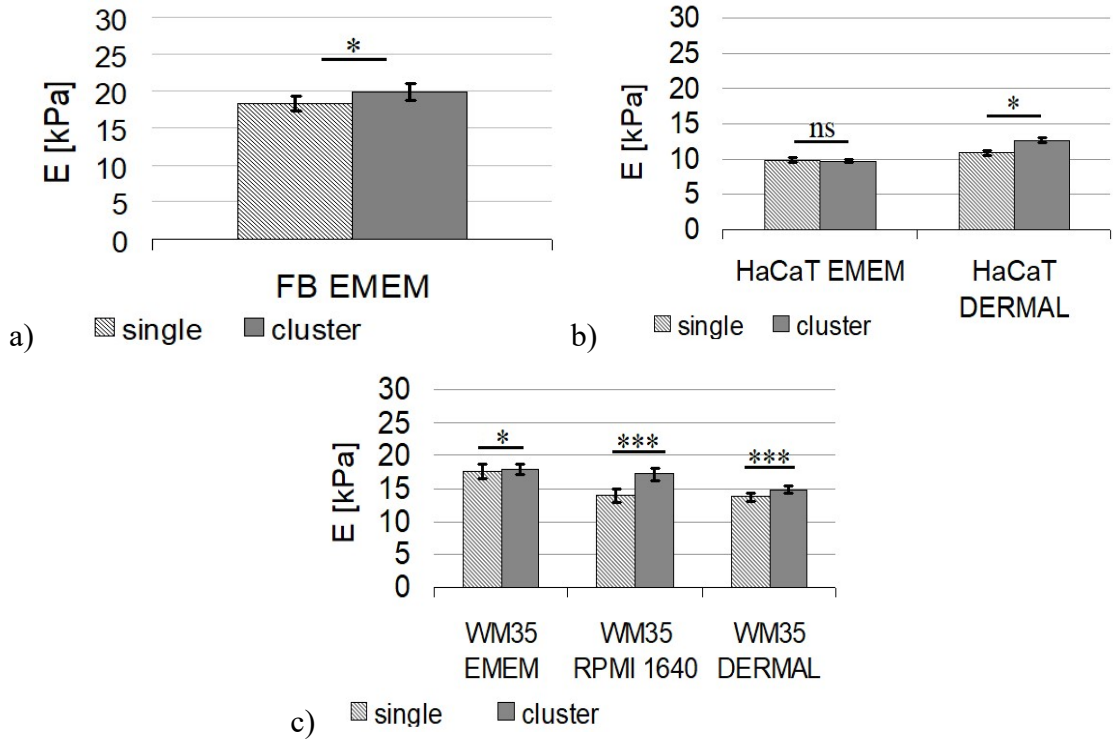

*Figure 11. Alterations in elasticity of (a) fibroblasts cultured in EMEM, (b) keratinocytes grown in DERMAL and EMEM media and, (c) WM35 cells cultured in EMEM, DERMAL and RPMI 1640 media. Elasticity of single cells and cells embedded in clusters of 5-10 cells is compared. All statistical tests were two-sided and p values of < 0.05 were considered statistically significant. The statistical significance is shown as asterisks: ***p < 0.001; **p < 0.01; *p < 0.1; ns – not statistically different.*

Fibroblasts were cultured only in *EMEM* conditions and only the difference between elastic properties of single cells and of cell clusters was evaluated (**Figure 11a**). Elastic modulus for single cells is 18.0 ± 1.0 kPa and for cell clusters - 19.8 ± 1.2 kPa. Keratinocytes (**Figure 11b**) cultured in *EMEM* medium do not change their mechanical properties depending on the cell neighborhood. Elastic modulus for single cells is 9.7 ± 0.3 kPa and for cell clusters - 9.9 ± 0.3 kPa. These cells alter their deformability when cultured in *DERMAL*.

Cells grown in clusters have become more rigid as single cells (12.6 ± 0.4 kPa and 10.9 ± 0.4 kPa, respectively, ***p < 0.001). WM35 melanoma cells (**Figure 11c**) are previsedto be cultured in RPMI 1640 medium. In this medium, elastic modulus for single cells is 13.9 ± 1.1 kPa while modulus for cell clusters is 17.0 ± 1.0 kPa. Cells become stiffer. Cells cultured in other conditions, i.e. in *DERMAL* or *EMEM*, show distinct level of cellular deformability. In *DERMAL* medium, elastic modulus slightly increases to 14.8 ± 0.6 kPa for single cells and decreases to 13.7 ± 0.7 kPa for cell clusters as compared to values obtained for cells grown in RMPI 1640 conditions. Once culture medium was changed to *EMEM*, deformability of melanoma cells decreased to c.a. 17 kPa and it remained constant for both single cells and cell clusters (17.6 ± 1.1 kPa and 17.9 ± 0.8 kPa, respectively).
To evaluate the influence of neighboring cells on single cell deformability, EMEM culture medium was chosen since it allows for minimization of the effect of neighboring cells on measured elasticity of cells. In this medium, elastic modulus for fibroblasts, keratinocytes and WM35 melanoma cells, remained at the same level independently of the presence or absence of neighboring cells of the same type. Thus, any further observed alterations in cellular mixtures can be directly referred to the effect of cellular neighbors of different type.

3.2.1. Cellular mixtures

To prepare a cell co-culture, two separate suspensions of cells were mixed together as schematically shown in **Figure 12.**

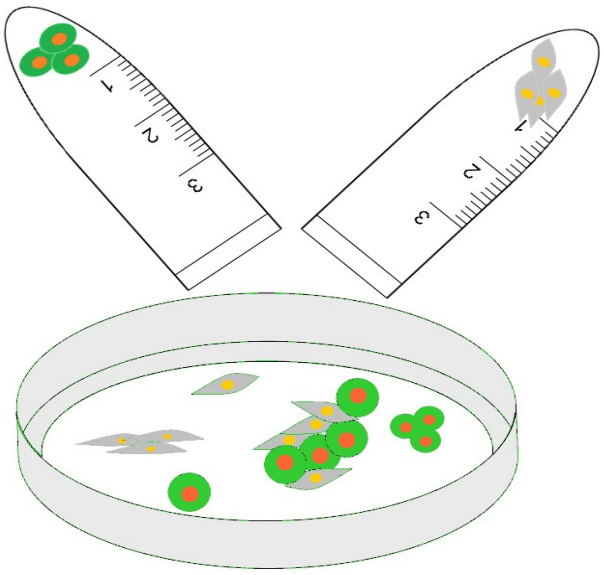

Figure 12. The idea of co-culture preparation. Two suspensions of cells to be studied were mixed together and placed on a surface of a glass coverslip immersed in the Petri dish, in optimized culture medium. Then, a mixture of cells was cultured in CO_2 incubator for a given time.

The concentration of cells in the suspensions were fixed for each single experiment. After mixing, cells were placed on a glass coverslip immersed in the Petri dish and then cultured for two chosen periods of time, typically for 24 and 48 hours. All cells in co-cultures were grown in an optimized medium i.e. EMEM at 37°C in 98% air/5% CO_2 atmosphere, in the

incubator (Nuaire). Additionally, as control samples, both cell types were cultured separately in the analogous conditions. For AFM and fluorescent microscopies, cells were moved from culture flasks to circular coverslips (with diameter of 2.5 cm). The following pairs of cells were mixed and cultured together:

- fibroblasts (CCL-110)/keratinocytes (HaCaT),
- fibroblasts (CCL-110)/melanoma cells (RGP WM35),
- keratinocytes (HaCaT)/melanoma cells (RGP WM35).

3.2.2. Summarizing cell cultures and media

Table 1 presents the summary of the cell cultures carried out within the presented thesis. It shows cell type, conditions (mono- or co-cultures) and culture media used during the experiment.

Table 1. Summary of cell cultures and conditions.

monoculture or *co-culture* / culture medium	FB	HaCaT	WM35	*FB & HaCaT*	*FB & WM35*	*WM35 & HaCaT*
EMEM	+	+	+	+	+	+
DERMAL	-	+	+	-	-	+
RPMI 1640	-	-	+	-	-	-

3.3. Sample preparation for AFM measurements

AFM measurements were carried out for cells cultured on glass coverslips. Initially, cells were seeded on a glass coverslip and placed in the Petri dish (Sarstedt) filled with the corresponding culture medium **(Table 1)** up to 2 ml of the volume, and cultured for 24 or 48 hours. Before each measurement, a coverslip with cells was moved into AFM liquid chamber filled with a fresh medium and placed on the AFM scanner.

3.4. Sample preparation to fluorescence imaging

Regardless of the fact whether cell cultures contained one type of specific cells or a mixture of cells, an analogous protocol for F-actin and cell nucleus staining was applied. Briefly, cells grown on coverslips were incubated with 3.7% paraformaldehyde solution for 20 minutes. Then, coverslips with cells were rinsed twice with the phosphate-buffered saline (PBS, Sigma) for 2 minutes. After rinsing, a cold solution of 0.2% Triton X-100 was added

for 4 minutes, and followed by washing coverslips with the PBS buffer for 2 minutes. Next, cells were incubated with phalloidin conjugated with 1:200 solution Alexa Fluor 488 dye (Invitrogen) for 30 minutes, and sub subsequently staining of cell nuclei with 1:5000 solution Hoechst dye (Sigma) for 14 minutes was performed.

3.5. Cytochalasin D treatment

Depolymerization of actin filaments was carried out by incubating cells with cytochalasin D (Sigma), an agent depolymerizing F-actin. Fibroblasts were incubated with 1μM cytochalasin D solution for 10 minutes whereas keratinocytes were treated with 7.8 μM cytochalasin D solution for 14 hours. Next, the cells were washed with PBS, and placed into AFM liquid chamber filled with a fresh culture medium (EMEM) and AFM measurements of cell elasticity properties were carried out.

3.6. MTT assay

Cells were cultured in multi-well plate (24 wells) in 1 ml of the corresponding culture medium (**Table 1)**. Next, viability of cells was verified using MTT assay (Sigma). Briefly, 100 μl of 3-(4,5-dimethylthiazol-2-yl)-2,5-diphenyltetrazolium bromide was added to the cells in culture medium. Then, cells were incubated at 37°C in 98% air/5% CO_2 atmosphere, in the incubator (Nuaire) for 4 hours. The MTT converts into formazan crystal which is later dissolved in dimethylsulfoxide (DMSO). Final volume of 2 ml was pipetted to a 96-well plate of 200 μl on one hole. The absorbance was determined in 96-well three times for each time spot of 24 h, 48 h, and 72 h.

3.7. Summary

In most cases, AFM-based elasticity measurements do not require any special sample preparation if single, isolated cells are studied and cell cultures conventional protocols are used. However, here, these protocols had to be optimized for measurements carried out on living cells grown as cellular mixtures. To minimize the effect of culture medium composition on cellular deformability, all chosen skin cell lines (fibroblasts, keratinocytes and melanoma cells) were cultured in three types of media. Consequently, it was possible to choose such culture conditions, in which deformability of all studied cells was not affected by medium composition regardless whether they were measured as single cells or cell clusters.

4. Methods

4.1. Cell viability assay

Viability and doubling time of cells were verified using the MTT colorimetric assay (Sigma) according to a protocol described in ***section 3.6***. Briefly, 3-(4,5-dimethylthiazol-2-yl)-2,5-diphenyltetrazolium bromide (MTT) added to cells in culture conditions is reduced by metabolically active cells. Particularly, by the action of dehydrogenase enzymes leading to the formation of formazan crystals.[61] Chemical reaction is as follows:

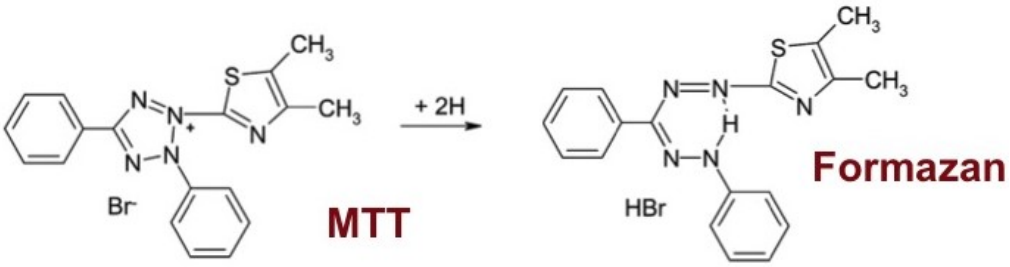

The amount of adsorbed light is mainly dependent on the concentration of substance in the solution, extinction coefficient of the substance, length of the path that the light travels by passing through the sample conditioned by the width of the measuring cuvette. According to the Lambert-Beer law:

$$A = k \cdot c \cdot l$$

where A is the absorbance, k is the radiation absorption coefficient, c is the substance concentration in solution, l is the thickness of the absorbing layer (the path through which the radiation passes through the solution). Intensity of transmitted light, after the radiation passed through the probe, decreases exponentially if each of the three factors increase.[62] The absorbance is, therefore, directly proportional to the concentration of the substance in solution at a given wavelength. Here, formazan concentration was verified using ELISA reader (BMG LABTECH) at 570 nm **(Figure 13)**.

Figure 13. SPECTROstar Nano - spectrophotometer for the ELISA method working at the IFJ PAN.

In solutions with suspended cells, absorbance corresponds to the number of alive cells. Thus, a plot of absorbance versus culture time can be created and fitted with the exponential function[63]:

$$y(t) = y_0 e^{kt}$$

where:
$y(t)$ – optical density at 570 nm at time point t,
y_0 – optical density at $t = 0$ *hour*,
k – growth constant,
t – time [*hour*].

From the fit, doubling time (t_d) can be derived as follows:

$$t_d = \frac{\ln 2}{k}$$

where k denotes the growth constant.

4.2. Atomic Force Microscope (AFM)

Atomic force microscope (AFM) is a tool widely applied to quantify mechanical properties of living cells as it provides high resolution images and a possibility to measure in liquid conditions mimicking the native ones. A scheme of the AFM is presented in **Figure 14a.** There are three main elements of the AFM system:

(1) AFM probe with a tip mounted at the free end of the cantilever,
(2) optical-based system used to detect cantilever deflection,
(3) piezoelectric system used to scan and move.

AFM probes are a central part of the system. They are usually made of silicon nitride (Si_3N_4) by applying photolithographic methods.[64] The tip is usually a four-sided pyramid, which height varies from 2 to 3 microns (**Figure 14b**). It is mounted at the free end of the cantilever being a flat, rectangular or triangular spring. Each cantilever is characterized by two parameters, spring constant and radius of curvature of the tip and/or open angle of the probing pyramid. Cantilevers, used in the presented experiments, had spring constant of 0.03 N/m, radius of curvature of 40 nm, and open angle of 36°.
Deflection of the cantilever is recorded by an optical system composed of a laser beam and position sensitive photodetector (often called *a photodiode*). Active area of the photodetector is divided into four quadrants, which allow to measure deflections in parallel and perpendicular direction to the investigated surface. Laser beam is focused on the back side of the free cantilever end and it is reflected into photodetector. When cantilever is far away from the surface, laser beam is focused in that manner that signals from all four quadrants are equal. Thus, the differences between two upper (or two right) and two lower (or two left) quadrants are zero. Force acting within a contact area induces cantilever deflection in perpendicular direction to the surface what results in the shift of the laser between two upper

and lower quadrants. The difference is proportional to the magnitude of force acting between the probing tip and the sample surface.

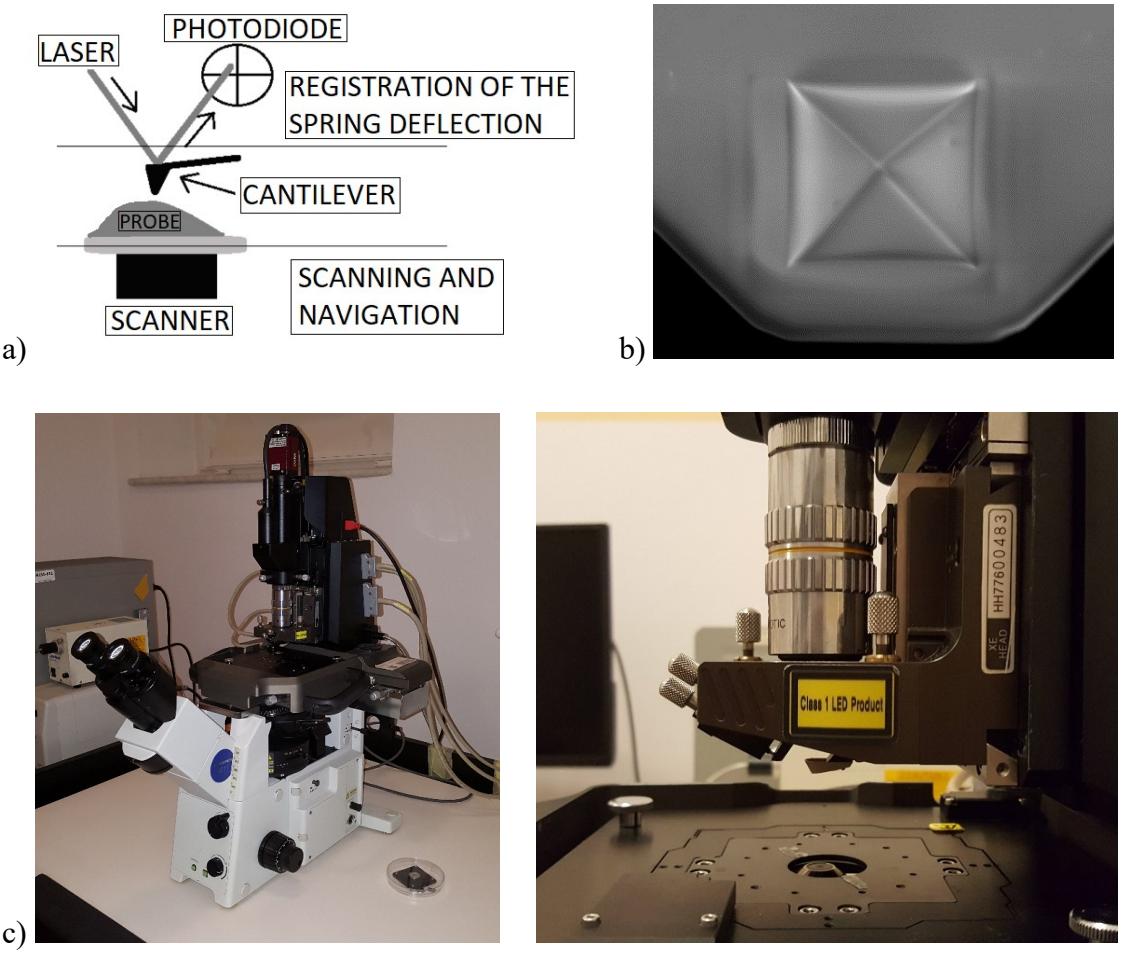

Figure 14. a) scheme of the AFM, b) SEM image of the AFM tip (PNP TR-B) – photo by Piotr Bobrowski, and c) photos of the AFM (Xe 120 Park Systems) working at the IFJ PAN.

Cantilever deflection (*deflection*) is converted into force (F) by multiplying the recorded signal by two factors, namely, cantilever spring constant and sensitivity of the photodetector according to the following equation:

$$F\,[nN] = deflection\,[V] \cdot k\,[\frac{N}{m}] \cdot PSD\,[\frac{nN}{V}]$$

where k is the cantilever spring constant and PDS denotes the photodetector sensitivity converting volts into nanometers. Scanning and sample movements are usually realized by piezoelectric elements operating basing on the inverted piezoelectric effect.[65]

4.3. Force curves

Elastic properties of studied samples are determined basing on measurements requiring AFM working in a force spectroscopy mode.[66]

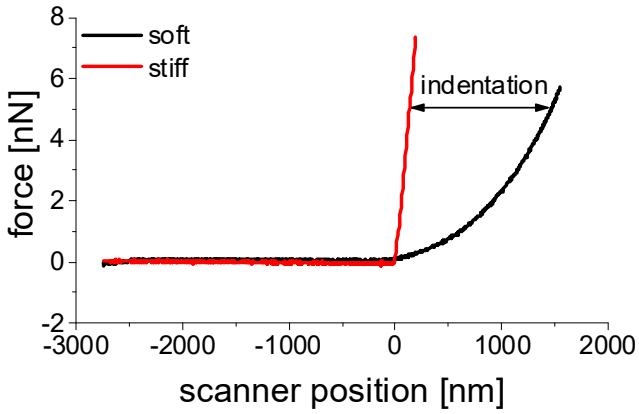

Figure 15. Comparison of the approach parts of force curves recorded on soft (a cell, i.e. an exemplary keratinocyte) and stiff (glass) surfaces.

Figure 15 presents a comparison of approach parts of two force curves recorded on a stiff, non-deformable glass surface and on an exemplary keratinocyte. The red curve shows two regions, a horizontal and a slopped ones. The first shows that deflection of the cantilever oscillates around a constant value (zero) indicating that interaction forces can be neglected. A slopped part corresponds to a displacement of the piezoelectric scanner. When a probing tip touches the surface of a non-deformable sample the forces start to push into the probing surface and the relation between scanner position and applied forces is linear. In most measurements of biological samples with AFM, force curves collected on glass, silicon or Petri dish surfaces reveal characteristics of non-deformable surfaces, thus, they can be used as calibration curves. In case of compliant materials, a cantilever deflection is usually much smaller due to indenting the sample. The relation between scanner/sample position and load force becomes nonlinear and characteristic for a material with given mechanical properties. Exemplary approach parts of force curves recorded for each studied cell type are shown in **Figure 16**.

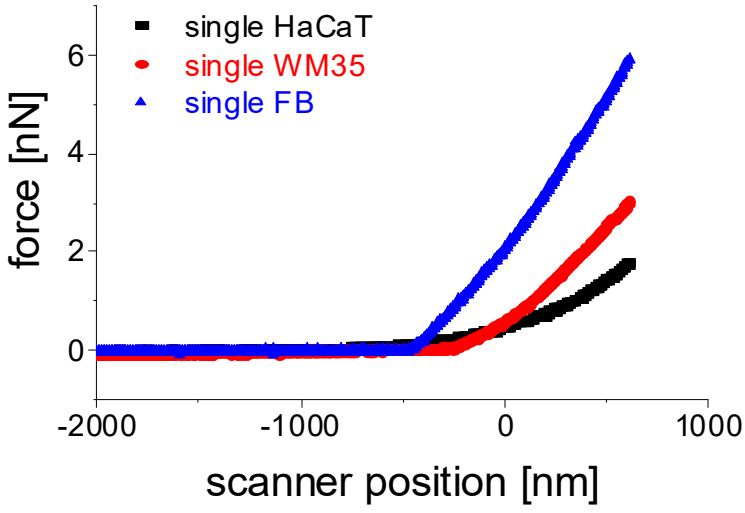

Figure 16. Approach parts of exemplary force curves recorded for single fibroblast (blue curve, keratinocyte (black curve) and melanoma cell (red curve).

The force-indentation curve is a result of the subtraction of two curves. A calibration force curve (recorded on a stiff non-deformable surface) is subtracted from a force curve recorded on a measured cell (**Figure 15)**.

4.4. Young's Modulus determination

Young's modulus describes elastic properties of a material. It is usually derived by fitting an appropriate model of contact mechanics to a relation between a load force and indentation. In the AFM domain, typically, Young's modulus is calculated basing on the Hertz contact mechanics with Sneddon's modifications. Initially, Hertz model described a deformation of two purely elastic spheres.[67] The model can be extended into a case of a sphere indenting an ideally elastic, isotropic half-space. In 1965, Sneddon delivered equations that take into account the shape of asymmetrical indenters.[68] Two of them are commonly used in the AFM to estimate the shape of four-sided pyramid, i.e. a cone and paraboloid. Thus, the relations between load force (F) and the resulting indentations (Δz) are:

$$F = \frac{2 \cdot \tan\alpha \cdot E` \cdot (\Delta z)^2}{\pi} \text{ (cone)}$$

and

$$F = \frac{4 \cdot \sqrt{R} \cdot E` \cdot (\Delta z)^{\frac{3}{2}}}{\pi} \text{ (paraboloid)}$$

where E' denotes the reduced Young's modulus:

$$\frac{1}{E`} = \frac{1 - \mu_{tip}^2}{E_{tip}} + \frac{1 - \mu_{sample}^2}{E_{sample}}$$

where E_{tip} and E_{sample} are the Young's modulus of the AFM tip and sample, respectively. The Poisson's ratio (μ) describes the way of deformation of a probed material which tends to expand in the perpendicular direction to the compressions directions.[69] It ranges between 0 and 0.5. For silicon nitride $\mu = 0.28 \pm 0.05$ [70] while for living cells it is frequently set to 0.5 (as for incompressible materials). Data presented within the thesis, were analyzed assuming that four-sided pyramid can be approximated as a paraboloid. The decision was taken basing on χ^2 value denoting the goodness of the fit.

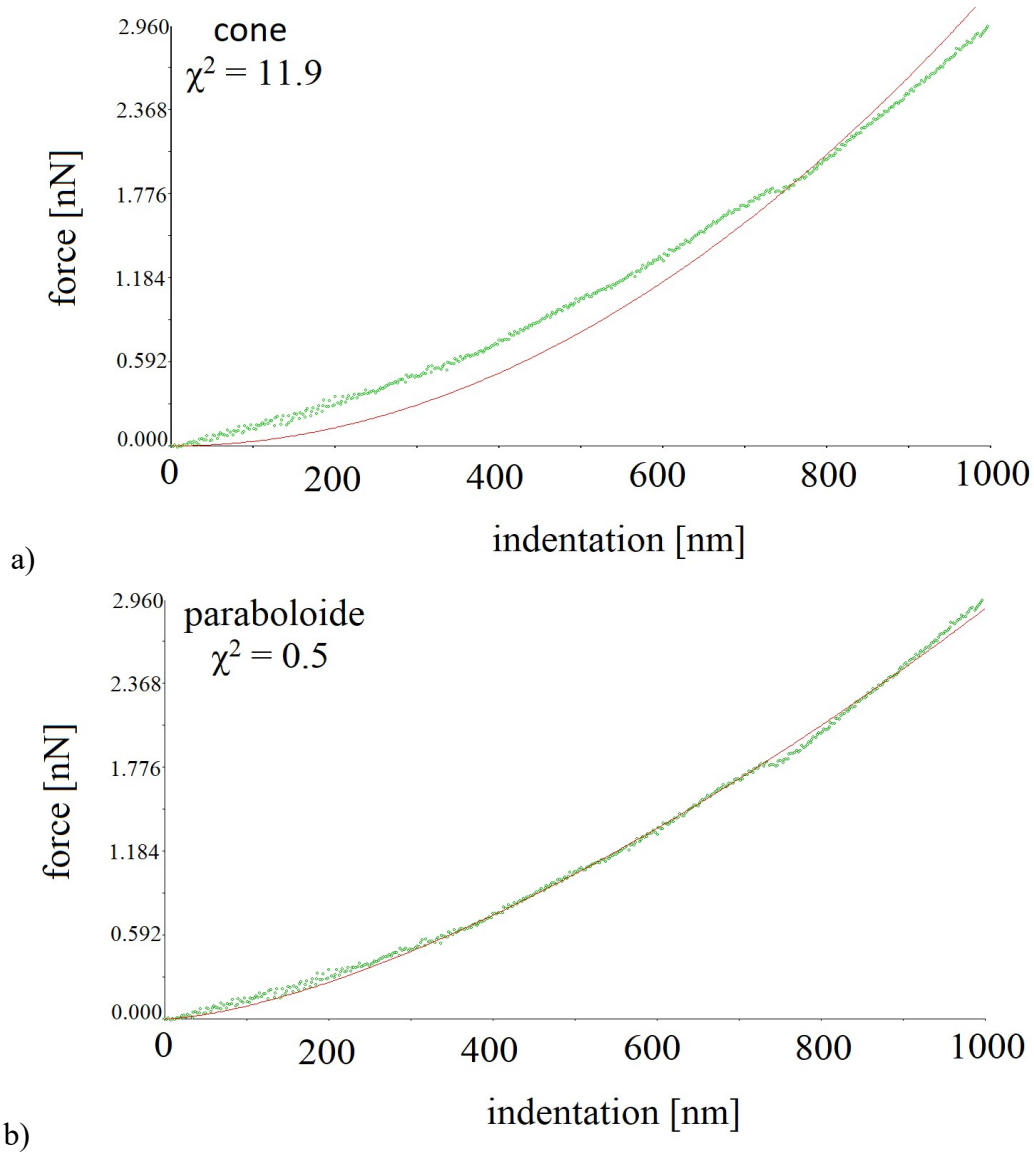

Figure 17. Exemplary fits obtained for a force-indentation curve recorded for a single fibroblast. Hertz model was fitted assuming that indenting AFM probe can be modelled as a cone (a) and paraboloid (b).

Figure 17 shows an exemplary force indentation curve fitted with two equations describing either conical or paraboloidal approximations of the indenting AFM tip. The calculated value of χ^2, denoting the goodness of the fit, was smaller for paraboloidal approximation (0.5) as compared to the conical one (11.9). Thus, for further data analysis, a model assuming paraboloidal shape of the AFM tip was chosen.

4.5. Young's moduli distributions – elastic modulus of cell populations.

In this section, a discussion how to calculate the final Young's modulus for a given cell population is presented as several approaches can be applied. The easiest way is to calculate an average value, however, on each single cell an elasticity map was recorded. Thus, Young's modulus of each single cell is represented as a mean ± standard deviation (SD). SD can be used to weight each modulus value delivering a ***weighted average*** value.

Another approach is to determine median from all measurements, which is a middle value that divides data into two sets. Most common approaches fit functions describing symmetric (Gauss function) or non-symmetric (Lognormal function) distributions of obtained data histograms.

4.5.1. Weighted average

Weighted average (avw) can be calculated for *n* observations with assigned appropriate weights, not correlated with each other using a formula:

$$avw = \frac{w_1 x_1 + w_2 x_2 + w_3 x_3 + ... + w_n x_n}{w_1 + w_2 + w_3 + ... + w_n}.$$

weighted standard deviation (*SDw*) is defined with formula:

$$SDw = \sqrt{\frac{w_1^2 x_1 + w_2^2 x_2 + w_3^2 x_3 + ... + w_n^2 x_n}{w_1 + w_2 + w_3 + ... + w_n} - awv^2}.$$

In his approach elements with larger weight influence more significantly on the average value.
The final Young's modulus determined using ***weighted average*** applied to collected data, was determined as follows:

a) for each single cell, the mean was calculated,
b) for each mean value, a weight was estimated basing on the number of curves recorded for this particular cell
c) final value of a given cell populations (e.g. single fibroblasts) was determined as a weighted average.

Illustration of this methodology is presented in **Table 4**.

Table 2. Exemplary Young's moduli determined for each cells.

number of cells	*cell name*	*mean [kPa]*	*number of recorded force curves*
1	cell 01	9.25	25
2	cell 02	7.98	15
3	cell 03	8.69	19

The final Young's modulus, determined as a *weighted average (avw)* ± *weighted standard deviation (SDw)*, is:

$$E_{avw} = \frac{9.25 \cdot 25 + 7.98 \cdot 15 + 8.69 \cdot 19}{25 + 15 + 19} \approx 8.75\ kPa,$$

$$E_{SDw} = \sqrt{\frac{9.25^2 \cdot 25 + 7.98^2 \cdot 15 + 8.69^2 \cdot 19}{25 + 15 + 19} - 8.75^2} \approx 0.45\ kPa.$$

4.5.2. Median

Median or the middle value is the value that separates larger half of data from the lower one. To calculate the median from the set of *n* observations, the data must be sorted crescively and numbered from 1 to *n*. When *n* is odd the median is the observation value in the middle (number of this value is determined as $\frac{n+1}{2}$ while for even *n*, the result is the arithmetic mean between two middle observations number $\frac{n}{2}$ and $\frac{n}{2}+1$. For example, for the data included in **Table 4**, the median is 7.98 kPa.

4.5.3. Gaussian distribution

Gauss function describes the symmetric (normal) distribution of data (**Figure 18**). It is defined by the formula:

$$y = y_0 + \frac{A}{w\sqrt{\frac{\pi}{2}}} e^{\frac{-2(x - x_c)^2}{w^2}}$$

where:

A – the area under the curve,

w – $\frac{FWHM}{\sqrt{2 \cdot \ln 2}}$ (*FWHM* denotes full width at half maximum),

x_c – expected value of the distribution, the center of Gauss distribution.

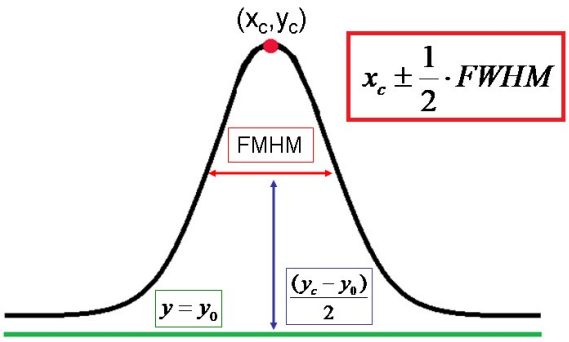

Figure 18. Gauss function. The distribution is described by a set of parameters such as x_c (the center of the distribution) and FWHM (full width at half maximum).

As a result of Gauss function fit to the data distribution, the most probable value can be obtained from a position of the distribution maximum (x_c), which, for normal distributions, corresponds to a mean. Deviation from center of the distribution is calculated as FWHM/2,

which delivers a value of the standard deviation. Examples of histograms are presented in **Figure 19**, obtained for all individual force curves of measured cell lines after 24 hours of culture.

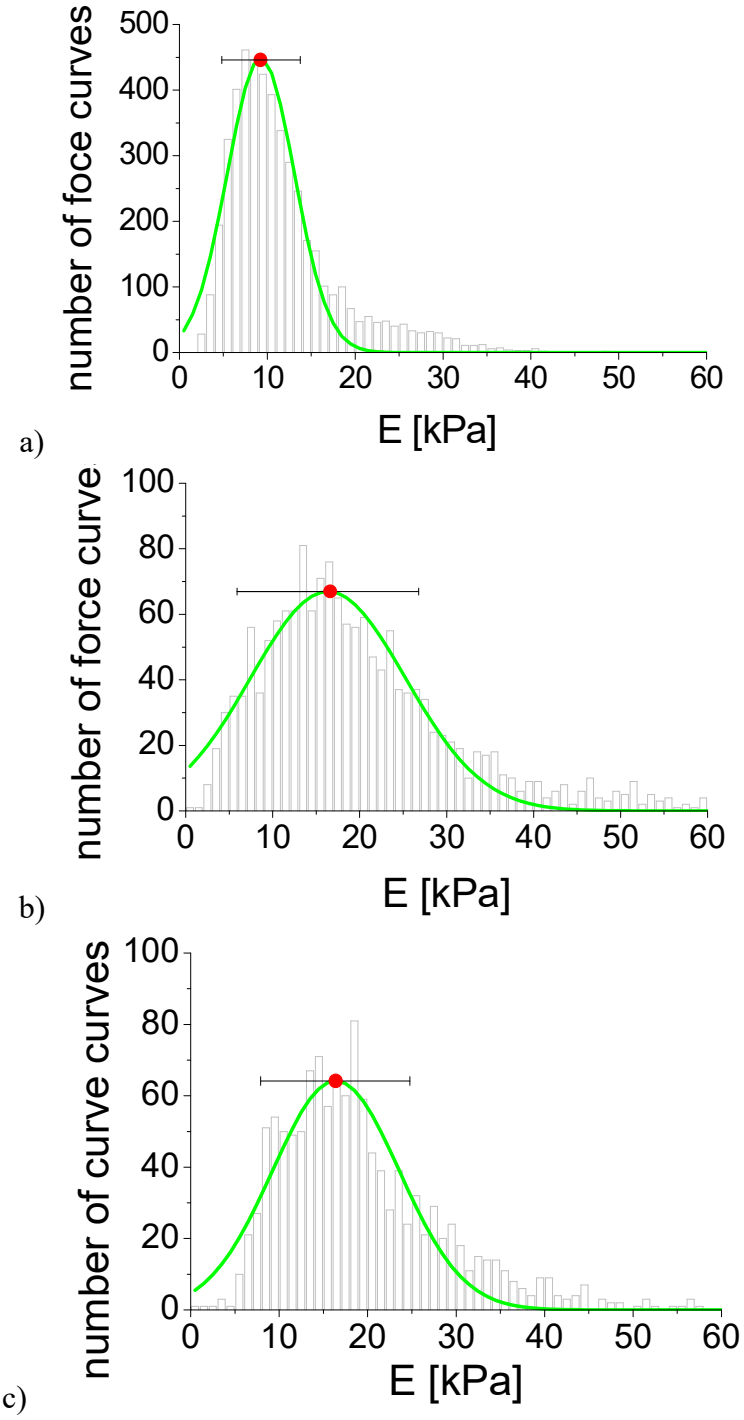

Figure 19. Histograms of Young's moduli determined from the analysis of all recorded force curves for: a) keratinocytes, b) fibroblasts and c) melanoma cells. Data distributions were fitted with Gaussian function (a green line). Red dot denotes the center of the distribution referring to a mean; horizontal line is FWHM corresponding to a standard deviation.

Gauss function can be applied only to data characterized by symmetric distributions (normal distributions). As shown in **Figure 19,** histograms obtained within the presented thesis are

not symmetric. What is more, right-sided tails are characteristic for these distributions, thus, it seems to be reasonable to use the lognormal function.

4.5.4. Lognormal distribution

Lognormal function describes a probability distribution of a random variable whose logarithm is normally distributed (**Figure 20**). The lognormal function is defined by the formula:

$$y = y_0 + \frac{A}{\sqrt{2\pi}wx} e^{\frac{-(\ln(\frac{x}{x_c})^2)}{2w^2}}$$

where:
A – the area under the curve,
w – logarithmic standard deviation,
x_c – expected value of the distribution.

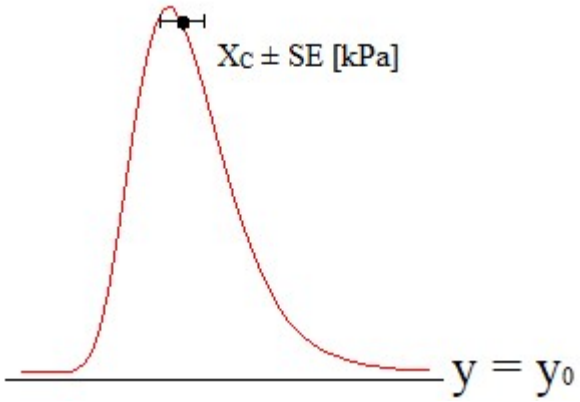

Figure 20. Lognormal function. The distribution can be described by x_c (the center of the distribution) ± SE (standard error).

As an error for lognormal expected value, standard error (SE) can be used. It is defined by the following formula:

$$SE = \frac{SD \cdot 3}{\sqrt{n-1}}$$

where:
SD – standard deviation,
n – probes number.

Figure 21 shows the Young's modulus distribution for all force curves recorded for all studied cells of the same type (analogously as in the case of **Figure 19**, data represent the case of single cells measured, after 24 of culture), i.e. keratinocytes (**Figure 21a**), fibroblasts (**Figure 21b)** and melanoma cells (**Figure 21c).** For all cases, lognormal function delivers a better approximation of the histogram shape.

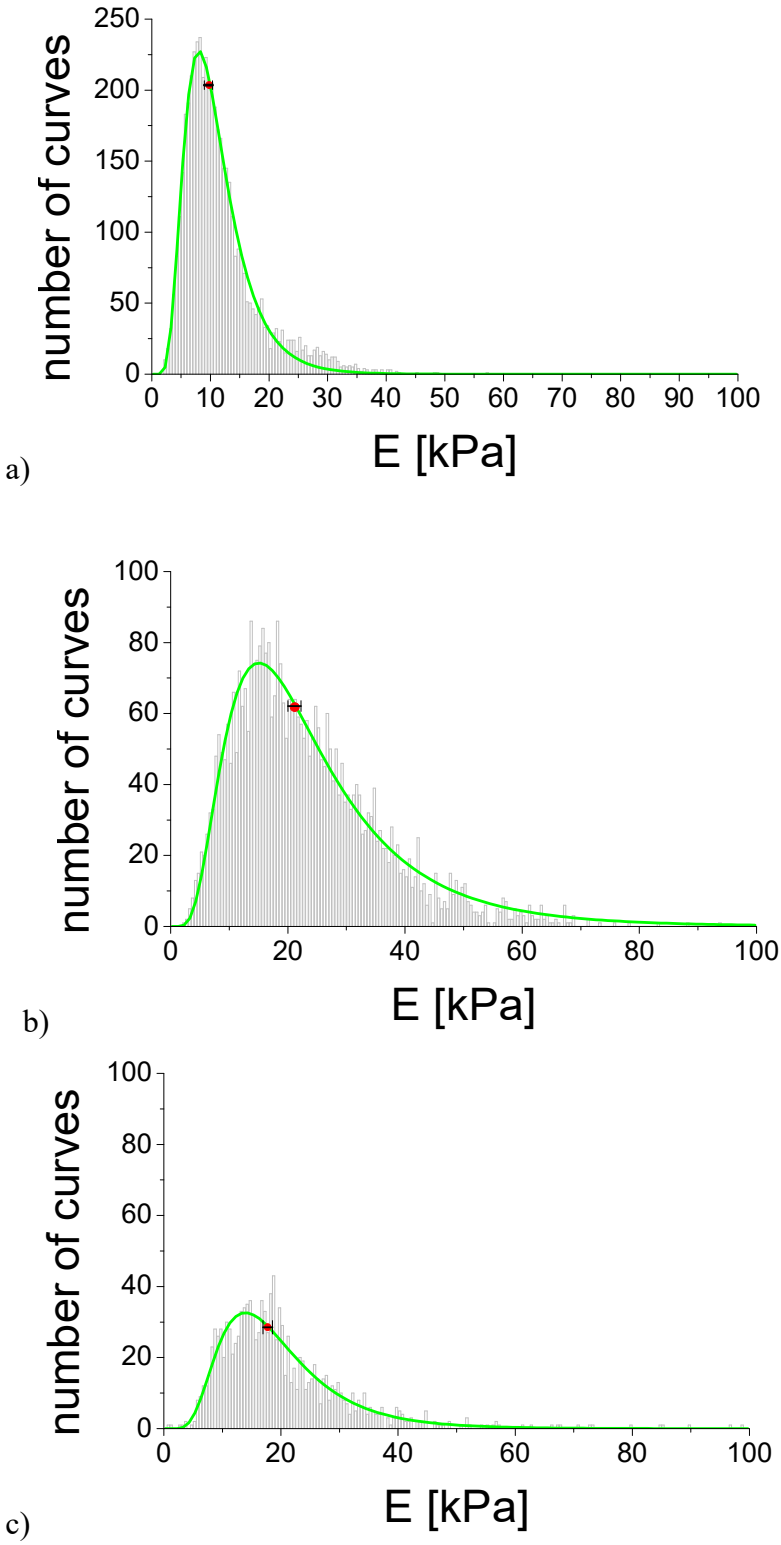

Figure 21. Histograms of Young's modulus determined from the analysis of all recorded force curves for: a) keratinocytes, b) fibroblasts and c) melanoma cells. Data distributions were fitted with lognormal function (a green line). Red dot denotes the expected value of the lognormal distribution.

4.6. Evaluating statistical significance of the obtained results.

In a population of cells originated from the same cell line, each cell is characterized by similar properties leading to a distribution of a defined maximum and width. This is also the case of data obtained from AFM-based elasticity measurements. Various papers report on symmetric and non-symmetric distributions of elastic modulus.[71] Thus, statistical tests have to be applied to validate the significance of obtained differences among various cell populations. Here, in the first step, normality test was performed. Its results define the applicability of a particular statistical test.

4.6.1. Normality tests

A set of normality tests, Shapiro – Wilk, Anderson – Darling, Lilliefors, and Jarque – Bera, was applied to all each of data sets. The variable from which the sample was extracted does not follow a normal distribution at p-values are lower than 0.001. The results indicate the abnormal distributions of data recorded for all measured cell lines or their combinations. These results direct the further analysis towards the use of the lognormal function to describe Young's modulus distributions.

4.6.2. Statistical significance – Mood's median test

A statistical difference among studied cell populations was verified by the use of the nonparametric ***Mood's median test,*** which shows the distinction between the medians calculated from given data sets. "Nonparametric" denotes that knowledge on the data distribution type (normal or abnormal) is not required before running the test.

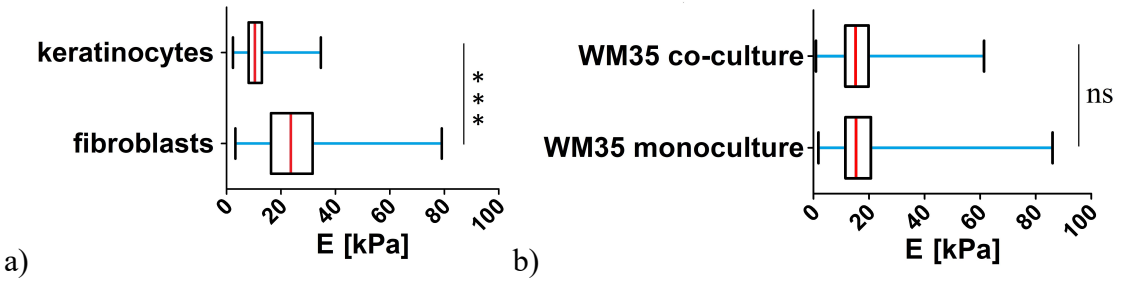

*Figure 22. The box chart plots showing the median (red line), width of distribution (blue line) and the results of Mood's median test applied to validate the difference between (a) keratinocytes and fibroblasts (p-value < 0.001, marked as ***), and (b) WM35 melanoma cells cultured as mono- and co-cultures (p-value > 0.05, ns – not significantly different).*

Mood's median test ($p < 0.001$) was applied to validate differences of elasticity parameters obtained for cells of various types and measurement conditions. **Figure 22** shows an exemplary comparison of Young's moduli determined for various cell populations shown as box charts plots with a median marked by red lines. A notable difference was observed between the deformability of keratinocytes and fibroblasts. WM35 melanoma cells cultured in various conditions did not reveal significant statistical difference ($p > 0.05$).

4.7. Adjusting indentation depths for data analysis.

The mechanical properties of living cells change with the indentation depth.[72,73] This is connected with a heterogeneity of their interior and, also, with a presence of various structures of distinct mechanical characteristics. During indentation, AFM probe meets consecutively glycocalix, cell membrane, actin filaments, cytosol components and cell nucleus (**Figure 23**). Each of these structures will respond differently to the load force. Thus, depth dependent analysis enables us to study the heterogeneity of the cell interior.

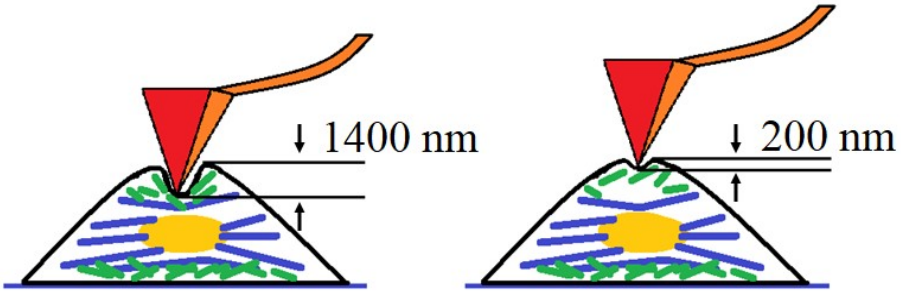

Figure 23. The indentation depth vs. heterogeneity of the cells interior structure. [adapted from Pogoda et al. Eur. Biophys. J. 41 (2012) 79-87]

Depending on the indentation depth, the contribution of the cell structural elements to mechanical response to the applied load force can be defined. Thus, the indentation depth up to 100 nm can be assumed to deliver mechanical information originating from cell glycocalix and, also, cell membrane. Indentations between 200 nm – 400 nm bring resistivity of actin cortex that lies beneath the cell membrane (but still one can remember that both glycocalix and cell membrane contribute to measured elasticity). The overall mechanical properties of a whole cell can be obtained for indentations larger than 500 nm. Herein, three indentation depths were initially considered, i.e. 200 nm, 400 nm, and 600 nm. Thus, information on superficial layers of the cells and on the overall elasticity of whole cells is expected to be obtained.

Figure 24 shows three lognormal functions fitted to data histograms for three chosen indentation depths (only fitted functions are shown for clarity). Distributions for 400 nm and 600 nm follow the same characteristics, regardless of the measurements conditions (either single cells or cell clusters). As expected, the only difference is observed for indentation depth equal to 200 nm, where distributions are characterized by the largest values of the distribution center. This is probably linked with a large mechanical heterogeneity of the cells probed for small indentations. Larger indentations depths like 400 nm or 600 nm reveal most probably the overall elasticity of cells.

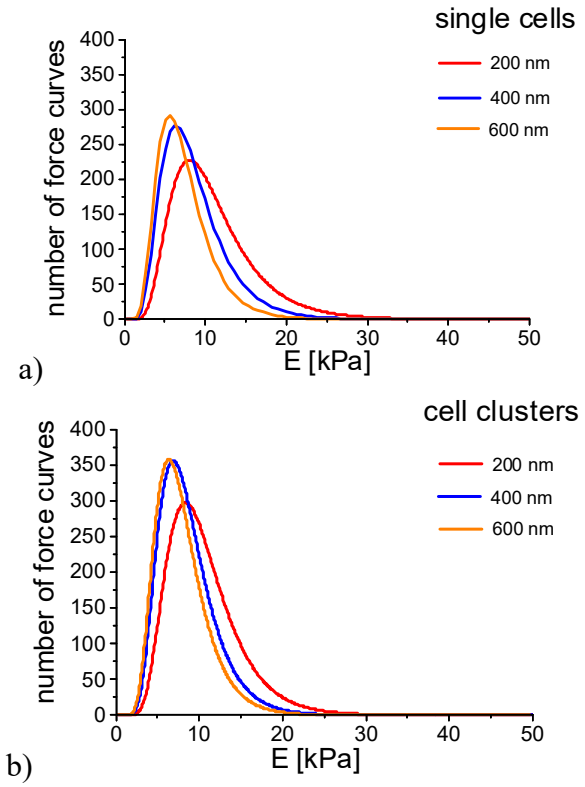

Figure 24. Lognormal functions describing histograms of elastic modulus at indentations of 200 nm, 400 nm, and 600 nm for keratinocytes measured as: a) single cells, b) cell clusters. Only fitted functions are shown. Histograms were removed due to clarity reasons.

Based on the lognormal fits to gathered data, expected values were determined at various indentation depths (Table 3).

Table 3. Expected value for each cell type determined by fitting lognormal function to the obtained data (single cells, 24 h of culture).

keratinocytes	E [kPa]		
indentation depth	200 nm	400 nm	600 nm
single cells	9.9 ± 0.3	7.8 ± 0.3	6.7 ± 0.2
cell clusters	9.7 ± 0.3	8.0 ± 0.2	7.4 ± 0.2

The expected value for single keratinocytes are 9.9 ± 0.3 kPa, 7.8 ± 0.3 kPa and 6.7 ± 0.2 kPa for 200 nm, 400 nm and 600 nm, respectively. The corresponding moduli for keratinocyte clusters are 9.7 ± 0.3 kPa, 8.0 ± 0.2 kPa and 7.4 ± 0.2 kPa. Analogously, as for keratinocytes, Young's moduli was determined for fibroblasts. Distributions are shown in **Figure 25** while results of the analysis in **Table 4**.

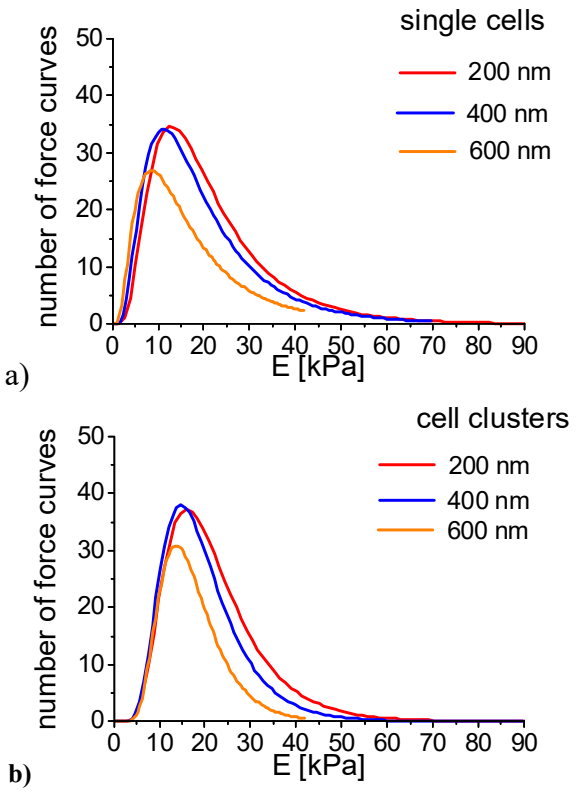

Figure 25. Lognormal functions describing histograms of elastic modulus at indentations of 200 nm, 400 nm, and 600 nm for fibroblasts measured as: a) single cells, b) cell clusters. Only fitted functions are shown. Histograms were removed due to clarity reasons.

Lognormal functions fitted to data histograms for three chosen indentation depths for fibroblasts show the same characteristics for 200 nm and 400 nm. This is probably linked with a large mechanical heterogeneity of the cells probed for small indentations. Larger indentations depths of 600 nm reveal most probably the overall elasticity of cells.

Table 4. Expected value for each cell type determined by fitting lognormal function to obtained data (single cells, 24 h of culture).

fibroblasts	E [kPa]		
indentation depth	200 nm	400 nm	600 nm
single cells	18.0 ± 1.0	16.7 ± 0.8	14.3 ± 0.8
cell clusters	19.8 ± 1.2	17.9 ± 0.8	16.1 ± 0.6

For single fibroblasts and fibroblast clusters, the expected values are 18.0 ± 1.0 kPa, 16.7 ± 0.8 kPa and 14.3 ± 0.8 for 200 nm, 400 nm and 600 nm, respectively. The corresponding moduli for cell clusters are 19.8 ± 1.2 kPa, 17.9 ± 0.8 kPa and 16.1 ± 0.6 kPa.
For melanoma cells, lognormal functions are presented in **Figure 26**. They show variability of distribution depending on the indentation depths.

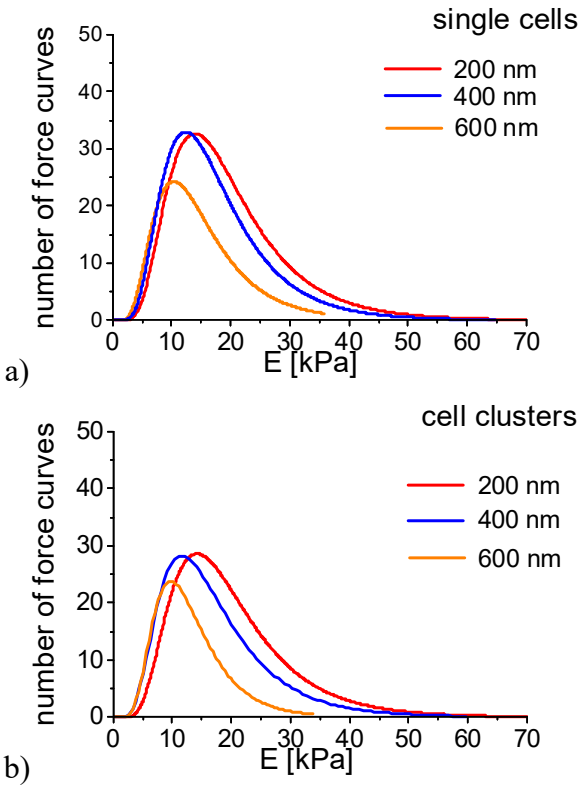

Figure 26. . Lognormal functions describing elastic modulus histograms of elastic modulus for indentations of 200 nm, 400 nm, and 600 nm for melanoma cells measured as: a) single cells, b) cell clusters. Only fitted functions are shown. Histograms were removed due to clarity reasons.

Table 5. Expected value for each cell type determined by fitting lognormal function to obtained data (single cells, 24 h of culture).

melanoma cells	E [kPa]		
indentation depth	200 nm	400 nm	600 nm
single cells	18.0 ± 1.0	15.7 ± 0.7	13.4 ± 0.7
cell clusters	17.9 ± 0.8	15.2 ± 0.8	11.9 ± 0.7

The expected value for single melanoma cells are 18.0 ± 1.0 kPa, 15.7 ± 0.7 kPa and 13.4 ± 0.7 for 200 nm, 400 nm and 600 nm, respectively. The corresponding moduli values for cell clusters are 17.9 ± 0.8 kPa, 15.2 ± 0.8 kPa and 11.9 ± 0.7 kPa.

4.8. Fluorescence microscope

The organization of actin filaments and cell nuclei was visualized *via* fluorescence microscope Olympus, IX53, equipped with an objective LUCPlanFLN (20x), 100 W mercury lamp (illuminating uniformly the whole cell area), and a set of filters enabling us to record emission at 594 nm and 420 nm. Images were collected using XC10 digital camera providing a 1376 × 1038 pixel image and analyzed with CellSense Dimensions software (Olympus). To estimate the cells area, free software – ImageJ has been used. Determination

of the surface area of individual cells was performed basing on the actin cytoskeleton and cells nuclei staining. Firstly, substrate coverage with visible stained cytoskeleton was summed up. Secondly, a number of cells nuclei was calculated. Then, the overall substrate coverage was divided by the number of cells nuclei and the mean single cell surface area was obtained. Details of this protocol has already been published by Prauzner-Bechcicki *et al.*[74]

4.9. Summary

Realization of the thesis objectives involves the application of several analytical approaches. The comparison between them allowed to identify mechanical fingerprints characteristic for each type of skin cells, namely, keratinocytes, fibroblasts and melanoma cells. In the presented approach elasticity data were fitted with lognormal function describing non-symmetric histograms (based on applied normality tests). In further chapters, the comparison will be performed on the grounds of an expected modulus value determined from the most probable moduli values, accompanied by a standard error. Statistical difference was estimated on the basis of Mood's median test. In that manner, the overall information on cells population mechanical properties can be obtained.

5. Mechanical and morphological changes of skin cells in wound healing

5.1. Objectives

During wound healing, the interaction between keratinocytes and fibroblasts proceeds through a double paracrine signaling pathway.[6,7] However, most of studies, showing details of signaling pathway involved, were performed using the Boyden Chamber system.[58] The classic Boyden Chamber system uses a hollow plastic chamber, an insert, which is suspended over a larger well. Cells are placed both in the insert and at the bottom of the well. Such experiments allow to study the role of signaling molecules,[7] however, the role of direct physical interactions is neglected. In the presented studies, the main stress has been placed on alterations in cellular deformability of skin cells. By determining deformability of single cells, any potential influence of paracrine signaling pathways can be obtained. In such a case, the direct cellular interaction is minimized. Studying cell clusters enabled to get insight on the interactions of cells being in direct contact. Here, paracrine signaling pathways is less pronounced. Dominant contribution in cell mechanical properties stem from physical contact between cells and is governed by the cytoskeleton.[7]

To realize the assumed objectives two types of skin cells, i.e. fibroblasts (FB) and keratinocytes (HaCaT) were cultured together at two time spots (24 and 48 hours). Morphological changes were quantified by the determination of their spreading area while their mechanical properties were obtained from AFM measurements. As stated in section *Materials*, elasticity of single cells and cell clusters was estimated for 8 groups of samples as presented in **Figure 27a**.

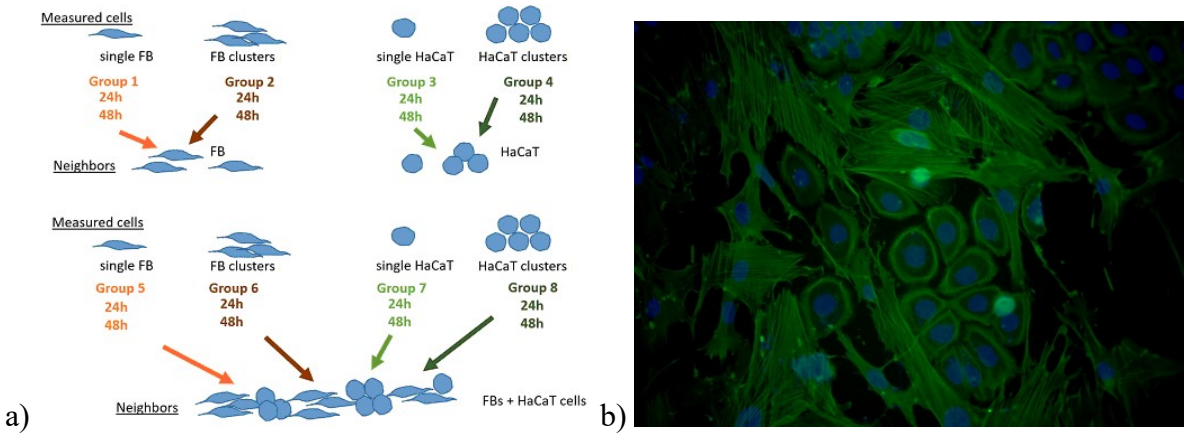

Figure 27. (a) Summary of experiments carried out for mixtures of keratinocytes and fibroblasts. (b) Fluorescence image of actin filaments (green) and cell nuclei (blue) in a cellular mixture of both FBs and HaCaT cells mixed at the ratio of 10:2 (FB : HaCaT cells).

Eight groups of samples were measured constituting various combinations of measured cells (single cells or cell clusters) and their environment (cells of the same type or cellular

mixtures). Each group was measured at two time spots, namely, after 24 and 48 hours of growth.
An exemplary image of a mixture of cells (**Figure 27b**) reveals cells of both types cultured for 48 hours. Actin filaments and cell nuclei were stained fluorescently with phalloidin conjugated with Alexa Fluor 488 and Hoechst, respectively (as described in ***Chapters 3&4***). Keratinocytes are oval-shaped cells whereas fibroblasts are spindle-like ones. Actin cytoskeleton of fibroblasts is well-differentiated with stress fibers spanning over the whole cell body. Oppositely, actin filaments in keratinocytes are poorly organized and forms mainly a ring-like structure located close to the edge of the cell. Due to distinct cellular shapes, it was possible to relate mechanical and morphological properties to a particular cell type.
The AFM-based force spectroscopy data were analyzed using the approach comparing changes of Young's modulus as a function of the indentation depth. The analysis allowed to discriminate cells response depending on various compartments of cell structures. Elasticity measurements were accompanied by the analysis of cell surface area.[74] Results described within the ***Chapter 5*** has already been published in paper by Orzechowska *et al.* [7]

5.2. Viability of skin cells in mixture

In the first step of the studies on the mechanical interaction between skin cells, fluorescent images were recorded to visualize cellular mixtures (**Figure 28**).

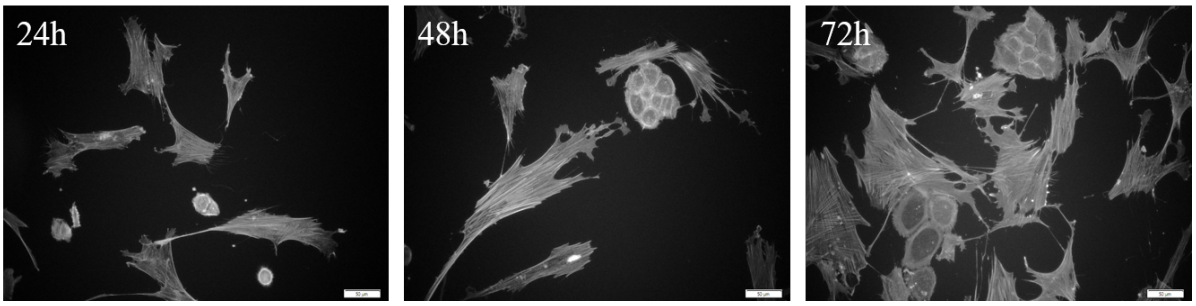

Figure 28. Fluorescence images of cellular mixture recorded after 24 h, 48 h and 72 h of culture - scale bar = 50 μm *(Orzechowska et al. J. Biomechanics, 2018[7]).*

Fluorescent images of cell mixtures composed of fibroblasts and keratinocytes show clearly two types of cell populations. Fibroblasts have a spindle-like morphology with stress fibers spanning over a whole cell. Keratinocytes grow as clusters composed of a few, rounded cells. Actin-rich rings are visible to surround cell nucleus.

Viability of cells was verified using MTT assay (described in ***Chapters 3&4***). Three types of samples were analyzed, i.e. only fibroblasts, only keratinocytes and a mixture of these two cell types (**Figure 29**).

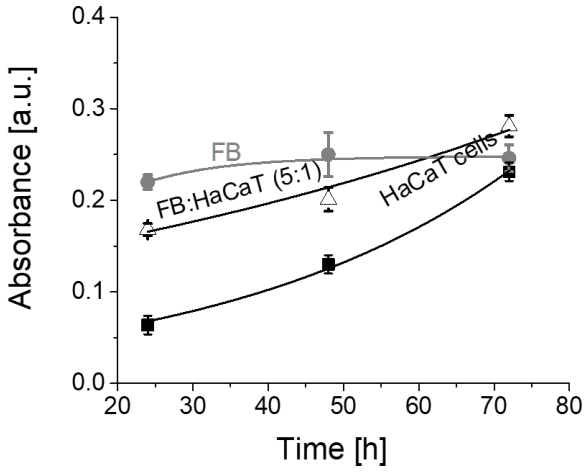

Figure 29. Viability of skin cells determined based on the MTT assay. Line denotes fitted model used to determine doubling time (Orzechowska et al. J. Biomechanics, 2018;[7]).

The number of fibroblasts, cultured separately within the time frame of 24–72 hours, increases only of about ~13% (this number was normalized to initial conditions, i.e. to the number of cells after 24 h of growth; doubling time for fibroblasts is ~120 h). HaCaT cells proliferate much faster (doubling time for HaCaT cells is 27.0 ± 1.7 h). The number of cells increases 3.5-fold as compared to initial conditions. A mixture of cells (FB : HaCaT; 5:1) proliferates faster than fibroblasts but slower than keratinocytes. The effective doubling time for the mixture is 64.8 ± 8.4 h. This indicates that growth of cellular mixtures is dominated by proliferation of keratinocytes.

5.3. The role of actin filaments in cellular deformability

Most of the AFM elasticity studies attribute mechanical properties of cells to the organization of actin filaments.[5,77,78] To verify whether, actin filaments are responsible for deformability of fibroblasts and keratinocytes, elasticity measurements were carried out on cells incubated with cytochalasin D, inhibiting the actin filament polymerization.[79–81] Here, fibroblasts were incubated with 1 μM cytochalasin D in phosphate buffered saline (PBS) for 10 minutes, while keratinocytes cells were treated with 7.9 μM cytochalasin D for longer time, i.e. for 14 hours (**Figure 30**.) As a result, larger deformability of cells is expected, characterized by a low value of the Young's modulus. The elasticity change is more pronounced for fibroblasts, for which a 10 minutes incubation in 1 μM concentration of cytochalasin D manifests in a dramatic drop of elastic modulus from 19.6 ± 4.3 kPa (n = 73 cells) to 9.3 ± 4.6 kPa (n = 19). Consequently, HaCaT cells were treated with the same cytochalasin D concentration during the same time, but the elasticity of these cells remained unchanged in comparison to the untreated ones. Then, I have been increasing both concentration and incubation time and small changes in cell mechanics after 14 hours of the expose to 7.9 μM cytochalasin D solution could be detected. The Young's modulus drops from 8.6 ± 1.6 kPa (n = 203 cells) to 6.5 ± 2.6 kPa (n = 16).

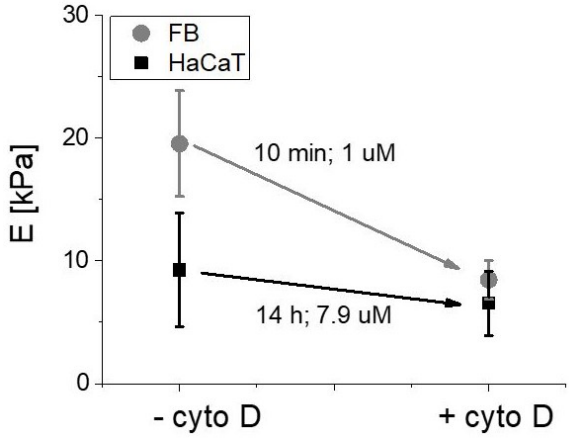

Figure 30. Mechanical properties of FB and HaCaT cells before and after the cytochalasin D treatment (Orzechowska et al. J. Biomechanics, 2018[7]).

Lack of pronounced elasticity changes is not surprising since our measurements were carried out above the cell nucleus. Moreover, our results confirmed the weak role of the actin cortex in maintaining keratinocytes mechanical integrity what agrees with results already reported.[82,83]

5.4. Deformability of single cells

Initially, single cells either fibroblasts or keratinocytes or both, measured at two culture times, i.e. 24 h and 48 h were analyzed. Elasticity measurements of single cells embedded in the environment composed of the same cell type allow to evaluate whether mechanical properties of these cells are modulated by the presence of distant neighbors of the same origin. Simultaneously, distinct indentations were probed to evaluate which parts of the cell, superficial or deeper layers, respond to the external stimuli, here, most probably by signaling molecules of the double paracrine signaling pathway.

Results obtained for single cells show that fibroblasts are more rigid as compared to HaCaT cells within the full range of the studied indentation depths and regardless of the culture time (**Figure 31**). The Young's modulus values for single keratinocytes cultured for 24 h at indentation depths of 200 nm, 400 nm and 600 nm are 9.9 ± 0.3 kPa (n = 203 cells), 8.0 ± 0.3 kPa (n = 202) and 6.7 ± 0.2 kPa (n = 202), respectively (**Figure 31a)**. Longer culture time leads to a decrease of the elastic modulus (an increase in cellular deformability). Obtained values are 8.5 ± 0.2 kPa (n = 239), 7.7 ± 0.2 kPa (n = 152) and 7.1 ± 0.2 kPa (n = 152), correspondingly. The elasticity varies from 5% to 14%. Single fibroblast deformability follows the similar pattern (**Figure 31b**). After 24 h of culture, individual fibroblasts are characterized by elastic moduli of 18.0 ± 1.0 kPa (n = 73), 16.6 ± 0.8 kPa (n = 72) and 14.0 ± 0.7 (n = 65) kPa at 200 nm, 400 nm and 600 nm respectively. After 48 h of culture, Young's moduli changes to 21.1 ± 0.6 kPa (n = 175), 16.0 ± 0.7 kPa (n = 75) and 13.8 ± 0.6 kPa (n = 68) at indentation depths of 200 nm, 400 nm and 600 nm, respectively.

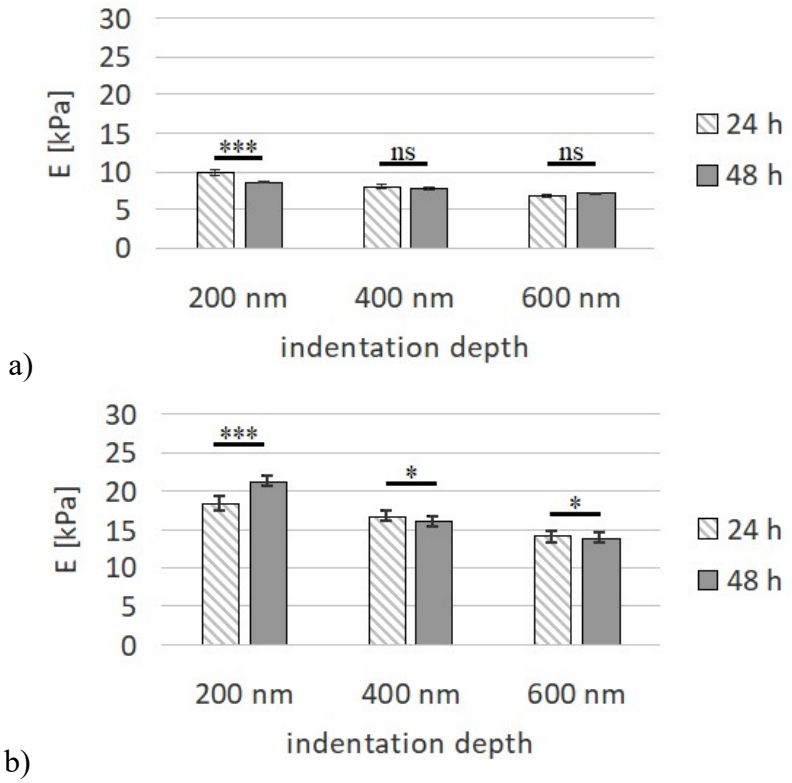

Figure 31. Deformability of single (a) keratinocytes and (b) fibroblasts calculated at three indentation depths of 200 nm, 400 nm and 600 nm, for cells cultured for 24 & 48 hours of culture. Data are presented as the expected value of the lognormal distribution ± standard error.

Summarizing, the presence of distant neighbors of the same origin (i.e. keratinocytes in the case of HaCaT cells and fibroblasts in the case of FBs) influences the elasticity of single cells, both HaCaT cells and fibroblasts. In both cases, the largest alterations were observed for superficial layer of the cells (indentation depth of 200 nm), indicating probably strong re-organization of actin filaments in response to cell expansion due to a free space around and signaling molecules receiving from distant cells. In case of deeper indentations mechanical response of single keratinocytes is contributed by the overall elasticity of a cell. Simultaneously, at these indentations, the information on actin filaments re-arrangements within the superficial layer of the cell vanishes.

Above-mentioned results show that in the case of single, individual cells measured in the presence of fibroblasts (or keratinocytes) that are relatively far away from the studied cell, it was possible to observe stiffness alterations induced by the presence of distant neighbors of the same origin. Thus, next question is whether the presence of two types of cellular neighbors (both FB and HaCaT cells) will influence deformability of a single cell. To elaborate on the issue, single keratinocytes and single fibroblasts were measured after 24 & 48 hours of culture in a mixture of cells.

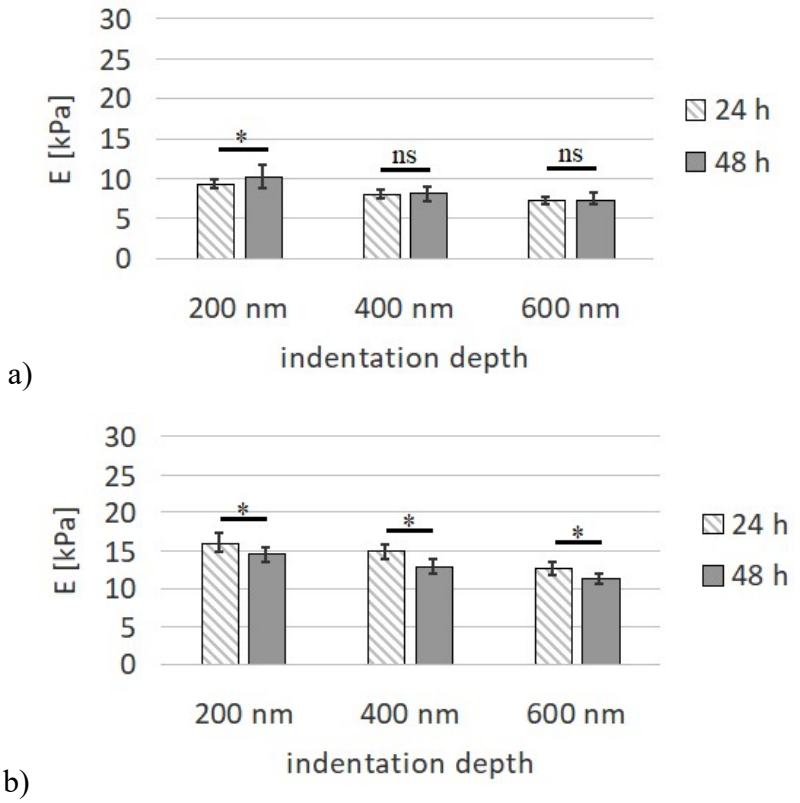

Figure 32. Deformability of single (a) keratinocytes and (b) fibroblasts calculated at three indentation depths of 200 nm, 400 nm and 600 nm, for cells cultured for 24 & 48 hours culture in cellular mixture.

The mechanical properties of single keratinocytes, cultured only in the presence of HaCaT cells and FBs for 24 hours, without physical contacts with these cells, remained at the same level independently of the indentation depths chosen for the analysis (**Figure 32**). The Young's moduli of single keratinocytes are 9.2 ± 0.6 kPa (n = 52 cells), 8.0 ± 0.6 kPa (n = 52) and 7.3 ± 0.6 kPa (n = 52), for indentations of 200 nm, 400 nm and 600 nm, respectively. Increasing the culture time did not change significantly the elasticity of single HaCaT cells 10.2 ± 1.5 kPa (n = 36 cells), 8.0 ± 0.9 kPa (n = 35 cells) and 7.4 ± 0.8 kPa (n = 33 cells) for indentation of 200 nm, 400 nm and 600 nm, respectively. This suggests that signaling molecules secreted by both keratinocytes and fibroblasts do not influence deformability of HaCaT cells. Single fibroblasts in cellular mixtures reveal larger deformability for longer culture time (48 h). A drop of elastic modulus was independent of the indentation depth. As for these culture conditions, cells have free space around themselves, one could expect that spreading of cells will be also influenced by distant neighbors of both the same and distinct origin. To elaborate this, spreading area of individual cells was determined from fluorescent images of actin filaments that bring information on cellular morphology (**Figure 33**).

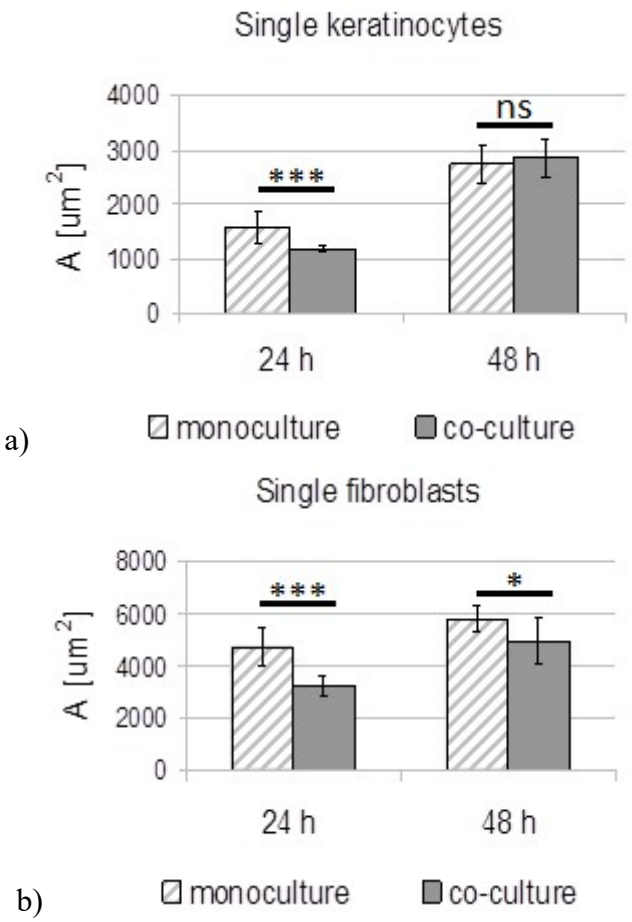

Figure 33. Surface area (A) of single (a) keratinocytes and (b) fibroblasts, determined after 24 h and 48 h of culture.

The surface area of both types of individual cells decreases with time of growth independently of the culture conditions, i.e. the presence of one type of cellular neighbors only or a mixture of cells. Changes in the cell spreading surface area are larger for single fibroblasts as compared to keratinocytes. They are probably linked with the organization of actin filaments. The reorganization was accompanied by a drop of elasticity. For keratinocytes, weak changes in cellular deformability were accompanied by diminished changes in a single cell surface area. This indicates that spreading of cells and elasticity changes are mutually dependent phenomena.

5.5. Deformability of cell clusters

Several research works have shown that an individual cell embedded within a cluster of cells is characterized by distinct mechanical properties as compared to an isolated, single cell.[7,55] Thus, in the presented studies, elasticity of single cells embedded within a cluster of 5 to 10 cells (referred here as cell clusters) was evaluated as a function of cell and cellular neighbor types (**Figure 34**). Moreover, studying single cells in clusters delivers information on the contribution of intercellular junctions to the overall elasticity of a single cell being in a direct contact with neighboring cells.

Analogously as for single cells, a depth-dependent analysis was performed. After 24 h of culture, keratinocyte clusters are characterized by the following elasticity parameter values 9.7 ± 0.3 kPa (n = 234 cells), 8.0 ± 0.2 kPa (n = 233) and 7.4 ± 0.2 (n = 229) kPa at 200 nm, 400 nm and 600 nm depths, respectively. Longer culture time (48 h) manifested in the decreased deformability of HaCaT cells. The corresponding moduli are 10.8 ± 0.2 kPa (n = 291), 10.4 ± 0.2 kPa (n = 206), 9.7 ± 0.2 kPa (n = 198). The increased rigidity of keratinocyte clusters (from 8% to 23%) indicates the influence of neighboring cells on maintaining mechanical resistance of cells to lateral deformations. Surprisingly, the increase of elastic modulus is the smallest for 200 nm of indentation depth at which largest re-organization of actin cytoskeleton is expected. This could be explained by the contributions of both keratin filaments[84] and cell-cell junctions of various structures[85,86] in mechanical properties.

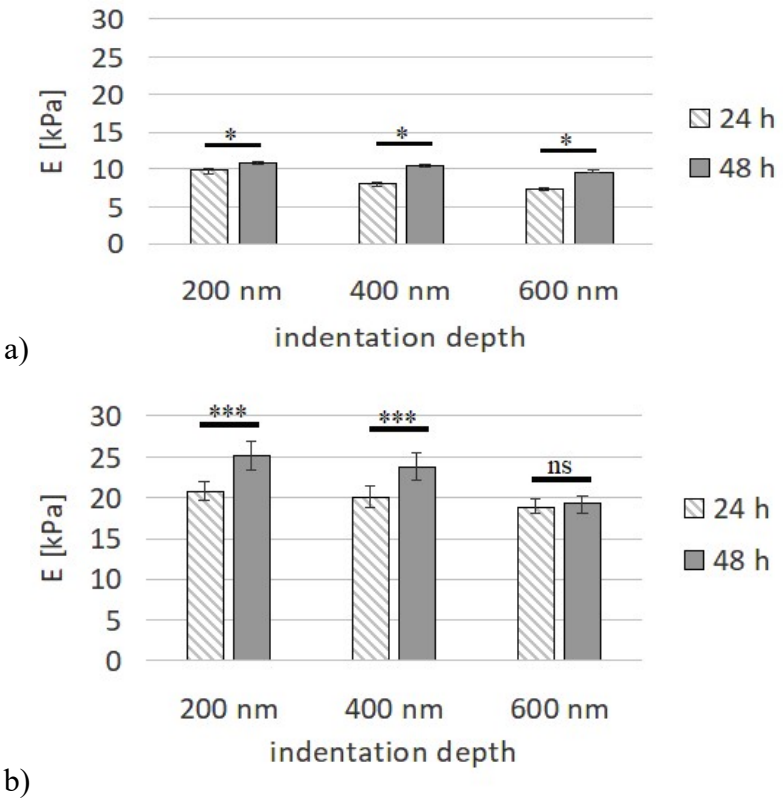

Figure 34. The mechanical properties of (a) keratinocyte and (b) fibroblast clusters after 24 h and 48 h of growth in the presence of cellular neighbors of the same origin.

Fibroblast clusters change their deformability in a depth-dependent manner. After 24 h of culture, FBs have elastic moduli of 19.8 ± 1.2 kPa (n = 69 cells), 17.9 ± 0.8 kPa (n = 67) and 16.0 ± 0.6 kPa (n = 60) for 200 nm, 400 nm and 600 nm, respectively. For longer time of growth (48 h) the obtained values were 21.9 ± 0.6 kPa (n = 177), 16.8 ± 0.8 kPa (n = 65) and 14.3 ± 0.6 kPa (n = 58), correspondingly. The change of about 6–10 %, either cell stiffening or softening, was observed depending on the indentation depth.

Mechanical properties of cell clusters in a cellular mixture are characterized by distinct deformability (**Figure 35**). After 24 h of culture, the Young's modulus of HaCaT cells is 10.6 ± 0.4 kPa (n = 43), 8.9 ± 0.4 kPa (n = 43) and 8.4 ± 0.4 kPa (n = 43) for indentations of 200 nm, 400 nm and 600 nm. Similarly, as for cell clusters measured in the

presence of keratinocytes only, an increase in elastic modulus is observed for 48 h of culture. The obtained values are 11.1 ± 0.7 kPa (n = 41), 9.2 ± 0.7 kPa (n = 41), 8.8 ± 0.5 kPa (n = 41), correspondingly.

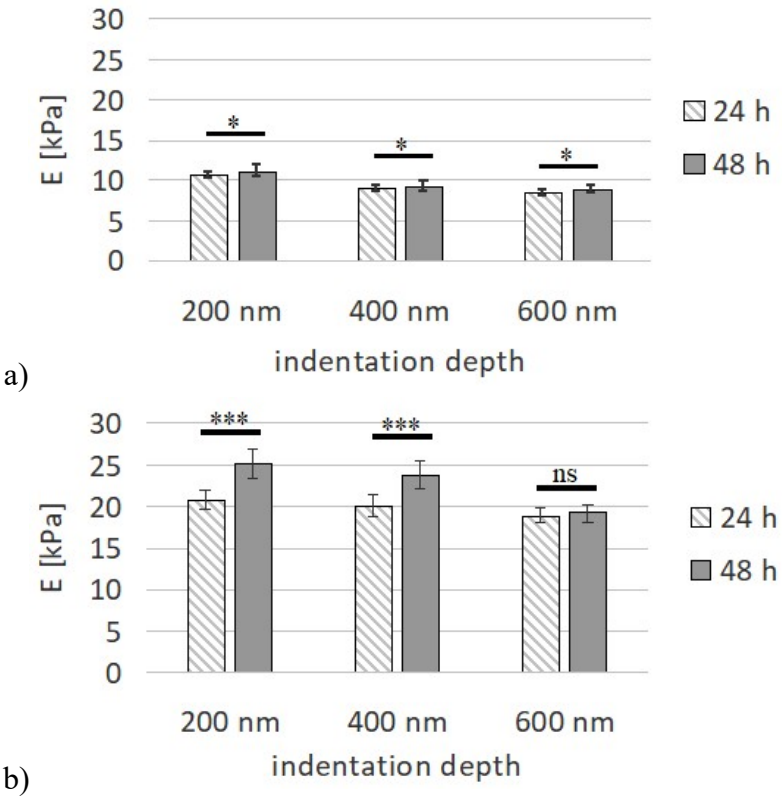

Figure 35. The mechanical properties of (a) keratinocyte and (b) fibroblast clusters after 24 h and 48 h of growth grown in the presence of a mixture of FBs and HaCaT cells.

Fibroblasts in clusters become more rigid during culture time. After 24 h of culture, the elastic modulus is 20.7 ± 1.2 kPa (n = 47), 20.1 ± 1.3 kPa (n = 47) and 18.9 ± 0.9 kPa (n = 40) for indentations of 200 nm, 400 nm and 600 nm, respectively. After 48 h of growth, the corresponding moduli are observed, i.e. 25.1 ± 1.7 kPa (n = 49), 23.8 ± 1.7 kPa (n = 46) and 19.1 ± 1.1 kPa (n = 29). These are larger as compared to both single cells and fibroblast clusters measured in the presence of fibroblasts only.

Analogously as for single cells the surface area of an effective cell was calculated. A surface area of a whole cluster was determined together with a number of nuclei of cells constituting the cluster. By dividing the surface area by the number of cell nuclei, a surface area of an effective cell was obtained (**Figure 36**).

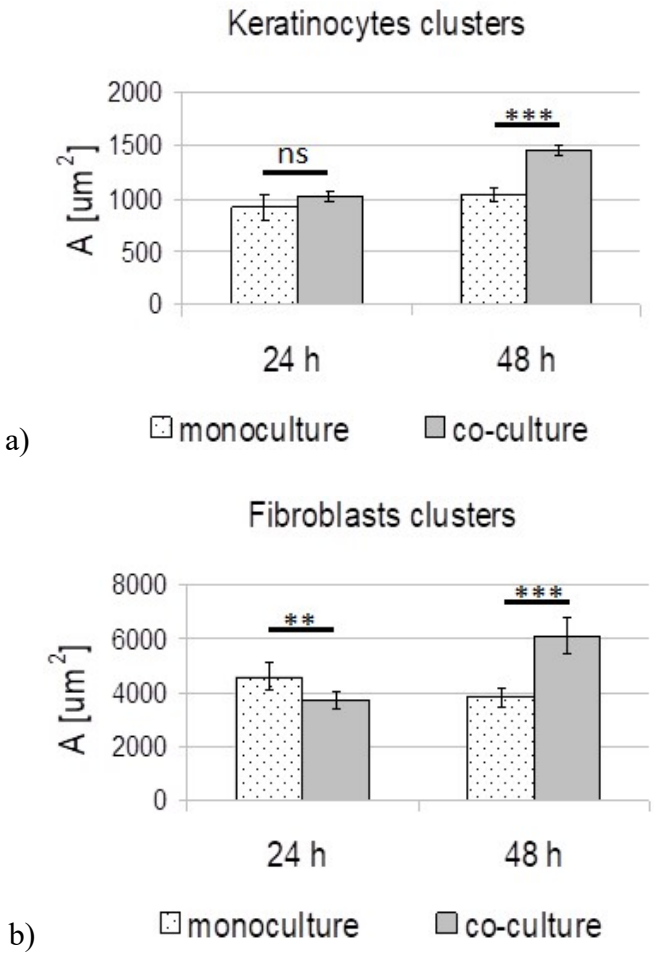

Figure 36. Surface area (A) of an effective, single (a) keratinocyte and (b) fibroblast cell embedded in cellular clusters, after 24 h and 48 h of culture.

The effective area of keratinocytes changes significantly only after 48 h of culture in the presence of both FBs and HaCaT cells. In case of fibroblasts grown in clusters the mechanical properties of these cells from mono- and co-cultures are on the same level which is connected with small changes in cells area. After 24 h of growth the mean area of single cell from the monoculture is slightly higher than the mean area of cells from the co-culture. Thus, in cellular mixtures, deformability of cells and their capability to spread out are independent phenomena.

5.6. Elasticity of border cells

Together with alterations in mechanical properties of single cells and cell clusters, another question arose, namely, how deformability changes for cells in contact with another cell of distinct origin. Therefore, Young's modulus was determined for keratinocytes being in contact with fibroblasts as well as for FBs in contact with HaCaT cells (**Figure 37**).

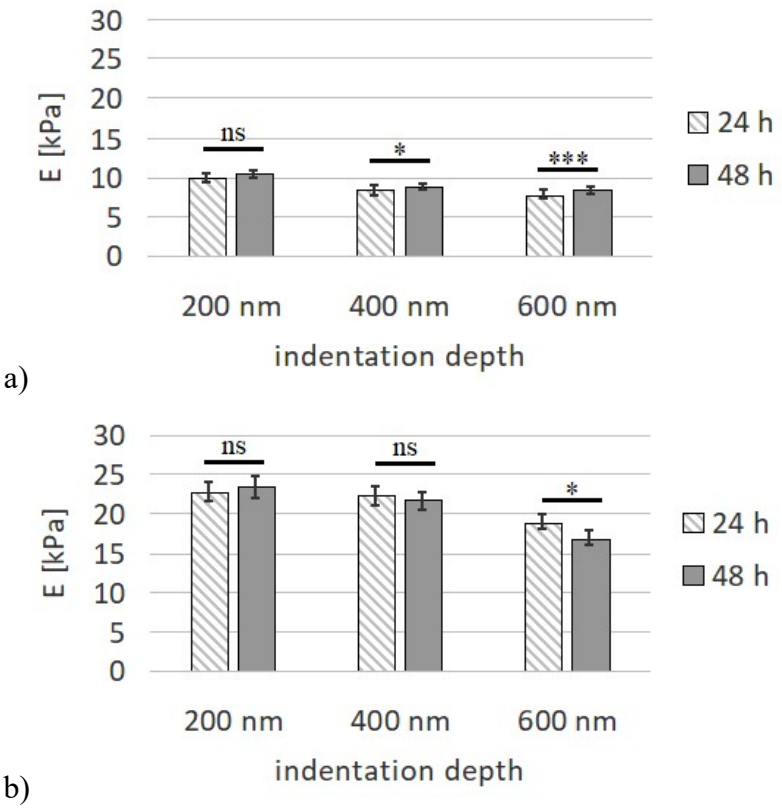

Figure 37. Deformability of (a) HaCaT cells and (b) FBs being in contact either with FB or HaCaT cell, determined for 24 h and 48 h of culture in cellular mixtures. Analogously, three indentations depth were considered.

Deformability of HaCaT cells, being in the direct contact with a fibroblast after 24 h of culture, is as follows: 9.8 ± 0.6 kPa (n = 53), 8.3 ± 0.6 kPa (n = 52), 7.7 ± 0.5 kPa (n = 52) for indentations of 200 nm, 400 nm and 600 nm, respectively. After 48 h of culture, it remains at the same level, 10.4 ± 0.4 kPa (n = 51), 8.7 ± 0.4 kPa (n = 51) and 8.3 ± 0.4 kPa (n = 51), correspondingly. Keratinocytes remained insensitive to the contact with fibroblasts, regardless of the culture time. The elastic moduli were 22.8 ± 1.3 kPa (n = 49 cells, 24h) and 23.3 ± 1.5 kPa (n = 47, 48 h) for indention of 200 nm; 22.3 ± 1.2 kPa (n = 49 cells, 24 h) and 21.6 ± 1.2 kPa (n = 45, 48 h) for indentation of 400 nm, and 18.9 ± 1.1 kPa (n = 34 cells, 24 h) and 16.8 ± 0.9 kPa (n = 33, 48h). Analogously, as for keratinocytes, fibroblasts remained almost insensitive to the contact with keratinocytes, regardless of the culture time. However, results obtained for deeper indentations (600 nm) show 10% FBs stiffening.

5.7. Summary

Measurements of mechanical properties of keratinocytes (HaCaT cells) and fibroblasts bring information on how deformability changes in the direct or indirect cellular interaction in cells involved in wound healing process. Cells communicate either through various signaling pathways induced by molecules secreted to surrounding environment or by direct connections realized by distinct types of cellular junctions. Thus, elasticity measurements of single cells, cell clusters and border cells deliver information on the role of cytoskeleton reorganization induced either through paracrine signaling pathways or by

physical contact between two adjacent cells. The main results, presented within this Chapter, are:

- Keratinocytes and fibroblasts can be cultured together in the same culture medium for 72 h. Fluorescent images show clearly two types of cell populations. An additional finding is that growth of cellular mixtures is dominated by proliferation of keratinocytes.
- Reorganization of actin filaments leads to elasticity changes of cells significantly in case of fibroblasts while keratinocytes seems to be unaffected by actin cytoskeleton remodeling.
- Single fibroblasts are more rigid as compared to keratinocytes within the full range of the studied indentation depths regardless of the culture time.
- The presence of distant neighbors of the same origin (i.e. keratinocytes in the case of keratinocytes and fibroblasts in the case of fibroblasts) influences the elasticity of single cells, both keratinocytes and fibroblasts. In both cases, the largest alterations were observed for superficial layer of the cells, indicating probably strong re-organization of actin filaments in response to cell expansion due to free space around it and signaling molecules receiving from distant cells.
- At deeper indentations mechanical response of single keratinocytes is mainly contributed by the elasticity of a whole cell. Simultaneously, at these indentations, the information on actin filaments re-arrangements within the superficial layer of the cell vanishes.
- Comparison of elasticity parameter changes with single cell spreading area reveals large changes in a cell surface area for single fibroblasts. For keratinocytes, weak changes in cellular deformability accompanied by small changes in a single cell surface area are mutually dependent phenomena.
- Culturing cells in clusters did not change the relation of cellular deformability. Fibroblasts remained stiffer than keratinocytes.
- The increased rigidity of keratinocyte clusters indicates the influence of neighboring cells on maintaining mechanical resistance of cells to lateral deformations. For fibroblasts, both stiffening and softening was observed depending on the culture time.
- Keratinocytes remained insensitive to the contact with fibroblasts, regardless of the culture time. Analogously, fibroblasts were also insensitive to the contact with keratinocytes, regardless of the culture time.

AFM-based elasticity measurements demonstrated that interaction between keratinocytes and fibroblasts that occurs during wound healing process cannot be only characterized by molecular and biochemical properties. The process also involves alterations in mechanical properties of both participating cell types. Understanding how biomechanical properties changes allow us to elaborate in details on mechanisms governing the behavior of fibroblasts and keratinocytes during wound healing.

6. Elasticity changes of melanoma cells interacting with normal skin cells

6.1. Objectives

Healthy skin cells such as fibroblasts and keratinocytes affect the growth of melanoma cells. Some exemplary research has shown that at early stage of melanoma progression, fibroblasts can inhibit growth of cancer cells whereas at more advanced tumor stages, especially, for metastasis, growth of melanoma cells can be stimulated.[9–11] Fibroblast-derived signals can allow cancer cells to escape from local growth place both in the primary tumor site and at distant tissue sites. These results have been verified for a variety of experimental systems, particularly for that composed of human dermal fibroblasts and melanoma cells from distinct stages of cancer progression.[11] One of the molecules involved is an interleukin-6, which is a result of double paracrine signaling pathways occurring in keratinocyte-fibroblast interaction, in a similar manner to that observed in wound healing process.[10] So far, there is no knowledge how such signaling induced changes influence deformability of melanoma cells, especially during early stages of melanoma progression, where interaction with normal skin cells has been reported to inhibit cancer development. Therefore, the main objective of the presented studies is to evaluate alterations in mechanical properties of melanoma cells derived from radial growth phase in the interactions with two types of skin cells (both keratinocytes and fibroblasts). To demonstrate that cells interact both indirectly through signaling molecules (secreted by other cells and attaching to receptors of target cells) and, also, directly by various types of cell-cell junctions, mechanical properties of single cells, cell clusters and border cells were investigated for cellular mixtures composed of a particular pair of cells either keratinocytes/WM35 melanoma cells or fibroblasts/WM35 melanoma cells. Mechanical properties of cells were measured after 48 h of culture, as a function of the type of neighboring cells.

6.2. Viability of cells in cellular mixtures

Analogously, as in the case of keratinocyte–fibroblasts interactions presented in ***Chapter 5***, as a first step, viability of cells in cellular mixtures using MTT assay was performed. **Figure 38** presents results obtained for five groups of studied cell cultures: *(i)* only FBs, *(ii)* only HaCaT cells, *(iii)* WM35 melanoma cells from radial growth phase, *(iv)* a mixture of FB:WM35 melanoma cells, and *(v)* a mixture of HaCaT:WM35 melanoma cells.

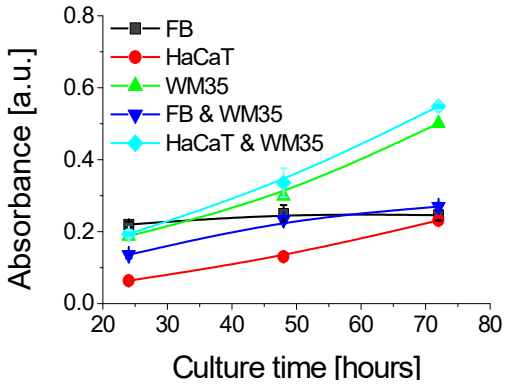

Figure 38. The results of MTT assay tests obtained for HaCaT cells, fibroblasts and WM35 melanoma cells and two types of cellular mixtures, namely, HaCaT & WM35 and FB & WM35.

Depending on the cell type, various characteristics were obtained. They were quantified by a doubling time describing the proliferation capability of cells.[63] The doubling times of keratinocytes and fibroblasts are 27.0 ± 1.7 h and 120 h ± 8 h, respectively (re-called data from ***Chapter 3***). WM35 melanoma cells were characterized by the doubling time of 33.8 ± 0.7 h. These cells were mixed either with HaCaT cells or FBs. Thus, analogously, the doubling time of a mixture was determined. The obtained results show that in the mixture of WM35 cells with FBs, cells proliferate with the doubling time of 48.5 ± 1.1 hours what is 2.5 times faster than the proliferation of fibroblasts alone. This means that the mixture of FB:WM35 is dominated by the growth of melanoma cells. The other cellular mixture studied is composed of WM35 and HaCaT cells. The obtained doubling time is 32.1 ± 0.7 h, which is similar to the doubling time of melanoma cells and is faster than for HaCaT cells alone. Analogously, as for FB:WM35 mixture, growth of cells in HaCaT:WM35 co-culture is dominated by melanoma cells.

6.3. Interaction of melanoma cells with keratinocytes

Melanoma cells origin from melanocytes that are embedded within a layer, mainly, consisting of keratinocytes. In such conditions, at initial stages of cancer progression, a single melanoma cell can interact either with keratinocytes or with extracellular matrix proteins. In the first step, stained cellular mixtures of HaCaT and melanoma cells were visualized with a fluorescent microscope, which clearly shows the presence of two types of cells. These cells not only co-exist but, as it has been shown with MTT assay, they also proliferate (**Figure 39**).

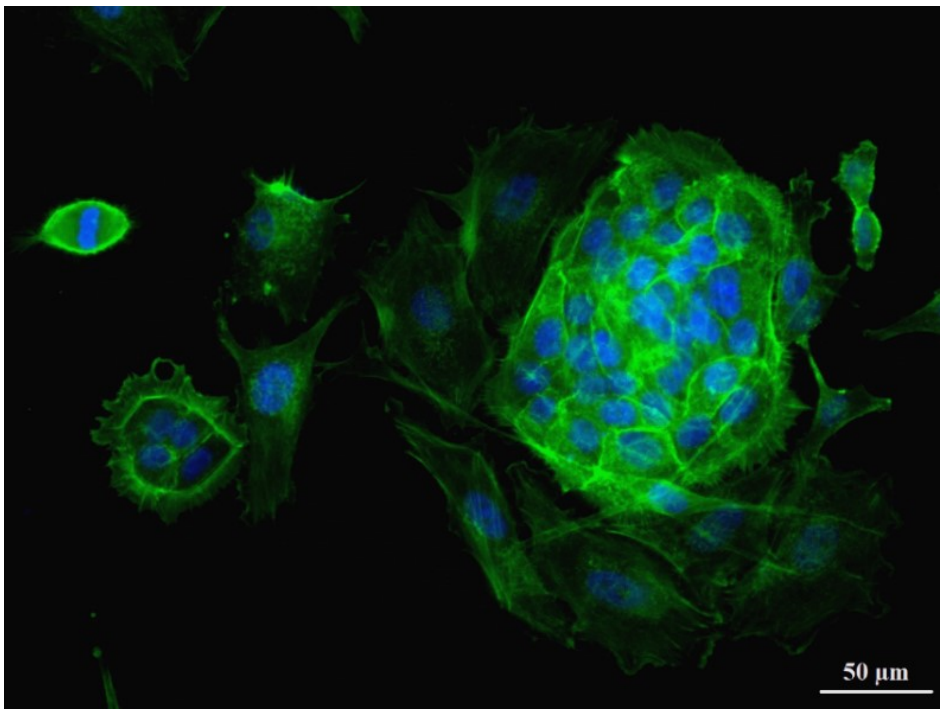

Figure 39. The fluorescence images of co-culture consisting of melanoma cells and keratinocytes after 48 h of culture.

Fluorescent visualization of the HaCaT:WM35 mixture was carried out by staining actin filaments with phalloidin conjugated with Alexa Fluor 488 dye. It clearly shows that actin-related intensity is much higher for keratinocytes as compared to melanoma cells what indirectly points out the lower amount of F-actin. Also, depending on the cell type, distinct organization of actin filaments is observed. HaCaT cells are round, with visible actin ring located close to the edge of this cell. In spindle-like melanoma cells, F-actin seems to be homogenously distributed over a whole cell body.

Mechanical properties of cells were determined from AFM-based elasticity measurements on three groups of cells, namely, on single cells, cell clusters, and border cells. Single, isolated cells cultured on a glass surface, have free space enabling them to spread out. There are no direct interactions between cells (neither between melanoma cells nor between melanoma and HaCaT cells). Thus, alterations of their biomechanical properties can arise due to attachment of signaling molecules secreted by distant neighbors either melanoma or HaCaT cells. Single cell embedded within a cluster of 5-10 cells represents a cell that can change their biomechanical properties *(i)* due to attachment of signaling molecules secreted by distant neighbors either melanoma or HaCaT cells or *(ii)* due to direct connections through various types of cell-cell junctions. Elasticity of border cells seems to be dominated only by a direct interaction between melanoma and HaCaT cells.

6.3.1. Deformability of single cells

Evaluation of mechanical properties of single cells participating in the interaction of melanoma cells with keratinocytes started from calculations of Young's modulus of HaCaT and WM35 melanoma cells. Cells were cultured separately, i.e., only either keratinocytes or

melanoma cells were present on measured glass coverslips. Measurements of single, isolated cells with no physical contact with any other cells revealed that HaCaT cells are more deformable as compared to WM35 melanoma cells (**Figure 40**), what can be partially linked with actin filament organization in both cell types (**Figure 39**).

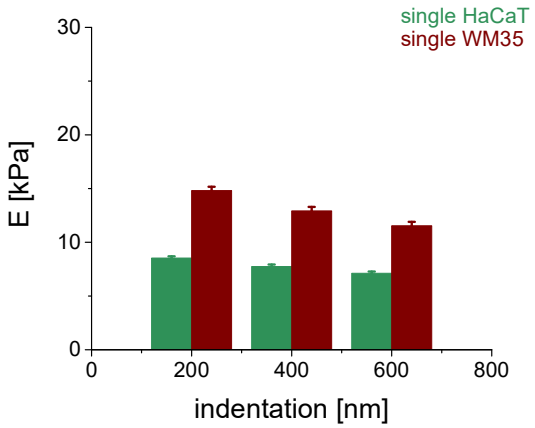

Figure 40. Young's modulus of single HaCaT and WM35 melanoma cells measured after 48h of growth. Both cell lines were cultured separately.

Obtained Young's moduli for HaCaT cells are 8.5 ± 0.2 kPa (n = 239 cells), 7.7 ± 0.2 kPa (n = 152), and 7.1 ± 0.2 kPa (n = 152) determined for indentations of 200 nm, 400 nm and 600 nm, respectively. The corresponding moduli for melanoma cells are 14.8 ± 0.4 kPa (n = 156 cells), 12.9 ± 0.4 kPa (n = 86), and 11.5 ± 0.4 kPa (n = 80). These data are in agreement with palpation approach to detect solid tumors used by clinicians[87,88]. In parallel, these results are also not in a contradiction with widely accepted results showing larger deformability of cancerous cells.[89] These results show that HaCaT cells cannot be used as a reference (a healthy counterpartner) to melanoma. Melanoma origins from melanocytes that were not under objective of studies presented here. The comparison of these cells to single cells of both types measured in cellular mixtures of HaCaT:WM35 melanoma cells is presented in **Figure 41**.

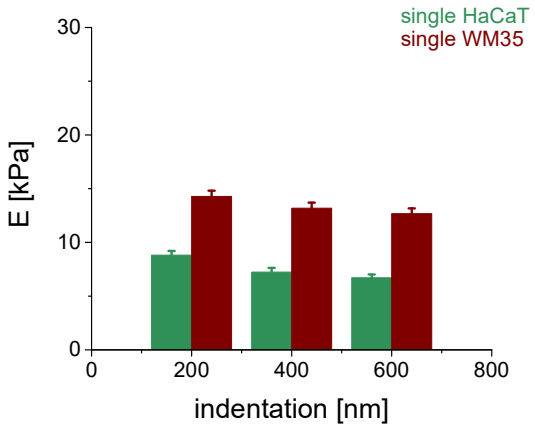

Figure 41. Young's modulus of single HaCaT and WM35 melanoma cells measured after 48h of growth in cellular mixture.

The relation between WM35 and HaCaT cells remained the same as for monocultures, i.e. melanoma cells are stiffer than keratinocytes within a whole range of the indentation depth.

Obtained Young's moduli for HaCaT cells are 8.8 ± 0.4 kPa (n = 39 cells), 7.2 ± 0.4 kPa (n = 39), and 6.7 ± 0.3 kPa (n = 39) determined for indentations of 200 nm, 400 nm and 600 nm, respectively. The corresponding moduli for melanoma cells are 14.3 ± 0.5 kPa (n = 58 cells), 13.2 ± 0.5 kPa (n = 58), and 12.7 ± 0.5 kPa (n = 47). Next, mechanical properties of both HaCaT and WM35 melanoma cells from monocultures and cellular mixtures were compared (**Figure 42**).

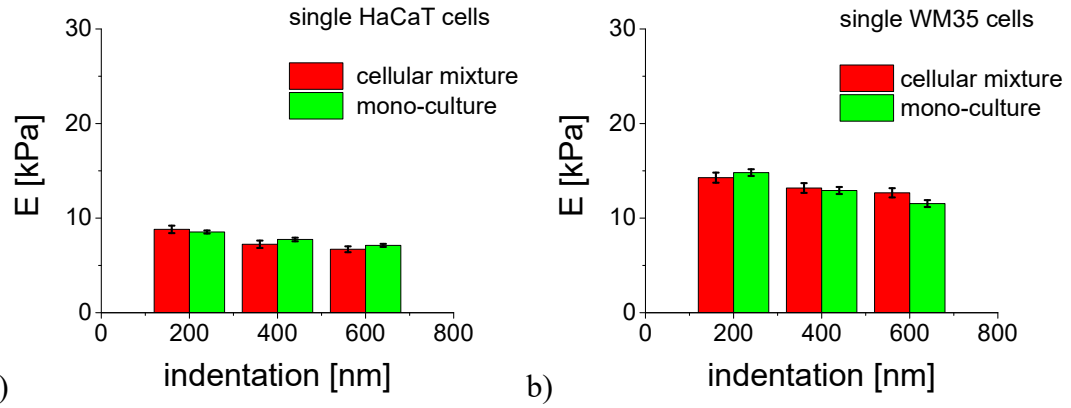

Figure 42. Comparison of Young's modulus of single (a) HaCaT and (b) WM35 melanoma cells measured after 48h of growth in both mono-cultures and cellular mixtures.

No significant difference in mechanical properties of single cells (either HaCaT or WM35 melanoma cells) cultured in monocultures and cellular mixtures is not surprising. These cells are not in direct contact with other cells, and, moreover, in cultures, there is a free space around them. The only way to influence mechanical properties by cellular neighbors located at distant places is to secrete signaling molecules that have to reach and bind to receptors present on the measured cells. Results show that the effect of neighboring cells of the same and distinct type is negligible. The presence of keratinocytes does not affect the elasticity of single melanoma cells and *vice versa* the presence of melanoma cells does not influence the stiffness of keratinocytes.

6.3.2. Deformability of cell clusters

Studies on deformability of cell clusters allows to quantify the effect of neighboring cells for cells being in direct contact with each other. Analogously, as for single cells, at first elastic properties of cell clusters were quantified in mono-cultures (for both HaCaT and WM35 melanoma cells cultured separately). Results show that also cell clusters composed of melanoma cells are more rigid as compared to clusters consisting of HaCaT cells (**Figure 43**).

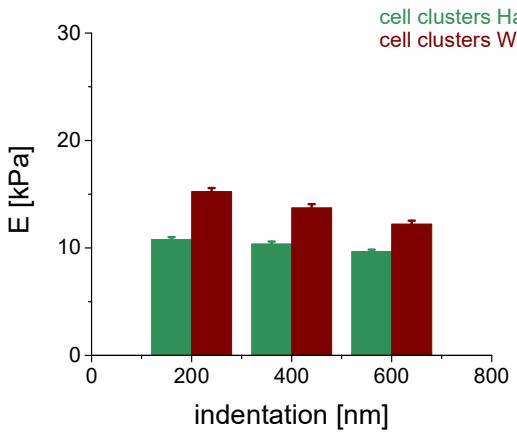

Figure 43. Young's modulus of HaCaT and WM35 melanoma cell clusters measured after 48h of growth. Both cell lines were cultured separately.

Obtained Young's moduli for HaCaT cells are 10.8 ± 0.2 kPa (n = 291 cells), 10.4 ± 0.2 kPa (n = 206), and 9.7 ± 0.2 kPa (n = 198) determined for indentations of 200 nm, 400 nm and 600 nm, respectively. The corresponding moduli for melanoma cells are 15.2 ± 0.3 kPa (n = 222 cells), 13.7 ± 0.3 kPa (n = 131), and 12.2 ± 0.3 kPa (n = 121). These values are of about 5%–30% larger as compared to elasticity of single cells, cultured at the same conditions. Since one can assume similar secretion level of signaling molecules as in the case of single cells, the increase in cell cluster deformability can be attributed to the presence of cellular junctions that stabilize the overall elasticity of a cell being in direct contact with neighboring cells. At this moment, cell clusters composed of cells of the same type were considered. Moreover, distant neighbors are also of the same origin as the measured cells.

To study whether the relation observed for cell clusters remains unaffected by the presence of distant neighbors of different type, mechanical properties of cell clusters were measured for cellular mixtures. Thus, it is possible to quantify the effect of HaCaT cells on WM35 cell clusters and WM35 cells on HaCaT cell clusters (**Figure 44).** Analogously as in previous results, melanoma cells remained stiffer than keratinocytes within the whole analyzed range of indentation depths.

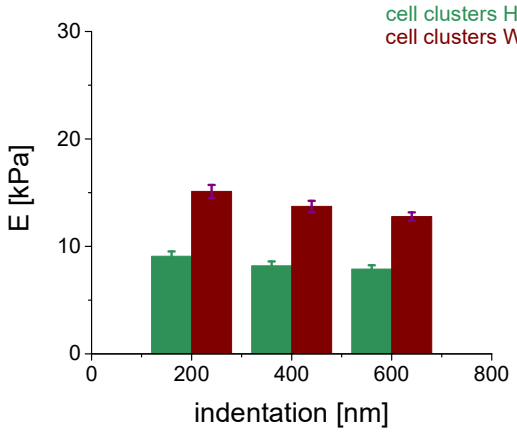

Figure 44. Young's modulus of HaCaT and WM35 melanoma cell clusters measured after 48h of growth in cellular mixtures.

Obtained Young's moduli for HaCaT cell clusters, measured at cellular mixtures, are 9.1 ± 0.5 kPa (n = 51 cells), 8.2 ± 0.4 kPa (n = 51), and 7.9 ± 0.4 kPa (n = 50) determined for indentations of 200 nm, 400 nm and 600 nm, respectively. The corresponding moduli of

melanoma cells are 15.1 ± 0.6 kPa (n = 67 cells), 13.7 ± 0.5 kPa (n = 67), and 12.8 ± 0.4 kPa (n = 63). Elastic modulus of HaCaT cells is lower of about 18%–28% as compared with cell clusters from mono-cultures (**Figure 45a)**.

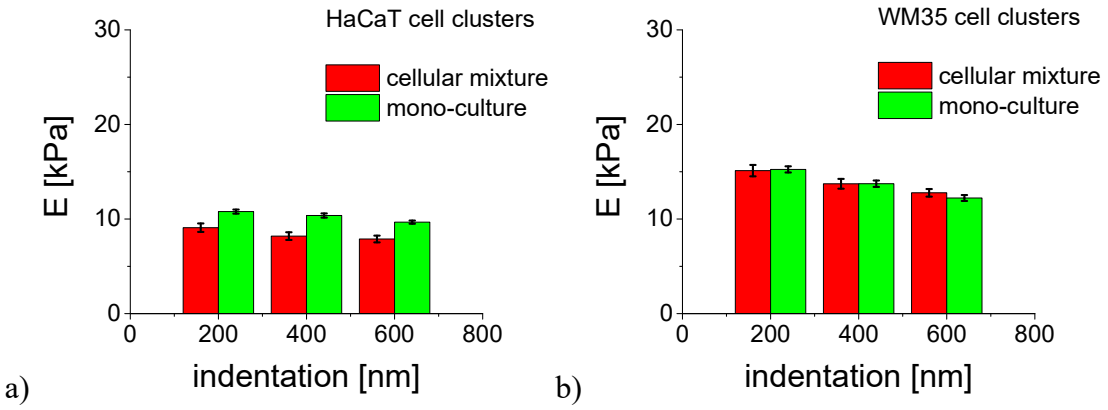

Figure 45. Comparison of Young's modulus of (a) HaCaT and (b) WM35 melanoma cell clusters measured after 48h of growth in both mono-cultures and cellular mixtures.

Cell clusters measured in the cellular mixture are composed of the same cell types, i.e. HaCaT cells that surround the measured cells. Conditions resemble that of mono-cultures where similar structures of clusters were analyzed. The difference between cellular mixture and monocultures lies in the types of cells at distant locations. In cellular mixtures, there are both HaCaT and WM35 cells while in monocultures there are only either HaCaT or melanoma cells. Lower elasticity modulus values indicate larger deformability of cell clusters in mixed cultures and suggest that this effect is induced by the presence of melanoma cells, located at various distant places from the measured cluster. This is the only parameter, which was changed. WM35 melanoma cells behave differently. Their deformability remained at the same level (**Figure 45b**) what allows to state that the presence of keratinocytes does not affect melanoma cells mechanical properties.

6.3.3. Deformability of border cells

To confirm that melanoma cells affect keratinocytes' mechanical properties border cells were analyzed. Therefore, the relation between HaCaT and WM35 melanoma cells was plotted (**Figure 46**).

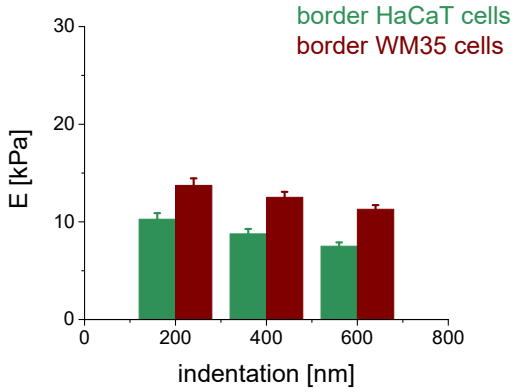

Figure 46. Young's modulus of HaCaT and WM35 melanoma border cells measured after 48h of growth in cellular mixtures.

It shows that even in the case of the direct contact between WM35 and HaCaT cells, melanoma cells preserve their deformability properties (Young's moduli are higher). Next, the question was whether two cells contacting each other mutually alter their mechanical properties. At first, keratinocytes were studied (**Figure 47a**).

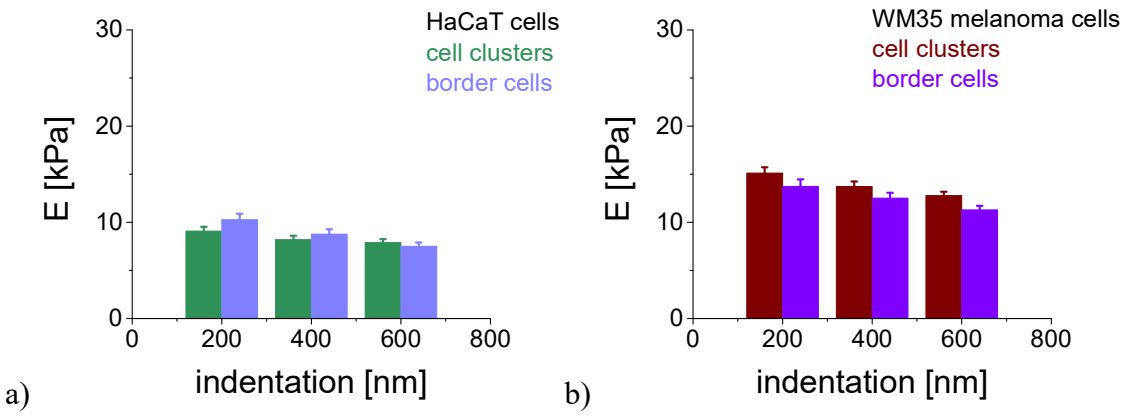

Figure 47. Comparison of Young's modulus of (a) HaCaT and (b) WM35 melanoma border cells measured after 48h of growth in cellular mixtures.

Obtained Young's moduli for HaCaT border cells, measured at cellular mixtures, are 10.3 ± 0.6 kPa (n = 49 cells), 8.8 ± 0.5 kPa (n = 49), and 7.5 ± 0.4 kPa (n = 48) determined for indentations of 200 nm, 400 nm and 600 nm, respectively. The corresponding moduli for cell clusters (recalled from section 6.3.2.) are 9.1 ± 0.5 kPa (n = 51 cells), 8.2 ± 0.4 kPa (n = 51), and 7.9 ± 0.4 kPa (n = 50). A decrease of Young's modulus suggests that melanoma cells effect on keratinocytes in the case of the direct cellular contact. However, these changes are not as pronounced as that observed for cell clusters. This is probably due to cell-cell junctions present within the contact area. Analogous analysis was performed for WM35 melanoma cells (**Figure 47b**). Here, obtained moduli for border cells are 13.7 ± 0.7 kPa (n = 49 cells), 12.5 ± 0.6 kPa (n = 49), and 11.3 ± 0.4 kPa (n = 43) for indentations of 200 nm, 400 nm and 600 nm, respectively. The corresponding moduli for cell clusters (recalled from section 6.3.2.) are 15.1 ± 0.6 kPa (n = 67 cells), 13.7 ± 0.5 kPa (n = 67), and 12.8 ± 0.4 kPa (n = 63). Results show that melanoma cells become softer (i.e. more deformable) in case of direct contact with keratinocytes. The effect is more pronounced for melanoma border cells as compared to melanoma cell clusters.

6.3.4. Summary of the interaction between melanoma cells & keratinocytes

The results gathered in this section characterize changes of mechanical properties of both HaCaT and WM35 cells involved in the interaction between melanoma cells and keratinocytes. Comparison between deformability of cells measured as single cells, cell clusters, and border cells resulted in the following conclusions:

- WM35 melanoma cells are stiffer than keratinocytes, regardless of the conditions they were measured under (single cells, cell clusters, border cells).

- When both types of cells are measured as single, isolated cells, there are no significant changes in cellular deformability of neither HaCaT nor WM35 cells. This probably stems from lack of the direct contact with neighboring cells, thus, the only possible way to influence cells mechanical properties is through signaling molecules secreted by distant neighbors and it is negligible. The presence of keratinocytes does not affect the elasticity of single melanoma cells and *vice versa* the presence of melanoma cells does not influence the stiffness of keratinocytes.
- When HaCaT cells are measured as cell clusters, deformability decreases (cells become more rigid) of about 5%–30%. Such a change can be attributed to the presence of cellular junctions that stabilize the overall elasticity of a cell being in the direct contact with neighboring cells. They seem to be affected by melanoma cells.
- When WM35 melanoma cells are measured as cell clusters, their deformability remained at the similar level. They seem to be unaffected by keratinocytes presence.
- Border cells either HaCaT or melanoma cells respond to the cell, to which they are directly linked. Keratinocytes become more rigid while melanoma cells soften (i.e. increase their deformability).

These results demonstrate that cellular interactions involve not only signaling molecules secreted by other cells. Cell junctions present within a contact area modulate mechanical properties of both interacting cells, particularly, HaCaT and WM35 melanoma cells.

6.4. Interaction of melanoma cells with skin fibroblasts

In further steps of melanoma progression, invading through epidermis, cancer cells break a basal membrane and reach the dermis where it may interact with skin fibroblasts being most abundant in this layer. Thus, the objective of this section is to quantify mechanical properties of melanoma cells interacting with skin fibroblasts. Analogously, as for the keratinocyte/melanoma interaction, the first step was a visualization of cellular mixtures composed of FBs and WM35 melanoma cells by means of optical microscope. Fluorescent images of actin filaments (stained with phalloidin conjugated with Alexa Fluor 488 dye) reveal two types of cells in a co-culture (**Figure 48**). Typically, a large spindle-like fibroblast was surrounded by much smaller, although spindle-like cells being WM35 melanoma cells. It should be noted here that FBs distinguished themselves in directionality as compared to melanoma cells.

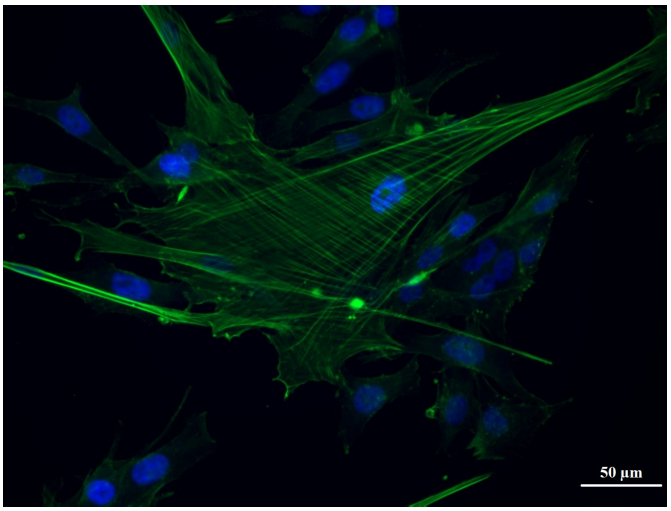

Figure 48. Fluorescence image of a mixture of fibroblasts (larger cells) and WM35 melanoma cells (smaller cells). Actin filaments (green) are stained with phalloidin conjugated with Alexa Fluor 488 dye while cell nuclei were visualized with Hoechst dye (blue).

Actin filaments in fibroblasts are well-organized with clearly visible stress fibers. In melanoma cells, F-actin is distributed over a whole cell body but the presence of stress fibers is hardly marked. For both cell types, FBs and WM35 cells, actin filaments are responsible for elastic properties (see section 5.3. showing the effect of cytochalasin D on FBs while results of cytochalasin D on melanoma cells have been already published).[89]
Analogously as for keratinocytes (HaCaT cells) and WM35 melanoma cells, three groups of cells, namely, single cells, cell clusters, and border cells were examined by means of AFM. Single, isolated cells cultured on a glass surface, have free space enabling them to spread out. There are no direct interactions between cells (neither between melanoma cells nor between melanoma cells and fibroblasts). Thus, alterations of their biomechanical properties can arise due to attachment of signaling molecules secreted by distant neighbors either melanoma cells or fibroblasts. Single cell embedded within a cluster of 5-10 cells represents a cell that can change its biomechanical properties *(i)* due to attachment of signaling molecules secreted by distant neighbors either melanoma cells or fibroblasts, or *(ii)* due to direct connections through various types of cell-cell junctions. Elasticity parameter of border cells seems to be dominated only by a direct interaction between melanoma cells and fibroblasts.

6.4.1. Deformability of single cells

Deformability of both cells, fibroblasts and WM35 melanoma cells, was determined for cells cultured for 48 hours in optimized conditions of growth (see Chapter 3). Elastic properties of single, isolated cells cultured in the presence of cellular neighbors of the same origin localized at distant places were measured. An isolated cell can be influenced only by signaling molecules secreted to the culture medium. Results of AFM-based elasticity measurements show larger deformability of melanoma cells (smaller Young's modulus) as compared to fibroblasts at each indentation depth value chosen for the analysis (**Figure 49**). Obtained moduli are 21.1 ± 0.6 kPa (n = 175 cells), 16.0 ± 0.7 kPa (n = 75), 13.8 ± 0.6 kPa

(n = 68) for indentations of 200 nm, 400 nm and 600 nm, respectively. The corresponding modulus values for melanoma cells are 14.8 ± 0.4 kPa (n = 156 cells), 12.9 ± 0.4 kPa (n = 86) and 11.5 ± 0.4 kPa (n = 80). However, one can see that difference between single fibroblasts and melanoma cells diminishes with indentation depth. Initially, it accounts for 30% while for indentation of 600 nm, it is only 6%.

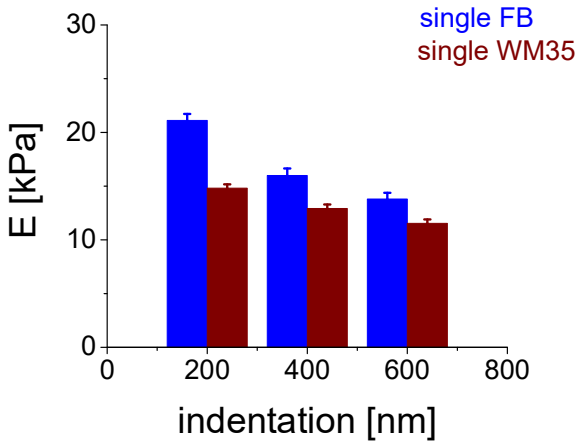

Figure 49. Young's modulus of single FBs and WM35 melanoma cells, determined for cells cultured separately after 48 h.

The comparison of mechanical properties of single fibroblasts cells from mono-cultures and cellular mixtures is presented in **Figure 50**.

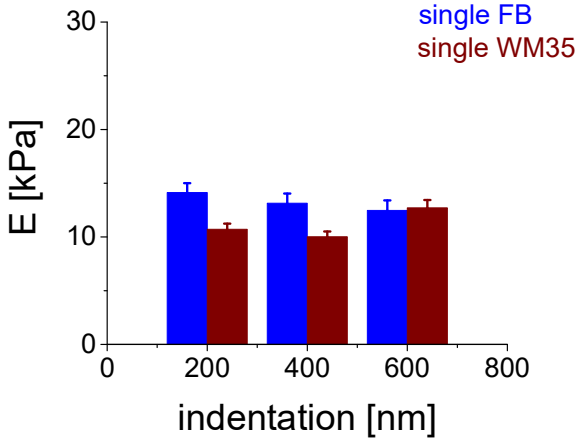

Figure 50. Young's modulus of single FBs and WM35 melanoma cells, determined for cells after 48 h culture in cellular mixtures.

The elasticity parameter of single fibroblasts, measured in co-cultures, changes in presence of melanoma cells and it is much lower than for the single fibroblasts grown in a monoculture. The larger difference between cells from mono- and co-culture is observed at 200 nm of indentation depth and it is about 7 kPa (Young's modulus for single fibroblasts is 21.1 ± 0.6 kPa and 14.1 ± 0.9 kPa, for mono- and co-cultures, respectively). This change gets smaller with the increase of indentation depth. For 400 nm, it is about 3 kPa (elastic moduli for single fibroblasts is 16.0 ± 0.7 kPa and 13.1 ± 0.9 kPa, for mono- and co-cultures, respectively). For 600 nm, it is about 1.3 kPa (elastic moduli for single fibroblasts is 13.8 ± 0.6 kPa and 12.5 ± 0.9 kPa, for mono- and co-cultures, respectively). A comparison

between single cells from monocultures and cellular mixtures, for both fibroblasts and WM35 melanoma cells is presented in **Figure 51.**

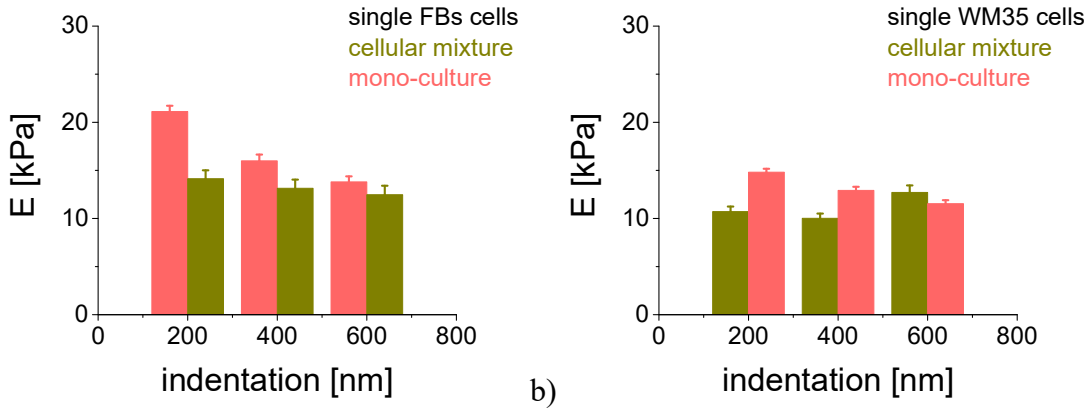

Figure 51. Comparison of Young's modulus of single (a) FBs and (b) WM35 melanoma cells measured after 48h of growth in both mono-cultures and cellular mixtures.

Results show that elasticity parameter values of single melanoma cells are lower than of single fibroblasts, regardless of the culture conditions. However, a comparison of deformability properties in mono-cultures and cellular mixtures reveals that *(i)* single fibroblasts are stiffer when cultured in the cellular mixture within the whole range of indentation depths, and *(ii)* single melanoma cells are softer when grown in the mono-culture, for indentations of 200 nm and 400 nm. As in both cases there is no physical contact between cells involved, the only difference stems from the composition of cells surrounding single cells. And thus, as single fibroblasts in mono-cultures are surrounded only by fibroblasts, a certain level of elasticity can be defined. An increased Young's modulus (cell stiffening) in cellular mixtures can be attributed to the signaling molecules produced by WM35 melanoma cells. In that manner they regulate fibroblasts deformability. In the opposite case, when single monocultured melanoma cells are probed, they can receive information only form melanoma cells. The presence of fibroblasts changes their properties – melanoma cells become altered in a depth-dependent manner. They are softer for smaller indentations (200 nm and 400 nm) and stiffer for larger indentations (above 600 nm). Young's modulus for single melanoma cells grown as monocultures are 14.8 ± 0.4 kPa, 12.9 ± 0.4 kPa and 11.5 ± 0.4 kPa for 200 nm, 400 nm and 600 nm, respectively. The corresponding elasticity parameters values obtained for single melanoma cells in co-cultures are 10.7 ± 0.5 kPa, 10.0 ± 0.5 kPa and 12.7 ± 0.7 kPa.

6.4.2. Deformability of cell clusters

The mechanical properties change when cell clusters are considered. However, still melanoma cells are softer than fibroblasts (**Figures 52**). The difference between these two cell types is indentation depth dependent and diminishes as the indentation increases.

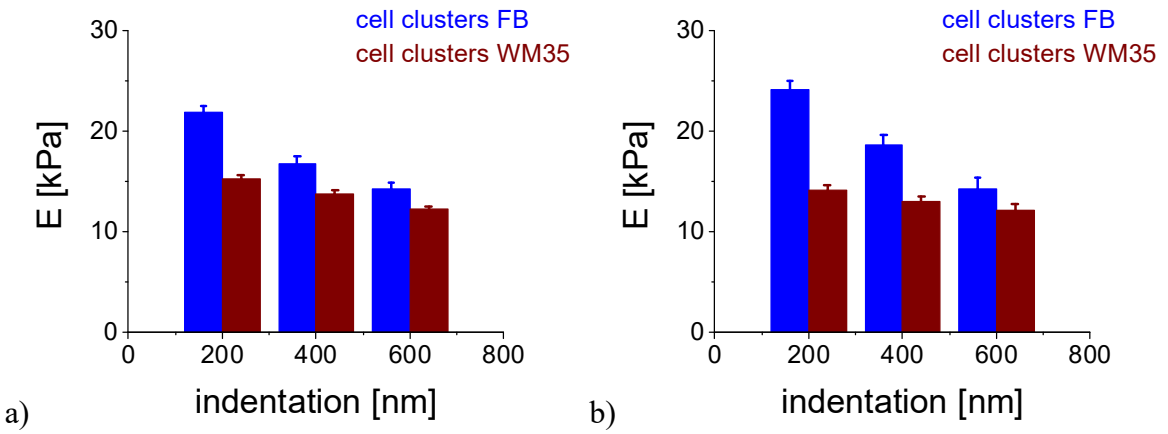

Figure 52. Young's modulus of FBs and WM35 melanoma cell clusters, determined for cells cultured (a) separately and (b) in cellular mixtures, after 48 h.

For fibroblasts cultured separately (i.e. a mono-culture), Young's moduli were 21.9 ± 0.6 kPa, 16.7 ± 0.8 kPa, 14.3 ± 0.6 kPa, for indentations of 200 nm, 400 nm, and 600 nm, respectively. The corresponding moduli for melanoma cells are 15.2 ± 0.3 kPa, 13.7 ± 0.3 kPa, 12.2 ± 0.3 kPa. When cellular mixtures are considered a clear increase in fibroblasts rigidity was observed for indentations up to 400 nm (**Figure 53a**), accompanied by weak changes in melanoma cells deformability (**Figure 53b**). For fibroblasts cultured separately (i.e. a mono-culture), Young's moduli were 24.1 ± 0.9 kPa, 18.6 ± 1.0 kPa, 14.3 ± 1.1 kPa, for indentations of 200 nm, 400 nm, and 600 nm, respectively. The corresponding moduli for melanoma cells are 14.1 ± 0.5 kPa, 12.9 ± 0.5 kPa, 12.1 ± 0.6 kPa.

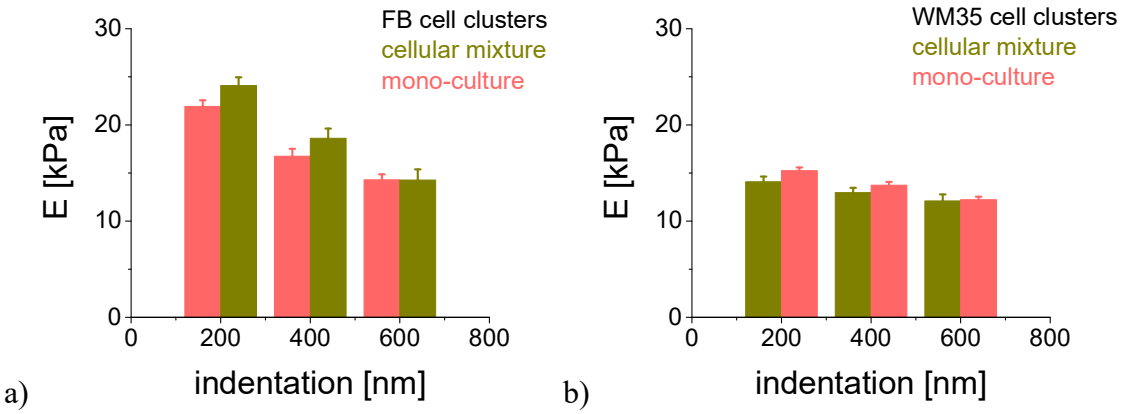

Figure 53. Comparison of Young's modulus of single (a) FB and (b) WM35 melanoma cells measured after 48h of growth in both mono-cultures and cellular mixtures.

These results suggest an important role of stress fibers in maintaining the mechanical properties of fibroblasts, usually leading to stiffening of cells (Young's modulus increases denoting that cells become more rigid). Similar stiffening of cells in clusters has already been reported for prostate and bladder cancer cells.[71,89] For melanoma cells weak relation in deformability was observed. Lack of clear, stress fibers (see e.g. fluorescent images in **Figure 48**), does not allow to transfer mechanical stress from one to another cell. Thus, the presence of neighboring cells belonging to melanoma family weakly influences the mechanical resistance of the measured cell.

6.4.3. Deformability of border cells

Deformability of border cells describes how cells interact with the neighbors of different type. Thus, both WM35 melanoma cells being in contact with fibroblasts and fibroblasts being in contact with melanoma cells were measured. Results, again, show that hen consider border cells fibroblasts are stiffer than melanoma cells for indentations up to 400 nm. For deeper indentations the difference vanishes (**Figure 54**).

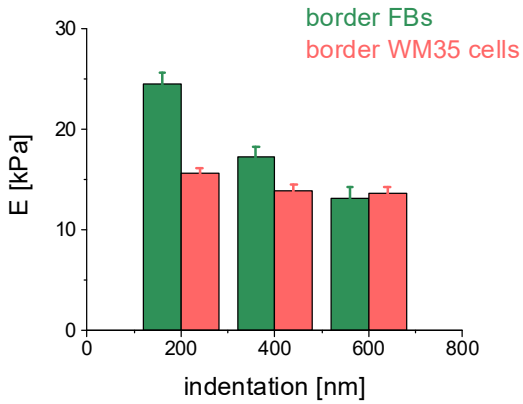

Figure 54. Young's modulus of FB and WM35 melanoma border cells measured after 48h of growth in cellular mixtures.

For fibroblasts cultured separately (i.e. a mono-culture), Young's moduli were 24.5 ± 1.1 kPa, 17.2 ± 1.0 kPa, 13.2 ± 1.1 kPa, for indentations of 200 nm, 400 nm, and 600 nm, respectively. The corresponding moduli for melanoma cells are 15.6 ± 0.6 kPa, 13.9 ± 0.6 kPa, 13.6 ± 0.6 kPa. When these results are compared to that obtained for cell clusters, they show that both fibroblasts and melanoma cells do not largely differ depending on the culture conditions. Results are very similar (**Figure 55**).

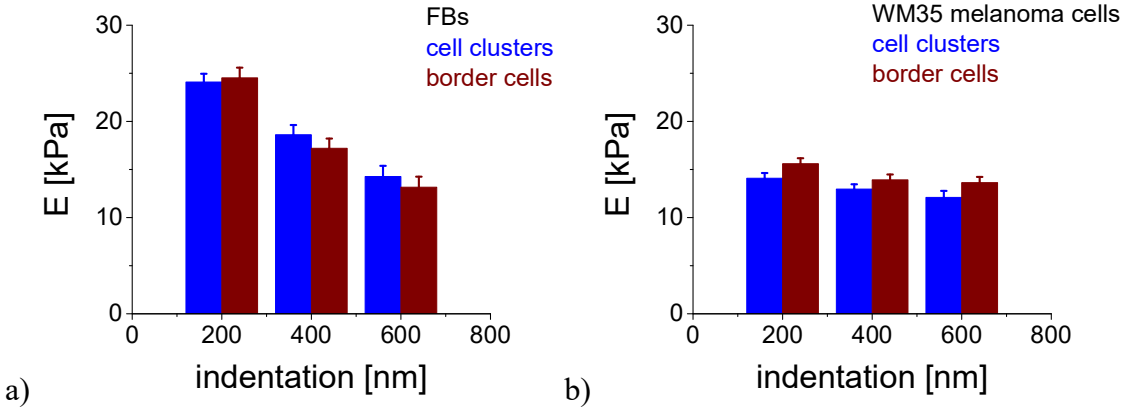

Figure 55. Comparison of Young's modulus of (a) FB and (b) WM35 melanoma border cells measured after 48h of growth in cellular mixtures.

The explanation for that again lies in the presence of stress fibers. They maintain cell's mechanical properties by cellular junctions involving actin filaments, which seems to be dependent on the number of junctions not on the type of adjacent cells connected.

6.4.4. Summary of the interaction between melanoma cells & fibroblasts

The results gathered in this section characterize changes of mechanical properties of both fibroblasts and WM35 melanoma cells. Comparison between deformability of cells measured as single cells, cell clusters, and border cells delivered following conclusions:

- WM35 melanoma cells can co-exist and proliferate in the presence of fibroblasts, whereas proliferation of cellular mixtures is dominated by melanoma cells.
- WM35 melanoma cells are softer than fibroblasts and such relation is independent on the conditions (single cells, cell clusters, border cells).
- The elasticity of single fibroblasts, measured in cellular mixtures, changes due to presence of melanoma cells and it is much lower than for the single fibroblasts grown in a monoculture. An increased Young's modulus (cell stiffening) in cellular mixtures can be attributed to the signaling molecules produced by WM35 melanoma cells, regulating fibroblasts' deformability in that manner.
- The presence of fibroblasts in the cellular mixture with melanoma cells changes their properties – melanoma cells become altered in a depth-dependent manner. They are softer for smaller indentations (200 nm and 400 nm) and stiffer for larger indentations (above 600 nm).
- Deformability of cell clusters revealed an important role of stress fibers present in fibroblasts. Their presence leads to stiffening of cells embedded in a cluster of 5-10 cells. Their absence or rather low abundance in melanoma cells does not induce changes in elastic properties.
- AFM-based elasticity measurements of border cells confirm the role of stress fibers in maintaining cellular deformability. Moreover, results show that the type cell being in contact is not significant.

Results of this section demonstrate that cellular interactions of melanoma cells are not only limited to keratinocytes that could be treated as melanoma environment at early stages of cancer progression (melanoma originates from melanocytes surrounded by keratinocytes). Migrating cancer cells interact also with fibroblasts in the dermis where they modulate mechanical properties of fibroblasts.

7. Conclusions

The main objective of the presented studies was to ascertain how the mechanical properties of living cells change in the processes of wound healing and melanoma formation being phenomena leading to disruption of basal membrane integrity. Therefore, the interactions between three chosen types of the skin cells (keratinocytes, fibroblasts, and melanoma cells from radial growth phase) were evaluated by using AFM-based elasticity measurements. The biochemical and biomolecular characteristics profile of these processes are relatively well-known. However, the knowledge how mechanics influences the process of cell migration or what is the effect of neighboring cells on deformability of single cells is still not well elaborated.
As majority of studies in cell mechanics realized by AFM are carried out on single isolated cells, thus, in the presented studies, an approach of cellular mixtures was developed. In most cases, AFM-based elasticity measurements do not require any special sample preparation if single, isolated cells are studied and cell cultures conventional protocols are used. However, here, these protocols had to be optimized for measurements carried out on living cells grown as cellular mixtures. The result from MTT assay and fluorescent microscope show that all pairs of cellular mixtures (fibroblasts/keratinocytes, fibroblasts/WM35 melanoma cells, and keratinocytes/WM35 melanoma cells) can grow together under a suitable ratio of cells. Additionally, MTT assay demonstrated that keratinocyte's proliferation dominates in the mixture with keratinocytes while in co-cultures with melanoma cells, the melanoma cells dominate in cellular growth. As cellular deformability is very sensitive to given experimental conditions, the effect of culture medium composition on cellular deformability for all chosen skin cell lines (fibroblasts, keratinocytes and melanoma cells) was elaborated. Consequently, it was possible to choose such a culture condition, in which deformability of all studied cells is not affected by medium composition regardless whether they were measured as single cells or cell clusters.

The comparison between various analytical approaches enabled to identify mechanical fingerprints characteristic for each of skin cell types, namely, keratinocytes, fibroblasts and melanoma cells. In the approach, presented here, elasticity data for were fitted with the lognormal function describing non-symmetric histograms (based on applied normality tests). Mood's median test was used to estimate statistical difference of the obtained data between studied cell populations. Cells communicate either through various signaling pathways induced by molecules secreted to surrounding environments or by direct connections realized by distinct types of cellular junctions. Thus, elasticity measurements of single cells, cell clusters and border cells delivers information on the role and cytoskeleton reorganization induced either through paracrine signaling pathways or by physical contact between two adjacent cells.

AFM-based elasticity measurements demonstrated that interaction between keratinocytes and fibroblasts that occur during wound healing process can be characterized not only by molecular and biochemical properties. Intuitively, mechanical forces might be involved as both participating cells are in direct and indirect contacts. These can lead to alterations in deformability of skin cells. Understanding how biomechanical properties

changes allow us to elaborate in details mechanisms governing the behavior of fibroblasts and keratinocytes during wound healing. Single fibroblasts are more rigid as compared to keratinocytes within the full range of the studied indentation depths and regardless of the culture time. Reorganization of actin filaments leads to elasticity changes of cells and dominates significantly in deformability of fibroblasts while keratinocytes seem to be unaffected by actin cytoskeleton remodeling. The presence of distant neighbors (i.e. keratinocytes in the case of keratinocytes and fibroblasts in the case of fibroblasts) influences the elasticity of single cells, regardless of the cell type studied. In both cases, the largest alterations were observed for the superficial layer of cells, indicating strong re-organization of actin filaments in a response to the cell expansion due to free space around and signaling molecules receiving from distant cells. For deeper indentations mechanical response of single keratinocytes, dominating contribution in the overall elasticity of a whole cell. Simultaneously, at these indentations, the information of actin filaments re-arrangements within the superficial layer of the cell vanishes. Comparing elasticity changes with single cell spreading area shows large changes in cell surface area for single fibroblasts. For keratinocytes, weak changes in cellular deformability accompanied by small changes in a single cell surface area indicate that these alterations are mutually dependent phenomena. Culturing cells in clusters did not change the relation between cellular deformability. Fibroblasts remained still stiffer than keratinocytes. Increased rigidity of keratinocyte clusters indicates the influence of neighboring cells in maintaining mechanical resistance of cells to lateral deformations. For fibroblasts, both stiffening and softening were observed depending on the culture time. This leads to a conclusion that in cellular mixtures, deformability of cells and their capability to spread out are independent phenomena. Consequently, both cells types remained insensitive to the presence of other cells, regardless of the culture time.

Studies on alterations in mechanical properties of melanoma cells and keratinocytes show that the former one are stiffer than then latter one, regardless of the conditions they were measured (single cells, cell clusters, border cells). When both types of cells are measured as single, isolated cells, there is no significant changes in cellular deformability of neither for HaCaT nor for WM35 melanoma cells. This probably stems from lack of direct contact with neighboring cells. The presence of keratinocytes does not affect the elasticity of single melanoma cells and *vice versa* the presence of melanoma cells does not influence the stiffness of single keratinocytes. When HaCaT cells are measured as cell clusters, deformability decreases (cells becomes more rigid) of about 5%–30%. Such a change can be attributed to the presence of cellular junctions that stabilize the overall elasticity of a cell being in direct contact with neighboring cells. They seem to be affected by melanoma cells. Deformability of WM35 melanoma cell clusters remains at the similar level. They seem to be unaffected by keratinocytes presence. Border cells either HaCaT or melanoma cells respond to the cell, to which they are directly attached. Keratinocytes become more rigid while melanoma cells soften (i.e. increase their deformability). Melanoma cell interaction with fibroblasts is different. As compared to fibroblasts, WM35 melanoma cells are softer. This relation appears to be independent on the conditions (single cells, cell clusters, border cells). The elasticity of single fibroblasts, measured in cellular mixtures, changes under the influence of presence of melanoma cells and it is much lower than for the single fibroblasts grown in the monoculture. An increased Young's modulus (cell stiffening) in cellular

mixtures can be attributed to the signaling molecules produced by WM35 melanoma cells, regulating fibroblasts' deformability in that manner. The presence of fibroblasts in the cellular mixture with melanoma cells changes their properties – melanoma cells became altered in a depth-dependent manner. They are softer for smaller indentations (200 nm and 400 nm) and stiffer for larger indentations (above 600 nm). Deformability of cell clusters revealed important role of stress fibers present in fibroblasts. Their presence leads to stiffening of cells embedded in a cluster of 5-10 cells. Their absence or rather low abundance in melanoma cells does not induce changes in elastic properties. AFM-based elasticity measurements of border cells underlined the role of stress fibers in maintaining cellular deformability, independently of the cell type studied.

Annex 1. Culture medium composition

EMEM – *Eagle's Minimum Essential Medium* (ATCC 30 - 2003) – modified to contain Earle's Balanced Salt Solution, nonessential amino acids, 2 mM Lglutamine, 1 mM sodium pyruvate, and 1500 mg/L sodium bicarbonate.

DERMAL – *Dermal Cell Basal Medium* (ATCC PCS - 200 - 030) – consist of a nutrient blend of amino acids, vitamins, organic and inorganic supplements and salts. With the exception of purified water, all ingredients are in concentrations of less than 1%. The concentrations of components of this formulation are considered a trade secret.

RPMI-1640 – (Sigma Aldrich, R8758) – liquid with sodium bicarbonate and L-glutamine, sterile-filtered, endotoxin and cell culture tested.

Annex 2. Summary of statistics

The statistic of collected data is very important in AFM measurement. In this chapter is presented a set of collected numbers of cells and curves for all cells type and probe measured in this study.

Table 6. Numbers of cells and curves recorded for all studied cell types (fibroblasts, keratinocytes and melanoma cells), cultured as mono-cultures for 24 h and 48 h.

monocultures 24 h		**200 nm**	**400 nm**	**600 nm**
single fibroblasts	**# cells**	73	72	65
	# curves	1579	1413	970
fibroblasts clusters	**# cells**	69	67	60
	# curves	1637	1404	906
single keratinocytes	**# cells**	203	202	202
	# curves	4833	4712	3967
keratinocytes clusters	**# cells**	234	233	229
	# curves	5632	5427	4774
single melanoma cells	**# cells**	52	52	48
	# curves	1247	1088	676
melanoma cells clusters	**# cells**	46	46	42
	# curves	1073	937	561

monocultures 48 h		**200 nm**	**400 nm**	**600 nm**
single fibroblasts	**# cells**	175	75	68
	# curves	3762	1601	1074
fibroblasts clusters	**# cells**	177	65	58
	# curves	3816	1349	872
single keratinocytes	**# cells**	239	152	152
	# curves	5831	3678	3441
keratinocytes clusters	**# cells**	291	206	198
	# curves	7067	4808	4083
single melanoma cells	**# cells**	156	86	80
	# curves	3638	1871	1237
melanoma cells clusters	**# cells**	222	131	121
	# curves	5260	2844	1879

Table 7. Numbers of cells and curves recorded for all studied cell types (fibroblasts, keratinocytes and melanoma cells), cultured as co-cultures for 24 h and 48 h.

co-cultures: FB & HaCaT (24 h)		200 nm	400 nm	600 nm
single fibroblasts	# cells	45	45	36
	# curves	1030	967	553
fibroblasts clusters	# cells	47	47	40
	# curves	1098	952	503
single keratinocytes	# cells	52	52	52
	# curves	1229	1205	995
keratinocytes clusters	# cells	43	43	43
	# curves	998	989	904
keratinocyte near to fibroblasts	# cells	53	52	52
	# curves	1236	1184	1034
fibroblasts near to keratinocytes	# cells	49	49	34
	# curves	1093	910	357

co-cultures: FB & HaCaT (48 h)		200 nm	400 nm	600 nm
single fibroblasts	# cells	38	38	36
	# curves	872	841	566
fibroblasts clusters	# cells	49	46	29
	# curves	1168	858	350
single keratinocytes	# cells	36	35	33
	# curves	823	756	611
keratinocytes clusters	# cells	41	41	41
	# curves	959	938	810
keratinocyte near to fibroblasts	# cells	51	51	51
	# curves	1231	1227	1153
fibroblasts near to keratinocytes	# cells	47	45	33
	# curves	1088	814	381

Table 8. Numbers of cells and curves recorded for fibroblasts and melanoma cells, cultured as co-culture for 48 h.

co-cultures: FB & WM35 (48 h)		200 nm	400 nm	600 nm
single fibroblasts	**# cells**	57	46	29
	# curves	1193	711	282
fibroblasts clusters	**# cells**	72	55	31
	# curves	1507	778	301
single melanoma cells	**# cells**	50	48	35
	# curves	1185	869	411
melanoma cells clusters	**# cells**	77	65	37
	# curves	1780	1086	503
fibroblasts near to melanoma cells	**# cells**	74	55	36
	# curves	1636	840	394
melanoma cells near to fibroblasts	**# cells**	81	71	35
	# curves	1907	1132	436

Table 9. Numbers of cells and curves recorded for keratinocytes and melanoma cells, cultured as co-culture for 48 h.

co-cultures: HaCaT & WM35 (48 h)		200 nm	400 nm	600 nm
single keratinocytes	**# cells**	39	39	39
	# curves	942	925	861
keratinocytes clusters	**# cells**	51	51	50
	# curves	1239	1209	1046
single melanoma cells	**# cells**	58	58	47
	# curves	1347	1218	704
melanoma cells clusters	**# cells**	67	67	63
	# curves	1646	1522	947
keratinocyte near to melanoma cells	**# cells**	49	49	48
	# curves	1199	1136	841
melanoma cells near to keratinocytes	**# cells**	49	49	43
	# curves	1161	1067	629

Table 10. Numbers of cells and curves recorded for melanoma cells, cultured as mono-culture in different culture media – DERMAL, RPMI -1640, after 48 h of growth.

different medium (Dermal, RPMI-1640)		200 nm	400 nm	600 nm
single melanoma cells RPMI-1640	# cells	41	41	41
	# curves	903	888	743
melanoma cells clusters RPMI-1640	# cells	56	55	54
	# curves	1259	1214	924
single melanoma cells DERMAL	# cells	44	44	44
	# curves	990	909	645
melanoma cells clusters DERMAL	# cells	57	56	56
	# curves	1299	1245	1002
single keratinocytes DERMAL	# cells	39	39	39
	# curves	876	833	516
keratinocytes clusters DERMAL	# cells	60	61	56
	# curves	1315	1235	867

List of figures

List of Tables

References

1. Wirtz, D., Konstantopoulos, K. & Searson, P. C. P. P. C. The physics of cancer: the role of physical interactions and mechanical forces in metastasis. *Nat. Rev. Cancer* **11,** 522 (2011).
2. Kumar, S. & Weaver, V. M. Mechanics, malignancy, and metastasis: The force journey of a tumor cell. *Cancer and Metastasis Reviews* **28,** 113–127 (2009).
3. Alibert, C., Goud, B. & Manneville, J. B. Are cancer cells really softer than normal cells? *Biology of the Cell* **109,** 167–189 (2017).
4. Cross, S. E. *et al.* AFM-based analysis of human metastatic cancer cells. *Nanotechnology* **19,** 384003 (2008).
5. Li, Q. S., Lee, G. Y. H., Ong, C. N. & Lim, C. T. AFM indentation study of breast cancer cells. *Biochem. Biophys. Res. Commun.* **374,** 609–613 (2008).
6. Werner, S., Krieg, T. & Smola, H. Keratinocyte-fibroblast interactions in wound healing. *Journal of Investigative Dermatology* **127,** 998–1008 (2007).
7. Orzechowska, B., Pabijan, J., Wiltowska-Zuber, J., Zemła, J. & Lekka, M. Fibroblasts change spreading capability and mechanical properties in a direct interaction with keratinocytes in conditions mimicking wound healing. *J. Biomech.* (2018). doi:10.1016/j.jbiomech.2018.04.033
8. Chen, L., Tredget, E. E., Wu, P. Y. G., Wu, Y. & Wu, Y. Paracrine factors of mesenchymal stem cells recruit macrophages and endothelial lineage cells and enhance wound healing. *PLoS One* **3,** (2008).
9. Lu, C., Vickers, M. F. & Kerbel, R. S. Interleukin 6: a fibroblast-derived growth inhibitor of human melanoma cells from early but not advanced stages of tumor progression. *Proc. Natl. Acad. Sci.* **89,** 9215–9219 (1992).
10. Boxman, I., Löwik, C., Aarden, L. & Ponec, M. Modulation of IL-6 production and IL-1 activity by keratinocyte-fibroblast interaction. *J. Invest. Dermatol.* (1993). doi:10.1111/1523-1747.ep12365474
11. Cornil, I. *et al.* Fibroblast cell interactions with human melanoma cells affect tumor cell growth as a function of tumor progression (metastasis/growth factors/tumor-host relationship). *Cell Biol.* **88,** 6028–6032 (1991).
12. Bouwstra, J. A., Honeywell-Nguyen, P. L., Gooris, G. S. & Ponec, M. Structure of the skin barrier and its modulation by vesicular formulations. *Progress in Lipid Research* **42,** 1–36 (2003).
13. El Ghalbzouri, A. & Ponec, M. Diffusible factors released by fibroblasts support epidermal morphogenesis and deposition of basement membrane components. *Wound Repair Regen.* **12,** 359–367 (2004).
14. Sorrell, J. M. Fibroblast heterogeneity: more than skin deep. *J. Cell Sci.* **117,** 667–675 (2004).
15. Marks, R. The stratum corneum barrier: the final frontier. *J. Nutr.* **134,** 2017S–2021S (2004).
16. Shetty, S. & Gokul, S. Keratinization and its disorders. *Oman Medical Journal* **27,** 348–357 (2012).
17. Tsatmali, M., Ancans, J. & Thody, A. J. Melanocyte function and its control by melanocortin peptides. *Journal of Histochemistry and Cytochemistry* **50,** 125–133 (2002).
18. Akomeah, F. K., Martin, G. P., Muddle, A. G. & Brown, M. B. Effect of abrasion induced by a rotating brush on the skin permeation of solutes with varying physicochemical properties. *Eur. J. Pharm. Biopharm.* **68,** 724–734 (2008).
19. Gairns, F. W. THE SENSORY NERVE ENDINGS OF THE HUMAN PALATE. *Q. J. Exp. Physiol. Cogn. Med. Sci.* **40,** 40–48 (1955).

20. Nadel, E. R., Bullard, R. W. & Stolwijk, J. A. J. Importance of skin temperature in the regulation of sweating. *J. Appl. Physiol.* **31,** 80–87 (1971).
21. Lips, P. Vitamin D physiology. *Progress in Biophysics and Molecular Biology* (2006). doi:10.1016/j.pbiomolbio.2006.02.016
22. Huang, C. T., Chen, M. L., Huang, L. L. & Mao, I. F. Uric acid and urea in human sweat. *Chin. J. Physiol.* **45,** 109–115 (2002).
23. Figdor, C. G., van Kooyk, Y. & Adema, G. J. C-type lectin receptors on dendritic cells and Langerhans cells. *Nat Rev Immunol* **2,** 77–84 (2002).
24. Carr, R. A., Taibjee, S. M. & Sanders, D. S. A. Basaloid skin tumours: Basal cell carcinoma. *Curr. Diagnostic Pathol.* **13,** 252–272 (2007).
25. Natsuga, K. Plectin-related skin diseases. *Journal of Dermatological Science* **77,** 139–145 (2015).
26. Segre, J. A. Epidermal barrier formation and recovery in skin disorders. *J. Clin. Investig.* **116,** 1150–1158 (2006).
27. Witte, R. P. & Kao, W. J. Keratinocyte-fibroblast paracrine interaction: The effects of substrate and culture condition. *Biomaterials* **26,** 3673–3682 (2005).
28. Diegelmann, R. F. Wound healing: an overview of acute, fibrotic and delayed healing. *Front. Biosci.* **9,** 283 (2004).
29. Spiekstra, S. W., Breetveld, M., Rustemeyer, T., Scheper, R. J. & Gibbs, S. Wound-healing factors secreted by epidermal keratinocytes and dermal fibroblasts in skin substitutes. *Wound Repair Regen.* **15,** 708–717 (2007).
30. Guo, S. & DiPietro, L. A. Factors Affecting Wound Healing. *J. Dent. Res.* **89,** 219–229 (2010).
31. Gosain, A. & DiPietro, L. A. Aging and Wound Healing. *World Journal of Surgery* **28,** 321–326 (2004).
32. Versteeg, H. H., Heemskerk, J. W. M., Levi, M. & Reitsma, P. H. New Fundamentals in Hemostasis. *Physiol. Rev.* **93,** 327–358 (2013).
33. Koh, T. J. & DiPietro, L. A. Inflammation and wound healing: the role of the macrophage. *Expert reviews in molecular medicine* **13,** (2011).
34. Tonnesen, M. G., Feng, X. & Clark, R. A. F. Angiogenesis in wound healing. *J. Investig. Dermatology Symp. Proc.* **5,** 40–46 (2000).
35. Pastar, I. *et al.* Epithelialization in Wound Healing: A Comprehensive Review. *Adv. Wound Care* **3,** 445–464 (2014).
36. Broughton, G., Janis, J. E. & Attinger, C. E. The basic science of wound healing. *Plastic and Reconstructive Surgery* **117,** (2006).
37. Siegel, R. L., Miller, K. D. & Jemal, A. Cancer statistics, 2018. *CA. Cancer J. Clin.* **68,** 7–30 (2018).
38. Cho, E., Rosner, B. A., Feskanich, D. & Colditz, G. A. Risk factors and individual probabilities of melanoma for Whites. *J. Clin. Oncol.* **23,** 2669–2675 (2005).
39. Queen, L. Skin Cancer: Causes, Prevention, and Treatment. *Sr. Honor. Theses* 1–29 (2017).
40. Lacy, K. & Alwan, W. Skin cancer. *Med. (United Kingdom)* **41,** 402–405 (2013).
41. Balch, C. M. Cutaneous melanoma: Prognosis and treatment results worldwide. *Semin. Surg. Oncol.* **8,** 400–414 (1992).
42. Arrangoiz, R. Melanoma Review: Epidemiology, Risk Factors, Diagnosis and Staging. *J. Cancer Treat. Res.* **4,** 1 (2016).
43. National Cancer Institute & Board, P. A. T. E. PDQ Melanoma Treatment. *PDQ Cancer Information Summaries* (2016). Available at: http://www.ncbi.nlm.nih.gov/pubmed/26389388%0Ahttp://www.cancer.gov/types/skin/patient/melanoma-treatment-pdq.
44. Bao, G. & Suresh, S. Cell and molecular mechanics of biological materials. *Nature Materials* **2,** 715–725 (2003).

45. Alberts, B. *et al. Alberts*. *Essential Cell Biology* (2009). doi:citeulike-article-id:4505949
46. Singer, S. J. & Nicolson, G. L. The Fluid Mosaic Model of the Structure of Cell Membranes. *Science (80-.).* **175,** 720–731 (1972).
47. Itel, F. *et al.* CO2permeability of cell membranes is regulated by membrane cholesterol and protein gas channels. *FASEB J.* **26,** 5182–5191 (2012).
48. Wang, Y., Ohkubo, Y. Z. & Tajkhorshid, E. Chapter 12 Gas Conduction of Lipid Bilayers and Membrane Channels. *Current Topics in Membranes* **60,** 343–367 (2008).
49. Loewenstein, W. R., Nakas, M. & Socolar, S. J. Junctional Membrane Uncoupling: Permeability transformations at a cell membrane junction . *J. Gen. Physiol.* **50,** 1865–1891 (1967).
50. Yeagle, P. L. Cholesterol and the cell membrane. *BBA - Reviews on Biomembranes* **822,** 267–287 (1985).
51. Simons, K. & Ikonen, E. Functional rafts in cell membranes. *Nature* **387,** 569–572 (1997).
52. Svitkina, T. The actin cytoskeleton and actin-based motility. *Cold Spring Harb. Perspect. Biol.* **10,** (2018).
53. Dix, C. L. *et al.* The Role of Mitotic Cell-Substrate Adhesion Re-modeling in Animal Cell Division. *Dev. Cell* **45,** 132–145.e3 (2018).
54. Sekino, Y., Kojima, N. & Shirao, T. Role of actin cytoskeleton in dendritic spine morphogenesis. *Neurochemistry International* **51,** 92–104 (2007).
55. Guo, X., Bonin, K., Scarpinato, K. & Guthold, M. The effect of neighboring cells on the stiffness of cancerous and non-cancerous human mammary epithelial cells. *New J. Phys.* **16,** (2014).
56. P., B. Wound healing and the role of fibroblasts. *J. Wound Care* **22,** 407–412 (2013).
57. Kim, S., Wong, P. & Coulombe, P. A. A keratin cytoskeletal protein regulates protein synthesis and epithelial cell growth. *Nature* **441,** 362–365 (2006).
58. Ryu, B., Kim, D. S., DeLuca, A. M. & Alani, R. M. Comprehensive Expression Profiling of Tumor Cell Lines Identifies Molecular Signatures of Melanoma Progression. *PLoS One* **2,** e594 (2007).
59. Moore, G. E., Ito, E., Ulrich, K. & Sandberg, A. A. Culture of human leukemia cells. *Cancer* **19,** 713–723 (1966).
60. Zemła, J. *et al.* Atomic force microscopy as a tool for assessing the cellular elasticity and adhesiveness to identify cancer cells and tissues. *Semin. Cell Dev. Biol.* **73,** (2018).
61. Supino, R. MTT assays. in *Methods in molecular biology, Vol 43: In V/fro ToxrCrty Testing Protocols* **43,** 137–149 (1995).
62. Ingle, J. D. J. & Crouch, S. R. Spectrochemical analysis. in *Spectrochemical Analysis* 325–351 (1988).
63. Maret, D. *et al.* Surface Expression of Precursor N-cadherin Promotes Tumor Cell Invasion. *Neoplasia* **12,** 1066-IN38 (2010).
64. Boisen, A., Hansen, O. & Bouwstra, S. AFM probes with directly fabricated tips. *J. Micromechanics Microengineering* **6,** 58–62 (1996).
65. Binnig, G. & Smith, D. P. E. Single-tube three-dimensional scanner for scanning tunneling microscopy. *Rev. Sci. Instrum.* **57,** 1688–1689 (1986).
66. Cappella, B. & Dietler, G. Force-distance curves by atomic force microscopy. *Surf. Sci. Rep.* (1999). doi:10.1016/S0167-5729(99)00003-5
67. Dintwa, E., Tijskens, E. & Ramon, H. On the accuracy of the Hertz model to describe the normal contact of soft elastic spheres. *Granul. Matter* (2008). doi:10.1007/s10035-007-0078-7
68. Sneddon, I. N. The relation between load and penetration in the axisymmetric Boussinesq problem for a punch of arbitrary profile. *Int. J. Engng Sci.* **3,** 47–57

(1965).
69. Lekka, M. *et al.* Elasticity of normal and cancerous human bladder cells studied by scanning force microscopy. *Eur. Biophys. J.* **28,** 312–316 (1999).
70. Vlassak, J. J. & Nix, W. D. A New Bulge Test Technique for the Determination of Young Modulus and Poisson Ratio of Thin-Films. *J. Mater. Res.* **7,** 3242–3249 (1992).
71. Lekka, M. *et al.* Cancer cell detection in tissue sections using AFM. *Arch. Biochem. Biophys.* **518,** 151–156 (2012).
72. Pogoda, K. *et al.* Depth-sensing analysis of cytoskeleton organization based on AFM data. *Eur. Biophys. J.* **41,** 79–87 (2012).
73. Gostek, J. *et al.* Nano-characterization of two closely related melanoma cell lines with different metastatic potential. *Eur. Biophys. J.* **44,** 49–55 (2015).
74. Prauzner-Bechcicki, S. *et al.* PDMS substrate stiffness affects the morphology and growth profiles of cancerous prostate and melanoma cells. *J. Mech. Behav. Biomed. Mater.* **41,** (2015).
75. Sieuwerts, A. M., Klijn, J. G. M. & Foekens, J. A. Assessment of the invasive potential of human gynecological tumor cell lines with the in vitro Boyden chamber assay: Influences of the ability of cells to migrate through the filter membrane. *Clin. Exp. Metastasis* **15,** 53–62 (1997).
76. Boyden, S. THE CHEMOTACTIC EFFECT OF MIXTURES OF ANTIBODY AND ANTIGEN ON POLYMORPHONUCLEAR LEUCOCYTES. *J. Exp. Med.* **115,** 453–466 (1962).
77. Lekka, M. *et al.* Cancer cell recognition - Mechanical phenotype. *Micron* **43,** 1259–1266 (2012).
78. Abidine, Y. *et al.* Mechanosensitivity of Cancer Cells in Contact with Soft Substrates Using AFM. *Biophys. J.* **114,** 1165–1175 (2018).
79. Klymenko, O., Wiltowska-Zuber, J., Lekka, M. & Kwiatek, W. M. Energy dissipation in the AFM elasticity measurements. in *Acta Physica Polonica A* **115,** 548–551 (2009).
80. Wakatsuki, T., Schwab, B., Thompson, N. C. & Elson, E. L. Effects of cytochalasin D and latrunculin B on mechanical properties of cells. *J. Cell Sci.* **114,** 1025–1036 (2001).
81. Wu, H. W., Kuhn, T. & Moy, V. T. Mechanical properties of L929 cells measured by atomic force microscopy: effects of anticytoskeletal drugs and membrane crosslinking. *Scanning* **20,** 389–397 (1998).
82. Lulevich, V., Yang, H. ya, Isseroff, R. R. & Liu, G. yu. Single cell mechanics of keratinocyte cells. *Ultramicroscopy* **110,** 1435–1442 (2010).
83. Ramms, L. *et al.* Keratins as the main component for the mechanical integrity of keratinocytes. *Proc. Natl. Acad. Sci.* **110,** 18513–18518 (2013).
84. Seltmann, K., Fritsch, A. W., Kas, J. A. & Magin, T. M. Keratins significantly contribute to cell stiffness and impact invasive behavior. *Proc. Natl. Acad. Sci.* **110,** 18507–18512 (2013).
85. Bambardekar, K., Clément, R., Blanc, O., Chardès, C. & Lenne, P.-F. Direct laser manipulation reveals the mechanics of cell contacts in vivo. *Proc. Natl. Acad. Sci.* (2015). doi:10.1073/pnas.1418732112
86. Schmidt, A. & Koch, P. J. Desmosomes: just cell adhesion or is there more? *Cell adhesion & migration* (2007). doi:10.4161/cam.4204
87. Bafounta, M. L., Beauchet, A., Chagnon, S. & Saiag, P. Ultrasonography or palpation for detection of melanoma nodal invasion: A meta-analysis. *Lancet Oncology* (2004). doi:10.1016/S1470-2045(04)01609-2
88. Prayer, L. *et al.* Sonography versus palpation in the detection of regional lymph-node metastases in patients with malignant melanoma. *Eur. J. Cancer Clin. Oncol.* (1990).